

Fermionic and Scalar Casimir Effect within the Scattering Approach

Andreas Wirzba
Institut für Kernphysik
Forschungszentrum Jülich

Fermionic and Scalar Casimir Effect within the Scattering Approach

Andreas Wirzba
Institut für Kernphysik
Forschungszentrum Jülich

1. General remarks about the Casimir effect and its geometry dependence

Fermionic and Scalar Casimir Effect within the Scattering Approach

Andreas Wirzba
Institut für Kernphysik
Forschungszentrum Jülich

1. General remarks about the Casimir effect and its geometry dependence
2. Generalization to bubbles in the Fermi sea

Fermionic and Scalar Casimir Effect within the Scattering Approach

Andreas Wirzba
Institut für Kernphysik
Forschungszentrum Jülich

1. General remarks about the Casimir effect and its geometry dependence
2. Generalization to bubbles in the Fermi sea
3. Map to a multi-scattering problem of a point particle

Fermionic and Scalar Casimir Effect within the Scattering Approach

Andreas Wirzba
Institut für Kernphysik
Forschungszentrum Jülich

1. General remarks about the Casimir effect and its geometry dependence
2. Generalization to bubbles in the Fermi sea
3. Map to a multi-scattering problem of a point particle
4. Interactions of two, three and four bubbles

Fermionic and Scalar Casimir Effect within the Scattering Approach

Andreas Wirzba
Institut für Kernphysik
Forschungszentrum Jülich

1. General remarks about the Casimir effect and its geometry dependence
2. Generalization to bubbles in the Fermi sea
3. Map to a multi-scattering problem of a point particle
4. Interactions of two, three and four bubbles
5. Interactions between superfluid bubbles

Fermionic and Scalar Casimir Effect within the Scattering Approach

Andreas Wirzba
Institut für Kernphysik
Forschungszentrum Jülich

1. General remarks about the Casimir effect and its geometry dependence
2. Generalization to bubbles in the Fermi sea
3. Map to a multi-scattering problem of a point particle
4. Interactions of two, three and four bubbles
5. Interactions between superfluid bubbles
6. Scalar Casimir effect

Fermionic and Scalar Casimir Effect within the Scattering Approach

Andreas Wirzba
Institut für Kernphysik
Forschungszentrum Jülich

1. General remarks about the Casimir effect and its geometry dependence
2. Generalization to bubbles in the Fermi sea
3. Map to a multi-scattering problem of a point particle
4. Interactions of two, three and four bubbles
5. Interactions between superfluid bubbles
6. Scalar Casimir effect
7. Conclusions

Fermionic and Scalar Casimir Effect within the Scattering Approach

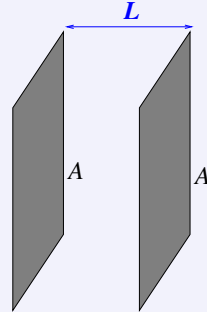
Andreas Wirzba
Institut für Kernphysik
Forschungszentrum Jülich

1. General remarks about the Casimir effect and its geometry dependence
2. Generalization to bubbles in the Fermi sea
3. Map to a multi-scattering problem of a point particle
4. Interactions of two, three and four bubbles
5. Interactions between superfluid bubbles
6. Scalar Casimir effect
7. Conclusions

Together with Aurel Bulgac (Seattle) and Piotr Magierski (Warsaw):

- A. Bulgac & A.W., *Phys. Rev. Lett.* **87** (2001) 120404;
- A. Bulgac, P. Magierski & A.W., *Europhys. Lett.* **72** (2005) 327;
- A. Bulgac, P. Magierski & A.W., *Phys. Rev. D* **73** (2006) 025007;
- A.W., A. Bulgac & P. Magierski, *J. Phys. A* **39** (2006) 6815;
- A.W., *J. Phys. A* **41** (2008) 164003.

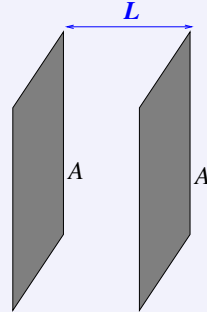
- H.B.G. Casimir (1948): two conducting, but uncharged parallel plates attract each other in vacuum 2



$$\frac{F^{\parallel}(L)}{A} = -\frac{\hbar c}{L^4} \frac{\pi^2}{240} \approx -1.3 \times 10^{-7} \frac{1}{L^4} \text{ N} \frac{\mu\text{m}^4}{\text{cm}^2}$$

$$\mathcal{E}^{\parallel}(L) = -\frac{\hbar c}{L^3} \frac{\pi^2}{720} A$$

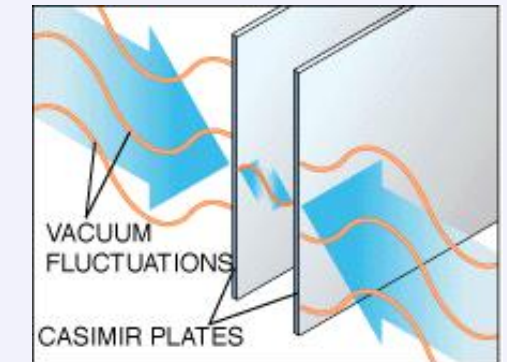
- H.B.G. Casimir (1948): two conducting, but uncharged parallel plates attract each other in vacuum 2



$$\frac{F^{\parallel}(L)}{A} = -\frac{\hbar c}{L^4} \frac{\pi^2}{240} \approx -1.3 \times 10^{-7} \frac{1}{L^4} \text{ N} \frac{\mu\text{m}^4}{\text{cm}^2}$$

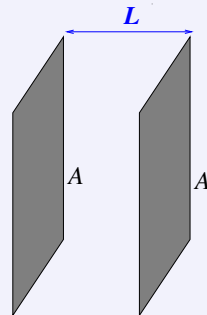
$$\mathcal{E}^{\parallel}(L) = -\frac{\hbar c}{L^3} \frac{\pi^2}{720} A$$

- Reason: zero-point fluctuations of the e.m. field modified by the presence of the plates **relative to the free case**



\Rightarrow change in the energy of the vacuum: $\sum \frac{1}{2} \hbar \omega_k |_{\text{plates}(L)} - \sum \frac{1}{2} \hbar \omega_k |_{\text{free}(L \rightarrow \infty)}$

- H.B.G. Casimir (1948): two conducting, but uncharged parallel plates attract each other in vacuum



$$\frac{F^{\parallel}(L)}{A} = -\frac{\hbar c}{L^4} \frac{\pi^2}{240} \approx -1.3 \times 10^{-7} \frac{1}{L^4} \text{ N} \frac{\mu\text{m}^4}{\text{cm}^2}$$

$$\epsilon^{\parallel}(L) = -\frac{\hbar c}{L^3} \frac{\pi^2}{720} A$$

- Reason: zero-point fluctuations of the e.m. field modified by the presence of the plates relative to the free case

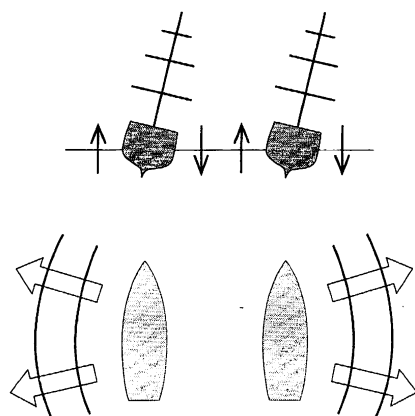
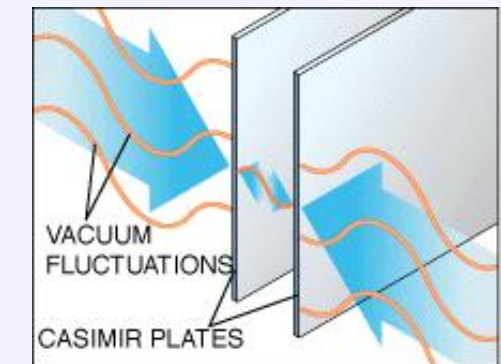
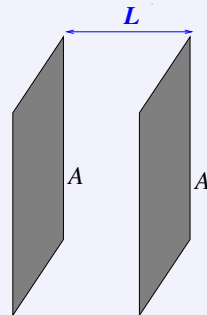


Figure 7.8 Two nearby ships rolling in a swell of ocean waves. Some waves are excluded from the region between the ships and the ships are forced together by the higher wave pressure on their outer sides.

P.C. Causeé: *l'Album du Marin*,
(Charpentier, Nantes, 1836);

S. L. Boersma:
A maritime analogy of the Casimir effect,
American J. Physics **64** (1996) 539;
J. D. Barrow, *The Book of Nothing*
(Random House, London, 2000)

- H.B.G. Casimir (1948): two conducting, but uncharged parallel plates attract each other in vacuum



$$\frac{F^{\parallel}(L)}{A} = -\frac{\hbar c}{L^4} \frac{\pi^2}{240} \approx -1.3 \times 10^{-7} \frac{1}{L^4} \text{ N} \frac{\mu\text{m}^4}{\text{cm}^2}$$

$$\epsilon^{\parallel}(L) = -\frac{\hbar c}{L^3} \frac{\pi^2}{720} A$$

- Reason: zero-point fluctuations of the e.m. field modified by the presence of the plates relative to the free case

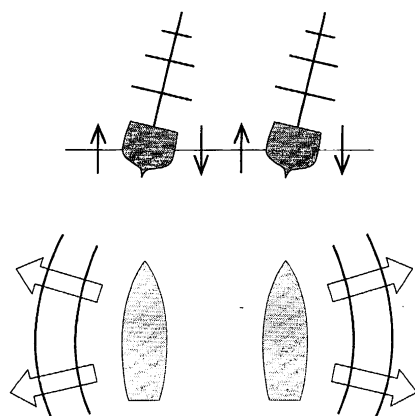
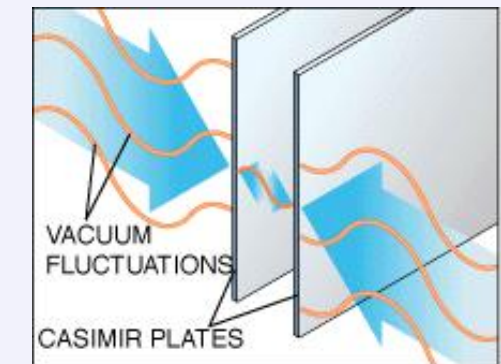


Figure 7.8 Two nearby ships rolling in a swell of ocean waves. Some waves are excluded from the region between the ships and the ships are forced together by the higher wave pressure on their outer sides.

P.C. Causeé: *l'Album du Marin*,
(Charpentier, Nantes, 1836);

S. L. Boersma:
A maritime analogy of the Casimir effect,
American J. Physics **64** (1996) 539;
J. D. Barrow, *The Book of Nothing*
(Random House, London, 2000)

- Distinctive Feature: Casimir calculations depend on the geometry in a non-intuitive way.

- Infinite zero-point energy can be subtracted (discarded) by suitable re-definition of the energy-origin (e.g. by normal ordering)

- Infinite zero-point energy can be subtracted (discarded) by suitable re-definition of the energy-origin (e.g. by normal ordering)
- However, energy-origin can be re-defined only *once*
(and only in homogeneous space (no b.c.'s) and only in the absence of gravity)

- Infinite zero-point energy can be subtracted (discarded) by suitable re-definition of the energy-origin (e.g. by normal ordering)
- However, energy-origin can be re-defined only *once*
(and only in homogeneous space (no b.c.'s) and only in the absence of gravity)

∴ Casimir effect = difference of (properly regularized)
eigen-mode sums of *constrained* QFT
– eigen-mode sums of *free* QFT

Casimir effect and vacuum energy of QFT:

- Infinite zero-point energy can be subtracted (discarded) by suitable re-definition of the energy-origin (e.g. by normal ordering)
- However, energy-origin can be re-defined only once
(and only in homogeneous space (no b.c.'s) and only in the absence of gravity)

\therefore Casimir effect = difference of (properly regularized)
eigen-mode sums of *constrained* QFT
– eigen-mode sums of *free* QFT

$$\begin{aligned}\varepsilon_C &= \lim_{V \rightarrow \infty} \frac{\mathcal{E}_C}{V} \quad (V : \text{quantization box}) \\ &= \lim_{\Lambda \rightarrow \infty} \underbrace{\lim_{V \rightarrow \infty} (-1)^{2S}}_{\text{statistic}} \left(\sum_{k, \nu_{\text{deg}}} \frac{1}{2} \hbar \omega_k |_{V, \Lambda, \textcolor{red}{C}} - \sum_{k, \nu_{\text{deg}}} \frac{1}{2} \hbar \omega_k |_{V, \Lambda, \emptyset} \right)\end{aligned}$$

Casimir effect and vacuum energy of QFT:

- Infinite zero-point energy can be subtracted (discarded) by suitable re-definition of the energy-origin (e.g. by normal ordering)
- However, energy-origin can be re-defined only once
(and only in homogeneous space (no b.c.'s) and only in the absence of gravity)

\therefore Casimir effect = difference of (properly regularized)
eigen-mode sums of *constrained* QFT
– eigen-mode sums of *free* QFT

$$\begin{aligned}\varepsilon_C &= \lim_{V \rightarrow \infty} \frac{\mathcal{E}_C}{V} \quad (V : \text{quantization box}) \\ &= \lim_{\Lambda \rightarrow \infty} \underbrace{\lim_{V \rightarrow \infty} (-1)^{2S}}_{\text{statistic}} \left(\sum_{k, \nu_{\text{deg}}} \frac{1}{2} \hbar \omega_k |_{V, \Lambda, \textcolor{red}{C}} - \sum_{k, \nu_{\text{deg}}} \frac{1}{2} \hbar \omega_k |_{V, \Lambda, \emptyset} \right) \\ \text{Constrained by } &\left\{ \begin{array}{ll} \text{gravity} & (\text{e.g. non-flat metric}) \end{array} \right.\end{aligned}$$

Casimir effect and vacuum energy of QFT:

- Infinite zero-point energy can be subtracted (discarded) by suitable re-definition of the energy-origin (e.g. by normal ordering)
- However, energy-origin can be re-defined only once
(and only in homogeneous space (no b.c.'s) and only in the absence of gravity)

\therefore Casimir effect = difference of (properly regularized)
eigen-mode sums of *constrained* QFT
– eigen-mode sums of *free* QFT

$$\varepsilon_C = \lim_{V \rightarrow \infty} \frac{\mathcal{E}_C}{V} \quad (V : \text{quantization box})$$

$$= \lim_{\Lambda \rightarrow \infty} \lim_{V \rightarrow \infty} \underbrace{(-1)^{2S}}_{\text{statistic}} \left(\sum_{k, \nu_{\text{deg}}} \frac{1}{2} \hbar \omega_k |_{V, \Lambda, \textcolor{red}{C}} - \sum_{k, \nu_{\text{deg}}} \frac{1}{2} \hbar \omega_k |_{V, \Lambda, \emptyset} \right)$$

Constrained by $\begin{cases} \text{gravity} & (\text{e.g. non-flat metric}) \\ \text{external fields} & (\text{e.g. anomalies}) \end{cases}$

Casimir effect and vacuum energy of QFT:

- Infinite zero-point energy can be subtracted (discarded) by suitable re-definition of the energy-origin (e.g. by normal ordering)
- However, energy-origin can be re-defined only once
(and only in homogeneous space (no b.c.'s) and only in the absence of gravity)

\therefore Casimir effect = difference of (properly regularized)
eigen-mode sums of *constrained* QFT
– eigen-mode sums of *free* QFT

$$\varepsilon_C = \lim_{V \rightarrow \infty} \frac{\mathcal{E}_C}{V} \quad (V : \text{quantization box})$$

$$= \lim_{\Lambda \rightarrow \infty} \lim_{V \rightarrow \infty} \underbrace{(-1)^{2S}}_{\text{statistic}} \left(\sum_{k, \nu_{\text{deg}}} \frac{1}{2} \hbar \omega_k |_{V, \Lambda, \textcolor{red}{C}} - \sum_{k, \nu_{\text{deg}}} \frac{1}{2} \hbar \omega_k |_{V, \Lambda, \emptyset} \right)$$

Constrained by $\begin{cases} \text{gravity} & (\text{e.g. non-flat metric}) \\ \text{external fields} & (\text{e.g. anomalies}) \\ \text{internal fields} & (\text{e.g. QCD vacuum}) \end{cases}$

Casimir effect and vacuum energy of QFT:

- Infinite zero-point energy can be subtracted (discarded) by suitable re-definition of the energy-origin (e.g. by normal ordering)
- However, energy-origin can be re-defined only once
(and only in homogeneous space (no b.c.'s) and only in the absence of gravity)

\therefore Casimir effect = difference of (properly regularized)
eigen-mode sums of *constrained* QFT
– eigen-mode sums of *free* QFT

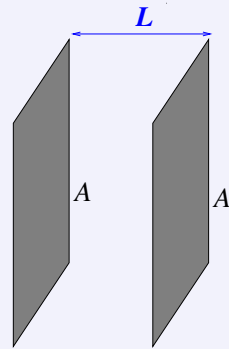
$$\varepsilon_C = \lim_{V \rightarrow \infty} \frac{\mathcal{E}_C}{V} \quad (V : \text{quantization box})$$

$$= \lim_{\Lambda \rightarrow \infty} \lim_{V \rightarrow \infty} \underbrace{(-1)^{2S}}_{\text{statistic}} \left(\sum_{k, \nu_{\text{deg}}} \frac{1}{2} \hbar \omega_k |_{V, \Lambda, \textcolor{red}{C}} - \sum_{k, \nu_{\text{deg}}} \frac{1}{2} \hbar \omega_k |_{V, \Lambda, \emptyset} \right)$$

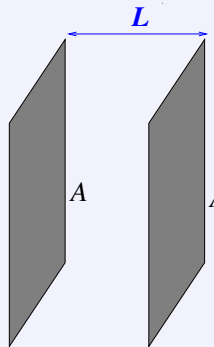
Constrained by $\left\{ \begin{array}{ll} \text{gravity} & (\text{e.g. non-flat metric}) \\ \text{external fields} & (\text{e.g. anomalies}) \\ \text{internal fields} & (\text{e.g. QCD vacuum}) \\ \text{geom.-dep. b.c.'s} & (2 \text{ plates, 2 half-spheres, ...}) \end{array} \right.$

Original Casimir effect:

4

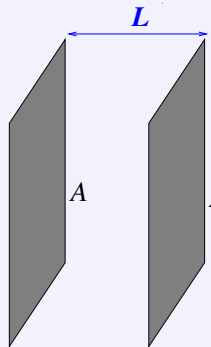


Original Casimir effect:



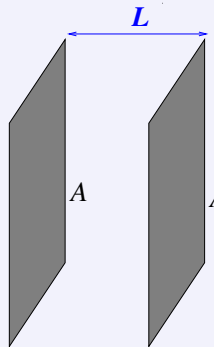
- 1) EM boundary conditions : $\mathbf{B}_\perp = 0$ & $\mathbf{E}_\parallel = 0,$
 - 2) quasi 1-dimensional “box”geometry
- $\left. \right\} \Rightarrow$ 2 decoupled scalar fields

Original Casimir effect:



- 1) EM boundary conditions : $\mathbf{B}_\perp = 0$ & $\mathbf{E}_\parallel = 0$, }
 2) quasi 1-dimensional “box”geometry } \Rightarrow 2 decoupled scalar fields:
 TE-modes (sin) with Dirichlet b.c.'s,
 TM-modes (cos) with Neumann b.c.'s

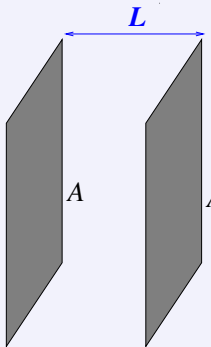
Original Casimir effect:



1) EM boundary conditions : $\mathbf{B}_\perp = 0$ & $\mathbf{E}_\parallel = 0$,
 2) quasi 1-dimensional “box”geometry } \Rightarrow 2 decoupled scalar fields:
 TE-modes (sin) with Dirichlet b.c.’s,
 TM-modes (cos) with Neumann b.c.’s

$$\begin{aligned} \epsilon_{\text{tot}}^{\parallel\text{EM}}(L) &= \lim_{\Lambda \rightarrow \infty} A \iint \frac{d^2 \mathbf{k}_\parallel}{(2\pi)^2} \left(\sum_{n_\perp=1}^{\infty} \underbrace{\frac{1}{2} \overbrace{\hbar\omega(\mathbf{k}_\parallel, n_\perp, L)}^{\hbar c \sqrt{\mathbf{k}_\parallel^2 + (\frac{n_\perp \pi}{L})^2}}}_{\text{background}} + \sum_{n_\perp=0}^{\infty} \underbrace{\frac{1}{2} \hbar\omega(\mathbf{k}_\parallel, n_\perp, L)}_{\text{bulk}} \right) e^{-\frac{\hbar\omega(\mathbf{k}_\parallel, n_\perp, L)}{\Lambda}} \\ &= \lim_{\Lambda \rightarrow \infty} \hbar c A L \left[\underbrace{\frac{3(\Lambda/\hbar c)^4}{\pi^2}}_{\text{background}} + \underbrace{(-1+1)\frac{(\Lambda/\hbar c)^3}{4\pi L}}_{\text{bulk}} - \underbrace{\frac{\pi^2}{720 L^4}}_{\epsilon_C^{\parallel\text{EM}}(L)} + \mathcal{O}\left((\hbar c)^2/\Lambda^2 L^6\right) \right] \end{aligned}$$

Original Casimir effect:

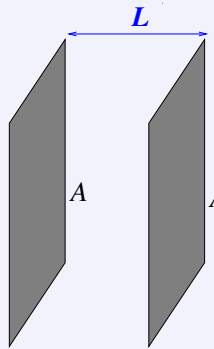


1) EM boundary conditions : $\mathbf{B}_\perp = 0$ & $\mathbf{E}_\parallel = 0$,
 2) quasi 1-dimensional “box”geometry } \Rightarrow 2 decoupled scalar fields:
 TE-modes (sin) with Dirichlet b.c.’s,
 TM-modes (cos) with Neumann b.c.’s

$$\begin{aligned} \epsilon_{\text{tot}}^{\parallel\text{EM}}(L) &= \lim_{\Lambda \rightarrow \infty} A \iint \frac{d^2 \mathbf{k}_\parallel}{(2\pi)^2} \left(\sum_{n_\perp=1}^{\infty} \frac{1}{2} \overbrace{\hbar\omega(\mathbf{k}_\parallel, n_\perp, L)}^{\hbar c \sqrt{\mathbf{k}_\parallel^2 + (\frac{n_\perp \pi}{L})^2}} + \sum_{n_\perp=0}^{\infty} \frac{1}{2} \hbar\omega(\mathbf{k}_\parallel, n_\perp, L) \right) e^{-\frac{\hbar\omega(\mathbf{k}_\parallel, n_\perp, L)}{\Delta}} \\ &= \lim_{\Lambda \rightarrow \infty} \hbar c A L \left[\underbrace{\frac{3(\Lambda/\hbar c)^4}{\pi^2}}_{\text{background}} + \underbrace{(-1+1)\frac{(\Lambda/\hbar c)^3}{4\pi L}}_{\text{bulk}} - \underbrace{\frac{\pi^2}{720 L^4}}_{\epsilon_C^{\parallel\text{EM}}(L)} + \mathcal{O}\left((\hbar c)^2/\Lambda^2 L^6\right) \right] \end{aligned}$$

- UV-cutoff Λ corresponds to plasma frequency.

Original Casimir effect:



1) EM boundary conditions : $\mathbf{B}_\perp = 0$ & $\mathbf{E}_\parallel = 0$,
 2) quasi 1-dimensional “box”geometry } \Rightarrow 2 decoupled scalar fields:
 TE-modes (sin) with Dirichlet b.c.’s,
 TM-modes (cos) with Neumann b.c.’s

$$\begin{aligned} \mathcal{E}_{\text{tot}}^{\parallel\text{EM}}(L) &= \lim_{\Lambda \rightarrow \infty} A \iint \frac{d^2 \mathbf{k}_\parallel}{(2\pi)^2} \left(\sum_{n_\perp=1}^{\infty} \underbrace{\frac{1}{2} \overbrace{\hbar\omega(\mathbf{k}_\parallel, n_\perp, L)}^{\hbar c \sqrt{\mathbf{k}_\parallel^2 + (\frac{n_\perp \pi}{L})^2}}}_{\text{background}} + \sum_{n_\perp=0}^{\infty} \frac{1}{2} \hbar\omega(\mathbf{k}_\parallel, n_\perp, L) \right) e^{-\frac{\hbar\omega(\mathbf{k}_\parallel, n_\perp, L)}{\Lambda}} \\ &= \lim_{\Lambda \rightarrow \infty} \hbar c A L \left[\underbrace{\frac{3(\Lambda/\hbar c)^4}{\pi^2}}_{\text{background}} + \underbrace{(-1+1)\frac{(\Lambda/\hbar c)^3}{4\pi L}}_{\text{bulk}} - \underbrace{\frac{\pi^2}{720 L^4}}_{\epsilon_C^{\parallel\text{EM}}(L)} + \mathcal{O}\left((\hbar c)^2/\Lambda^2 L^6\right) \right] \end{aligned}$$

- UV-cutoff Λ corresponds to plasma frequency.
- When the (infinitely) far separated plates are brought into a finite distance L , the background terms as well as the bulk terms of the single plates are unaffected and therefore removable \Rightarrow the Casimir energy is finite, even in the limit $\Lambda \rightarrow \infty$.

“Generalization” of concept of Casimir energy:

1) the geometry dependence

“Generalization” of concept of Casimir energy:

1) the geometry dependence

Casimir energy ≡ vacuum energy from the *geometry-dependent* part
of the **density of states (d.o.s)**

“Generalization” of concept of Casimir energy:

1) the geometry dependence

Casimir energy

≡ vacuum energy from the *geometry-dependent* part
of the **density of states (d.o.s)**

(\leftrightarrow *shell* correction energy in Nucl. Phys.)

“Generalization” of concept of Casimir energy:

1) the geometry dependence

Casimir energy \equiv vacuum energy from the *geometry-dependent* part
of the **density of states (d.o.s)**
(\leftrightarrow *shell* correction energy in Nucl. Phys.)

d.o.s.: $\rho(E) \equiv \sum_{E_k} \delta(E - E_k) = \underbrace{\rho_0(E)}_{\text{free case}} + \underbrace{\rho_{\text{bulk}}(E)}_{L \rightarrow \infty} + \underbrace{\delta\rho_C(E, \text{geom.-dep.})}_{L \text{ finite}}$

“Generalization” of concept of Casimir energy:

1) the geometry dependence

Casimir energy \equiv vacuum energy from the *geometry-dependent* part
of the **density of states (d.o.s)**
(\leftrightarrow *shell* correction energy in Nucl. Phys.)

$$\text{d.o.s.: } \rho(E) \equiv \sum_{E_k} \delta(E - E_k) = \underbrace{\rho_0(E)}_{\text{free case}} + \underbrace{\rho_{\text{bulk}}(E)}_{L \rightarrow \infty} + \underbrace{\delta\rho_C(E, \text{geom.-dep.})}_{L \text{ finite}}$$

$$\hookrightarrow \text{Casimir Energy: } \mathcal{E}_C \equiv \int_0^\infty dE E \delta\rho_C(E, \text{geom.-dep.}) = - \int_0^\infty dE \mathcal{N}_C(E, \text{geom.-dep.})$$

“Generalization” of concept of Casimir energy:

1) the geometry dependence

Casimir energy \equiv vacuum energy from the *geometry-dependent* part
of the **density of states (d.o.s)**
(\leftrightarrow *shell* correction energy in Nucl. Phys.)

$$\text{d.o.s.: } \rho(E) \equiv \sum_{E_k} \delta(E - E_k) = \underbrace{\rho_0(E)}_{\text{free case}} + \underbrace{\rho_{\text{bulk}}(E)}_{L \rightarrow \infty} + \underbrace{\delta\rho_C(E, \text{geom.-dep.})}_{L \text{ finite}}$$

$$\hookrightarrow \text{Casimir Energy: } \mathcal{E}_C \equiv \int_0^\infty dE E \delta\rho_C(E, \text{geom.-dep.}) = - \int_0^\infty dE \mathcal{N}_C(E, \text{geom.-dep.})$$

$$\text{where } \mathcal{N}_C(E) = \int_0^E dE' \delta\rho_C(E') \quad (\text{geom-dep. part of the integrated d.o.s})$$

“Generalization” of concept of Casimir energy:

2) matter fields

“Generalization” of concept of Casimir energy:

2) matter fields

- *Here*: space not “filled” with *fluctuating* EM modes, but with a gas of *non-interacting* (non-relativistic) fermions.

“Generalization” of concept of Casimir energy:

2) matter fields

- *Here*: space not “filled” with *fluctuating* EM modes, but with a gas of *non-interacting* (non-relativistic) fermions.
- *Similarity*: Existence of mode sums $\sum \hbar\omega_k$ with *constant* degeneracy factor (because of Pauli’s exclusion principle).

“Generalization” of concept of Casimir energy:

2) matter fields

- *Here*: space not “filled” with *fluctuating* EM modes, but with a gas of *non-interacting* (non-relativistic) fermions.
- *Similarity*: Existence of mode sums $\sum \hbar\omega_k$ with *constant* degeneracy factor (because of Pauli’s exclusion principle).
- *Difference*: Existence of a 2nd scale: Fermi energy = *chem. potential* (at $T \approx 0$) (in addition to the geometrical scales).

“Generalization” of concept of Casimir energy:

2) matter fields

- *Here*: space not “filled” with *fluctuating* EM modes, but with a gas of *non-interacting* (non-relativistic) fermions.
- *Similarity*: Existence of mode sums $\sum \hbar\omega_k$ with *constant* degeneracy factor (because of Pauli’s exclusion principle).
- *Difference*: Existence of a 2nd scale: Fermi energy = *chem. potential* (at $T \approx 0$) (in addition to the geometrical scales).
Physics dominated by UV scale
in contrast to long-wave behavior of usual Casimir effect.

“Generalization” of concept of Casimir energy:

2) matter fields

- *Here*: space not “filled” with *fluctuating* EM modes, but with a gas of *non-interacting* (non-relativistic) fermions.
- *Similarity*: Existence of mode sums $\sum \hbar\omega_k$ with *constant* degeneracy factor (because of Pauli’s exclusion principle).
- *Difference*: Existence of a 2nd scale: Fermi energy = *chem. potential* (at $T \approx 0$) (in addition to the geometrical scales).
Physics dominated by UV scale
in contrast to long-wave behavior of usual Casimir effect.
- *Concrete*: Matter fields (fermions) in the space between voids

“Generalization” of concept of Casimir energy:

2) matter fields

- *Here*: space not “filled” with *fluctuating* EM modes, but with a gas of *non-interacting* (non-relativistic) fermions.
- *Similarity*: Existence of mode sums $\sum \hbar\omega_k$ with *constant* degeneracy factor (because of Pauli’s exclusion principle).
- *Difference*: Existence of a 2nd scale: Fermi energy = *chem. potential* (at $T \approx 0$) (in addition to the geometrical scales).
Physics dominated by UV scale
in contrast to long-wave behavior of usual Casimir effect.
- *Concrete*: Matter fields (fermions) in the space between voids
→ the voids obstruct the free motion of the fermions

“Generalization” of concept of Casimir energy:

2) matter fields

- *Here*: space not “filled” with *fluctuating* EM modes, but with a gas of *non-interacting* (non-relativistic) fermions.
- *Similarity*: Existence of mode sums $\sum \hbar\omega_k$ with *constant* degeneracy factor (because of Pauli’s exclusion principle).
- *Difference*: Existence of a 2nd scale: Fermi energy = *chem. potential* (at $T \approx 0$) (in addition to the geometrical scales).
Physics dominated by UV scale
in contrast to long-wave behavior of usual Casimir effect.
- *Concrete*: Matter fields (fermions) in the space between voids
 - the voids obstruct the free motion of the fermions,
 - quantum pressure of the fermions on the voids depends on geometry.

“Generalization” of concept of Casimir energy:

2) matter fields

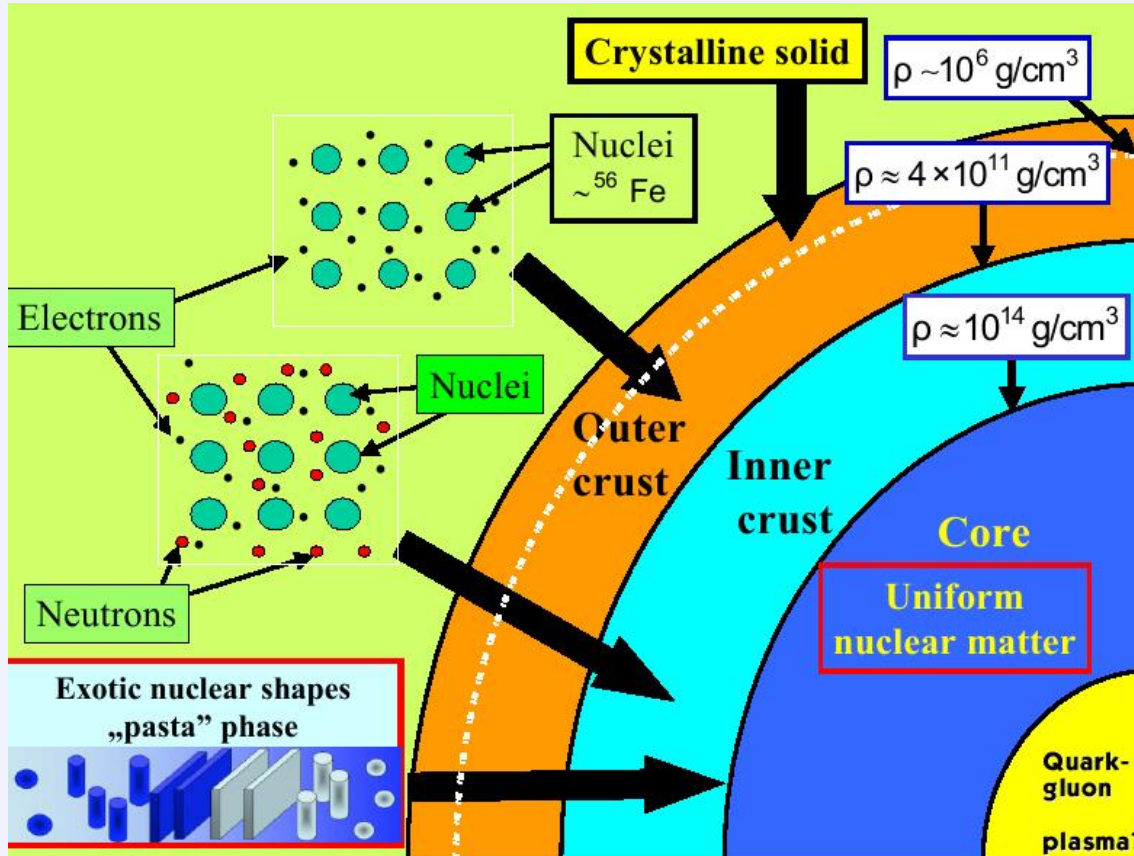
- *Here*: space not “filled” with *fluctuating* EM modes, but with a gas of *non-interacting* (non-relativistic) fermions.
- *Similarity*: Existence of mode sums $\sum \hbar\omega_k$ with *constant* degeneracy factor (because of Pauli’s exclusion principle).
- *Difference*: Existence of a 2nd scale: Fermi energy = *chem. potential* (at $T \approx 0$) (in addition to the geometrical scales).
Physics dominated by UV scale
in contrast to long-wave behavior of usual Casimir effect.
- *Concrete*: Matter fields (fermions) in the space between voids
 - the voids obstruct the free motion of the fermions,
 - quantum pressure of the fermions on the voids depends on geometry.

∴ effective *Casimir-type interaction* between empty regions of space
in the background of *non-interacting* fermionic fields

Applications

In the inner crust of a neutron star:

7

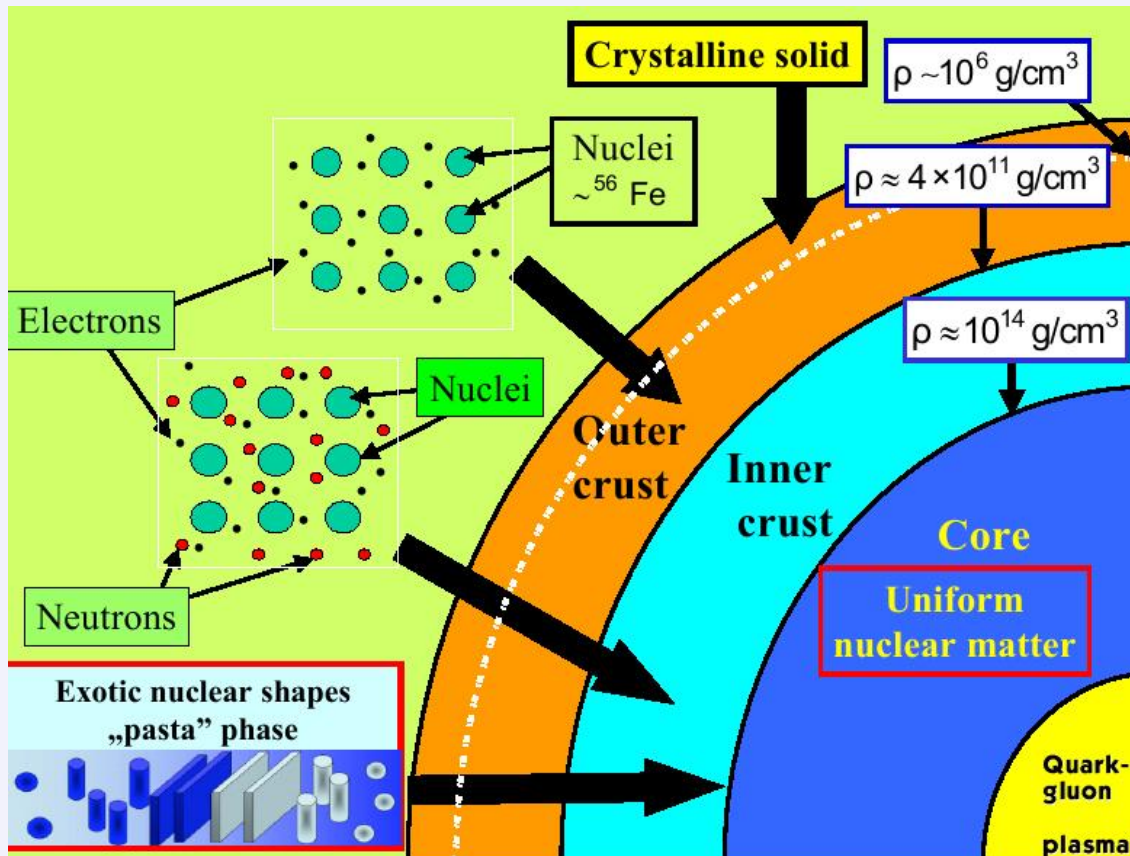


- nuclei lose neutrons due to increasing pressure and density: below the saturation density \Rightarrow chain of phases between 0.03 fm^{-3} and 0.1 fm^{-3} .

Applications

In the inner crust of a neutron star:

7

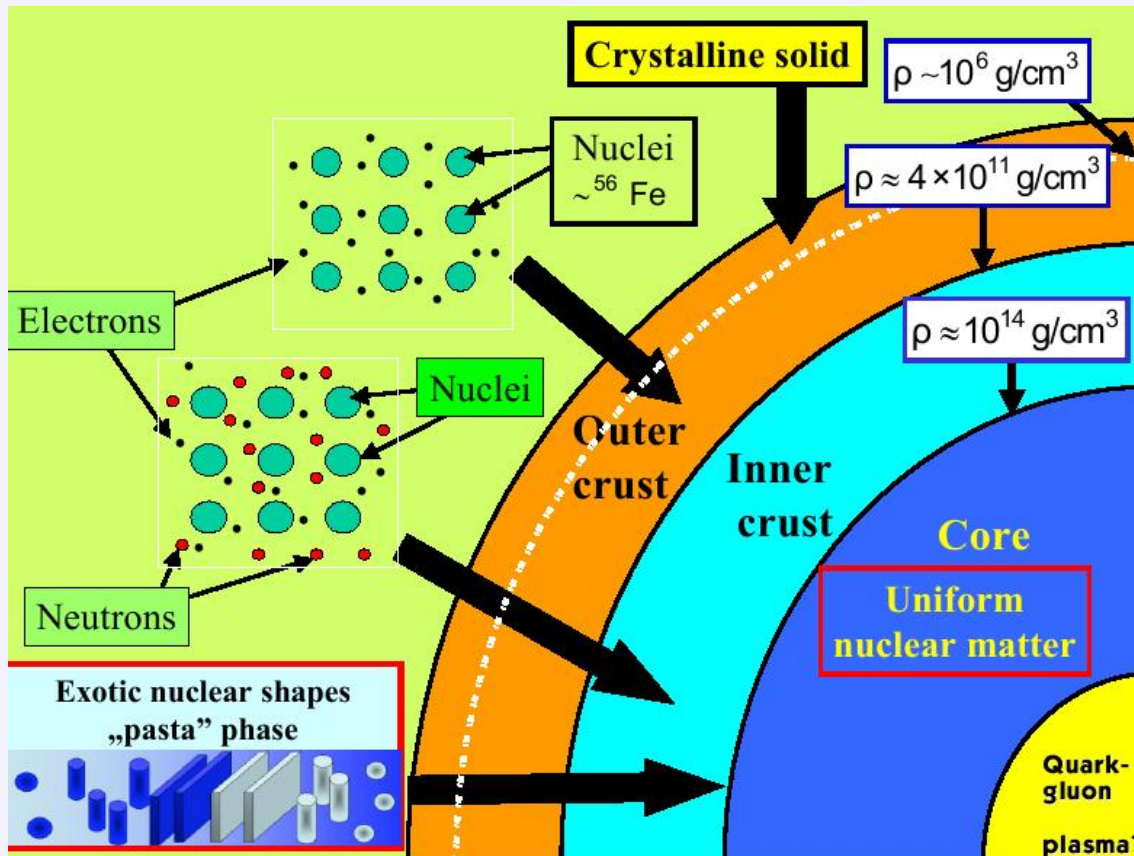


- nuclei lose neutrons due to increasing pressure and density: below the saturation density \Rightarrow chain of phases between 0.03 fm^{-3} and 0.1 fm^{-3} .
- liquid-drop model (interplay of Coulomb- and surface energies): nuclei \rightarrow rods \rightarrow slabs \rightarrow tubes \rightarrow bubbles \rightarrow uniform matter
(G. Baym, H.A. Bethe, C. Pethick, *N.P. A* 175 ('71))

Applications

In the inner crust of a neutron star:

7

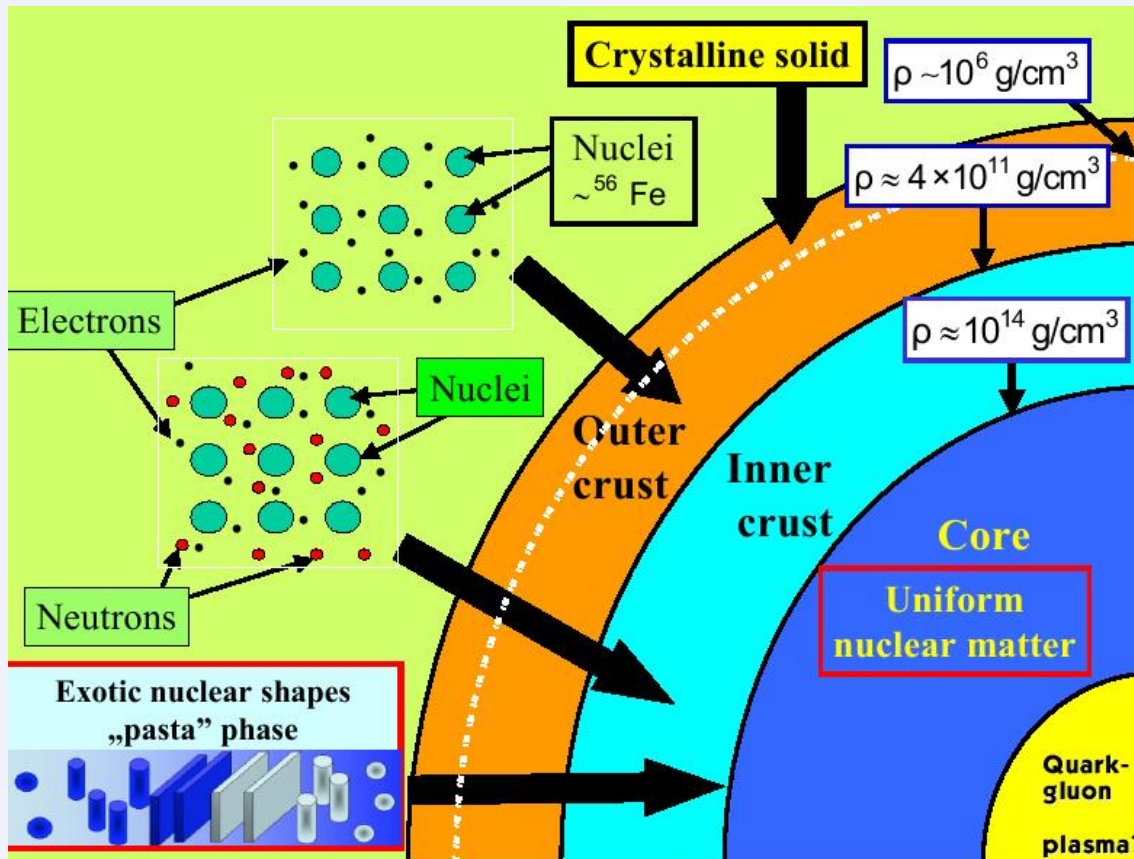


- nuclei lose neutrons due to increasing pressure and density: below the saturation density \Rightarrow chain of phases between 0.03 fm^{-3} and 0.1 fm^{-3} .
- liquid-drop model (interplay of Coulomb- and surface energies): nuclei \rightarrow rods \rightarrow slabs \rightarrow tubes \rightarrow bubbles \rightarrow uniform matter
(G. Baym, H.A. Bethe, C. Pethick, *N.P. A 175* ('71))
- However, the neglected “shell energy” of the outer neutrons is of the same order (keV/fm^3) !
(A. Bulgac & P. Magierski, *Nucl. Phys. A 683* ('01).)

Applications

In the inner crust of a neutron star:

7



- nuclei lose neutrons due to increasing pressure and density: below the saturation density \Rightarrow chain of phases between 0.03 fm^{-3} and 0.1 fm^{-3} .

- liquid-drop model (interplay of Coulomb- and surface energies): nuclei \rightarrow rods \rightarrow slabs \rightarrow tubes \rightarrow bubbles \rightarrow uniform matter

(G. Baym, H.A. Bethe, C. Pethick, *N.P. A 175* ('71))

- However, the neglected “shell energy” of the outer neutrons is of the same order (keV/fm^3) !

(A. Bulgac & P. Magierski, *Nucl. Phys. A 683* ('01).)

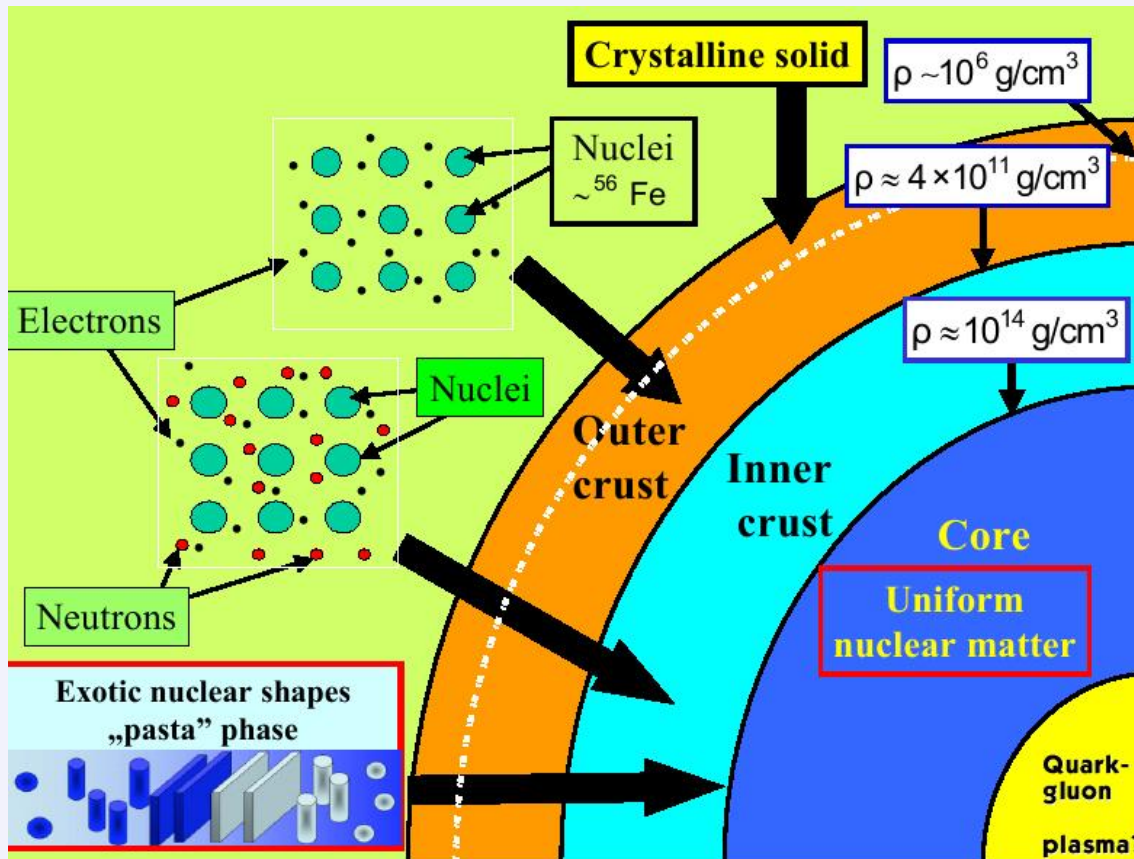
Inside a neutron/quark star:

- Quark droplets immersed in hadronic matter at $\rho \gg \rho_{nm}$

Applications

In the inner crust of a neutron star:

7



- nuclei lose neutrons due to increasing pressure and density: below the saturation density \Rightarrow chain of phases between 0.03 fm^{-3} and 0.1 fm^{-3} .

- liquid-drop model (interplay of Coulomb- and surface energies): nuclei \rightarrow rods \rightarrow slabs \rightarrow tubes \rightarrow bubbles \rightarrow uniform matter
(G. Baym, H.A. Bethe, C. Pethick, *N.P. A 175* ('71))

- However, the neglected “shell energy” of the outer neutrons is of the same order (keV/fm^3) !
(A. Bulgac & P. Magierski, *Nucl. Phys. A 683* ('01).)

Inside a neutron/quark star:

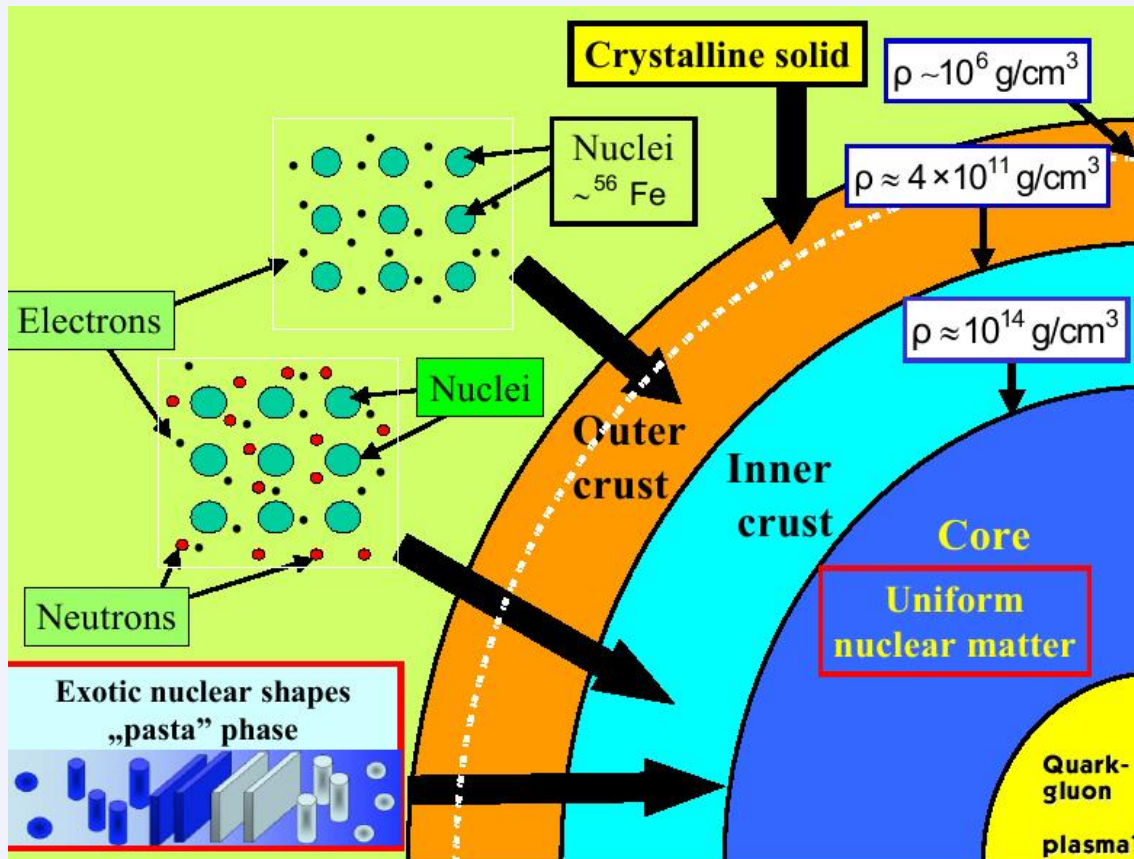
- Quark droplets immersed in hadronic matter at $\rho \gg \rho_{nm}$
 - Buckyballs immersed in an electron gas (in liquid mercury)

In the lab:

Applications

In the inner crust of a neutron star:

7



- nuclei lose neutrons due to increasing pressure and density: below the saturation density \Rightarrow chain of phases between 0.03 fm^{-3} and 0.1 fm^{-3} .

- liquid-drop model (interplay of Coulomb- and surface energies): nuclei \rightarrow rods \rightarrow slabs \rightarrow tubes \rightarrow bubbles \rightarrow uniform matter

(G. Baym, H.A. Bethe, C. Pethick, *N.P. A 175* ('71))

- However, the neglected “shell energy” of the outer neutrons is of the same order (keV/fm^3) !

(A. Bulgac & P. Magierski, *Nucl. Phys. A 683* ('01).)

Inside a neutron/quark star:

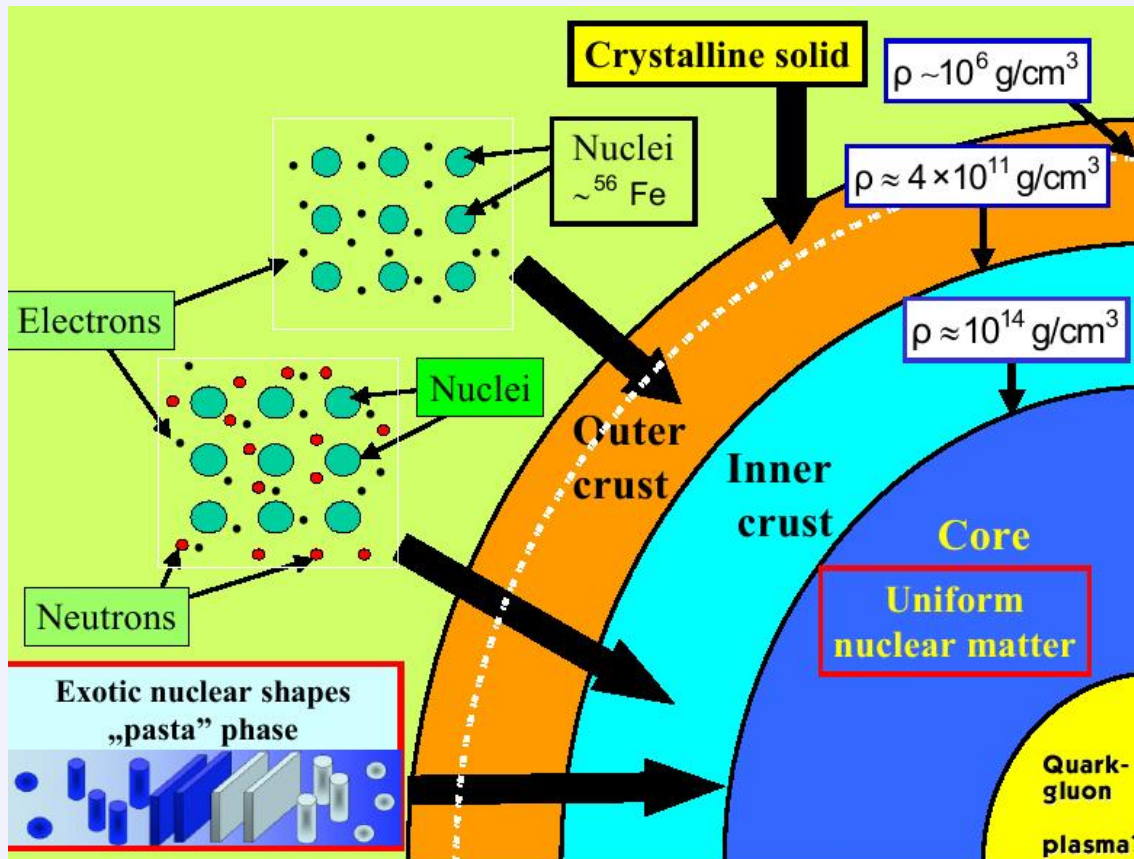
- Quark droplets immersed in hadronic matter at $\rho \gg \rho_{nm}$
 - Buckyballs immersed in an electron gas (in liquid mercury)
 - or buckyballs in liquid ${}^3\text{He}$.

In the lab:

Applications

In the inner crust of a neutron star:

7



- nuclei lose neutrons due to increasing pressure and density: below the saturation density \Rightarrow chain of phases between 0.03 fm^{-3} and 0.1 fm^{-3} .

- liquid-drop model (interplay of Coulomb- and surface energies): nuclei \rightarrow rods \rightarrow slabs \rightarrow tubes \rightarrow bubbles \rightarrow uniform matter

(G. Baym, H.A. Bethe, C. Pethick, *N.P. A 175* ('71))

- However, the neglected “shell energy” of the outer neutrons is of the same order (keV/fm^3) !

(A. Bulgac & P. Magierski, *Nucl. Phys. A 683* ('01).)

Inside a neutron/quark star:

- Quark droplets immersed in hadronic matter at $\rho \gg \rho_{nm}$
 - Buckyballs immersed in an electron gas (in liquid mercury)
 - or buckyballs in liquid ${}^3\text{He}$.
 - Bose-Einstein *droplets* in diluted **atomic Fermi-condensates**.

In the lab:

- Casimir energy for fermions between two impenetrable (parallel) planes at distance L :

$$\mathcal{E}_C = \mu F(k_F L) \quad \text{with} \quad \mu = \hbar^2 k_F^2 / 2m \quad \text{as natural scale .}$$

- Casimir energy for fermions between two impenetrable (parallel) planes at distance L :

$$\mathcal{E}_C = \mu F(k_F L) \quad \text{with} \quad \mu = \hbar^2 k_F^2 / 2m \quad \text{as natural scale .}$$

- More complicated geometries → demanding calculations, in general

- Casimir energy for fermions between two impenetrable (parallel) planes at distance L :

$$\mathcal{E}_C = \mu F(k_F L) \quad \text{with} \quad \mu = \hbar^2 k_F^2 / 2m \quad \text{as natural scale .}$$

- More complicated geometries → demanding calculations, in general
- However, case of immersed non-overlapping *spherical* voids still relatively simple:
 - *Krein (1953) trace-formula* : level density $\delta\rho(E) \leftrightarrow$ phase shift $\frac{1}{2i} \ln \det S_n(E)$

Calculation

- Casimir energy for fermions between two impenetrable (parallel) planes at distance L :

$$\mathcal{E}_C = \mu F(k_F L) \quad \text{with} \quad \mu = \hbar^2 k_F^2 / 2m \quad \text{as natural scale .}$$

- More complicated geometries → demanding calculations, in general
- However, case of immersed non-overlapping *spherical* voids still relatively simple:
 - *Krein (1953) trace-formula* : level density $\delta\rho(E) \leftrightarrow$ phase shift $\frac{1}{2i} \ln \det S_n(E)$

$$\delta\rho(E) = \bar{\rho}(E) - \bar{\rho}_0(E) = \frac{1}{2\pi i} \frac{d}{dE} \text{tr} \ln S_n(E) \quad \text{of the } n\text{-sphere S-matrix}$$

Calculation

- Casimir energy for fermions between two impenetrable (parallel) planes at distance L :

$$\mathcal{E}_C = \mu F(k_F L) \quad \text{with} \quad \mu = \hbar^2 k_F^2 / 2m \quad \text{as natural scale .}$$

- More complicated geometries → demanding calculations, in general
- However, case of immersed non-overlapping *spherical* voids still relatively simple:

- *Krein (1953) trace-formula* : level density $\delta\rho(E) \leftrightarrow$ phase shift $\frac{1}{2i} \ln \det S_n(E)$

$$\delta\rho(E) = \bar{\rho}(E) - \bar{\rho}_0(E) = \frac{1}{2\pi i} \frac{d}{dE} \text{tr} \ln S_n(E) \quad \text{of the } n\text{-sphere S-matrix}$$

- Extract *geometry-dependent* Casimir fluctuations from *multiple*-scattering part

Calculation

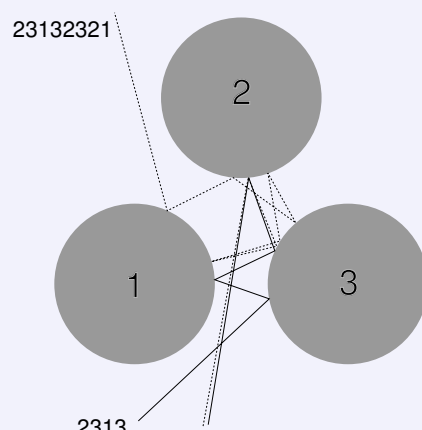
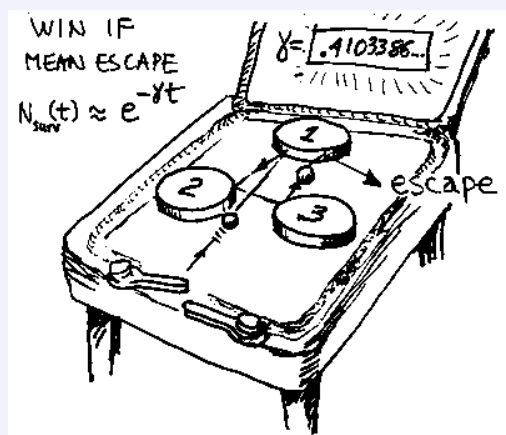
- Casimir energy for fermions between two impenetrable (parallel) planes at distance L :

$$\mathcal{E}_C = \mu F(k_F L) \quad \text{with} \quad \mu = \hbar^2 k_F^2 / 2m \quad \text{as natural scale .}$$

- More complicated geometries → demanding calculations, in general
- However, case of immersed non-overlapping *spherical* voids still relatively simple:
 - *Krein (1953) trace-formula* : level density $\delta\rho(E) \leftrightarrow$ phase shift $\frac{1}{2i} \ln \det S_n(E)$

$$\delta\rho(E) = \bar{\rho}(E) - \bar{\rho}_0(E) = \frac{1}{2\pi i} \frac{d}{dE} \text{tr} \ln S_n(E) \quad \text{of the } n\text{-sphere S-matrix}$$

- Extract *geometry-dependent* Casimir fluctuations from *multiple*-scattering part
 ⇒ Calculation mapped onto a quantum mechanical *billiard* problem:
hyperbolic point-particle scattering off n spheres or *n disks*



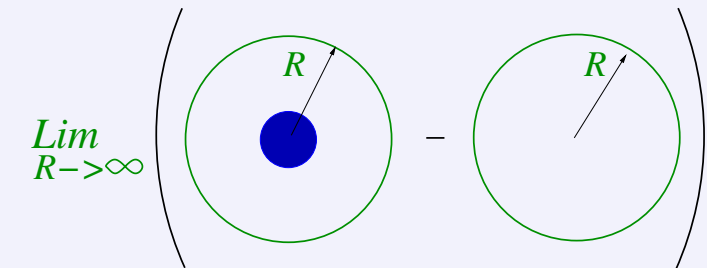
References:

- B. Eckhardt, *J. Phys.* **A20** (1987);
 P. Gaspard & S. Rice, *J. Chem. Phys.* **90** (1989);
 P. Cvitanović & B. Eckhardt, *Phys. Rev. Lett.* **63** (1989);
 M. Henseler, A. Wirzba & T. Guhr, *Ann. Phys.* **258** (1997).

Digression: E.Beth & G.E. Uhlenbeck (1937)

predecessor of *Krein (1962)* formula for *spherical* potential:

Idea: *spherical scattering box minus empty reference box*:



Asymptotically:

$$u_{k\ell}(r) \sim \sin(kr - \frac{1}{2}\ell\pi + \eta_\ell(k))$$

$$u_{k\ell}^{(0)}(r) \sim \sin(kr - \frac{1}{2}\ell\pi)$$

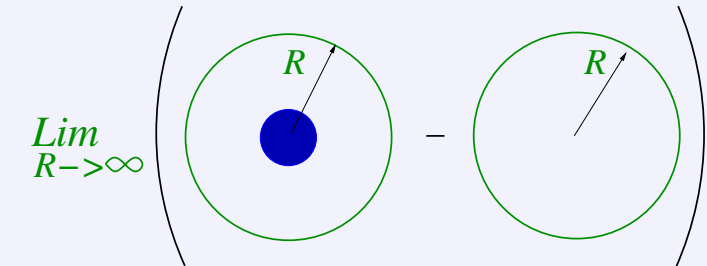
Digression: E.Beth & G.E. Uhlenbeck (1937)

predecessor of *Krein (1962)* formula for *spherical* potential:

Idea: *spherical scattering box minus empty reference box*:

Asymptotically:

$$\begin{aligned} u_{k\ell}(r) &\sim \sin(kr - \frac{1}{2}\ell\pi + \eta_\ell(k)) \\ u_{k\ell}^{(0)}(r) &\sim \sin(kr - \frac{1}{2}\ell\pi) \end{aligned}$$



and Dirichlet b.c.'s:

$$u_{k\ell}(R) = u_{k\ell}^{(0)}(R) = 0.$$

EV conditions ((2ℓ+1)-fold degenerate):

$$\Rightarrow \begin{aligned} k_{\ell,n}R - \frac{1}{2}\ell\pi + \eta_\ell(k_{\ell,n}) &= \pi n, \quad n=0,1,2,\dots && \text{(with potential)} \\ k_{\ell,n}^{(0)}R - \frac{1}{2}\ell\pi &= \pi n, \quad n=0,1,2,\dots && \text{(without potential)} \end{aligned}$$

A change of the radial quantum number n by one unit, for fixed angular momentum ℓ , implies

$$\Delta k_\ell \left(R + \frac{\partial}{\partial k} \eta_\ell(k) \right) = \pi = \Delta k_\ell^{(0)} R,$$

such that the conditions $\bar{\rho}_\ell(k)\Delta k_\ell = \bar{\rho}_\ell^{(0)}(k)\Delta k_\ell^{(0)} = 2\ell + 1$ (note the averaging !)

induce the formula

$$\bar{\rho}_\ell(k) - \bar{\rho}_\ell^{(0)}(k) = \frac{2\ell+1}{\pi} \frac{\partial}{\partial k} \eta_\ell(k) \quad \text{(independently of } R\text{)}$$

Digression 2: Semiclassical interpretation of Krein formula

Digression 2: Semiclassical interpretation of Krein formula

Determinant of scattering matrix is semiclassically a sum over periodic orbits (+Weyl terms)

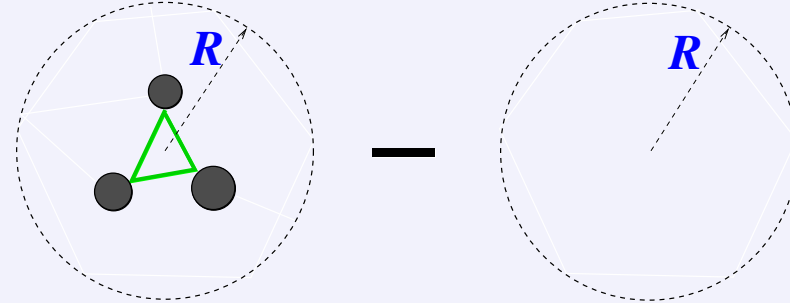


$$\frac{1}{2\pi} \text{Im} \left. \frac{d}{dk} \ln \det \mathbf{S}^{(n)}(k) \right|_{k \text{ real}}$$

Digression 2: Semiclassical interpretation of Krein formula

Determinant of scattering matrix is semiclassically a sum over periodic orbits (+Weyl terms)

Consider the difference of the densities of states of two *bounded reference systems*:

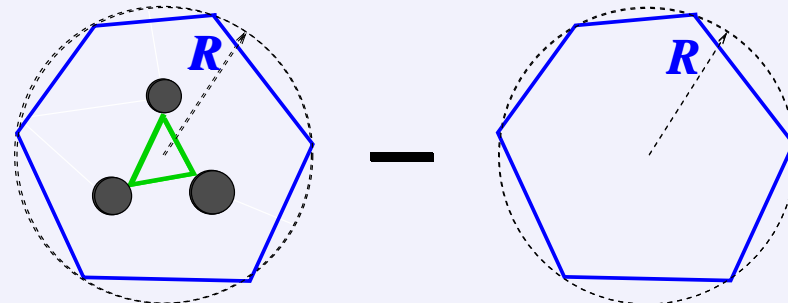


$$\begin{aligned} & \left\{ \rho^{(n)}(k ; \mathbf{R}) - \rho^{(0)}(k ; \mathbf{R}) \right\} \\ &= \frac{1}{2\pi} \text{Im} \left. \frac{d}{dk} \ln \det \mathbf{S}^{(n)}(k) \right|_{k \text{ real}} \end{aligned}$$

Digression 2: Semiclassical interpretation of Krein formula

Determinant of scattering matrix is semiclassically a sum over periodic orbits (+Weyl terms)

Consider the difference of the densities of states of two *bounded reference systems*:



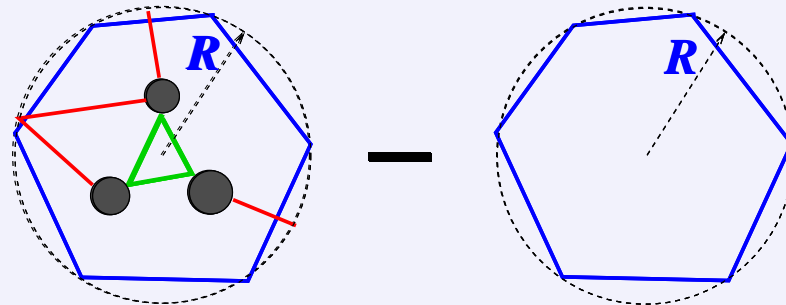
- The *container-induced* periodic orbits cancel!

$$\begin{aligned} & \left\{ \rho^{(n)}(k ; \mathbf{R}) - \rho^{(0)}(k ; \mathbf{R}) \right\} \\ &= \frac{1}{2\pi} \text{Im} \left. \frac{d}{dk} \ln \det \mathbf{S}^{(n)}(k) \right|_{k \text{ real}} \end{aligned}$$

Digression 2: Semiclassical interpretation of Krein formula

Determinant of scattering matrix is semiclassically a sum over periodic orbits (+Weyl terms)

Consider the difference of the densities of states of two *bounded reference systems*:



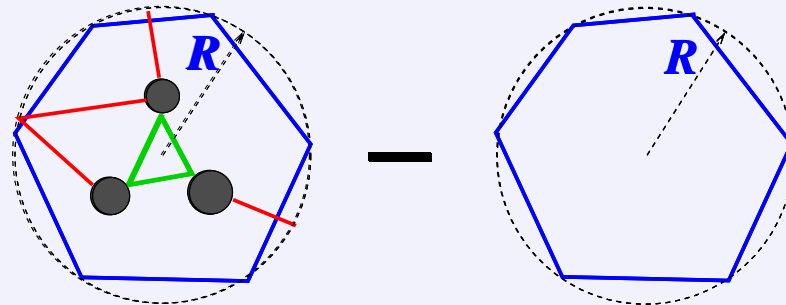
- The *container-induced periodic orbits* cancel!
- However, \exists further *spurious periodic orbits* whose lengths grow with increasing R .

$$\begin{aligned} \lim_{R \rightarrow \infty} & \left\{ \rho^{(n)}(k \quad ; R) - \rho^{(0)}(k \quad ; R) \right\} \\ &= \frac{1}{2\pi} \text{Im} \left. \frac{d}{dk} \ln \det \mathbf{S}^{(n)}(k) \right|_{k \text{ real}} \end{aligned}$$

Digression 2: Semiclassical interpretation of Krein formula

Determinant of scattering matrix is semiclassically a sum over periodic orbits (+Weyl terms)

Consider the difference of the densities of states of two *bounded reference systems*:



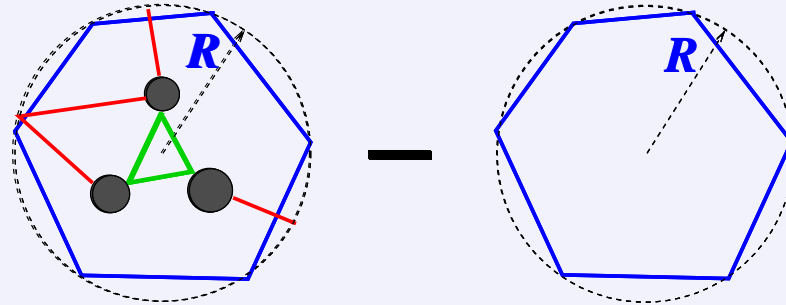
- The *container-induced* periodic orbits cancel!
- However, \exists further *spurious periodic orbits* whose lengths grow with increasing R .
- Removal of long orbits by exponential damping or averaging:

$$\begin{aligned} \lim_{\epsilon \rightarrow 0+} \lim_{R \rightarrow \infty} & \left\{ \rho^{(n)}(k + i\epsilon; R) - \rho^{(0)}(k + i\epsilon; R) \right\} \\ &= \frac{1}{2\pi} \text{Im} \left. \frac{d}{dk} \ln \det \mathbf{S}^{(n)}(k) \right|_{k \text{ real}} \end{aligned}$$

Digression 2: Semiclassical interpretation of Krein formula

Determinant of scattering matrix is semiclassically a sum over periodic orbits (+Weyl terms)

Consider the difference of the densities of states of two *bounded reference systems*:



- The *container-induced* periodic orbits cancel!
- However, \exists further *spurious periodic orbits* whose lengths grow with increasing R .
- Removal of long orbits by exponential damping or averaging:

$$\lim_{\epsilon \rightarrow 0^+} \lim_{R \rightarrow \infty} \left\{ \rho^{(n)}(k + i\epsilon; R) - \rho^{(0)}(k + i\epsilon; R) \right\}$$

$$= \frac{1}{2\pi} \text{Im} \left. \frac{d}{dk} \ln \det \mathbf{S}^{(n)}(k) \right|_{k \text{ real}}$$

Note the order of the limits!

Digression 3: Casimir energy in fermionic background

chem. potential $\mu = \hbar^2 k_F^2 / 2m$ or Fermi momentum k_F *natural UV-cutoff* ($\Lambda_{UV} = \mu$ or $k_{UV} = k_F$)

Digression 3: Casimir energy in fermionic background

chem. potential $\mu = \hbar^2 k_F^2 / 2m$ or Fermi momentum k_F *natural UV-cutoff* ($\Lambda_{UV} = \mu$ or $k_{UV} = k_F$)

Casimir energy at *fixed* total number of fermions \mathcal{N} :

Digression 3: Casimir energy in fermionic background

chem. potential $\mu = \hbar^2 k_F^2 / 2m$ or Fermi momentum k_F *natural UV-cutoff* ($\Lambda_{UV} = \mu$ or $k_{UV} = k_F$)

Casimir energy at *fixed* total number of fermions \mathcal{N} :

⇒ chem. potentials μ & μ_0 at *finite* and *infinite* separation of the scatterers differ

Digression 3: Casimir energy in fermionic background

chem. potential $\mu = \hbar^2 k_F^2 / 2m$ or Fermi momentum k_F *natural UV-cutoff* ($\Lambda_{UV} = \mu$ or $k_{UV} = k_F$)

Casimir energy at *fixed* total number of fermions \mathcal{N} :

⇒ chem. potentials μ & μ_0 at *finite* and *infinite* separation of the scatterers differ:

$$\mathcal{N} = \int_0^\mu \rho(E) dE = \int_0^{\mu_0} [\rho_0(E) + \rho_W(E)] dE$$

Digression 3: Casimir energy in fermionic background

chem. potential $\mu = \hbar^2 k_F^2 / 2m$ or Fermi momentum k_F *natural UV-cutoff* ($\Lambda_{UV} = \mu$ or $k_{UV} = k_F$)

Casimir energy at *fixed* total number of fermions \mathcal{N} :

\Rightarrow chem. potentials μ & μ_0 at *finite* and *infinite* separation of the scatterers differ:

$$\begin{aligned}\mathcal{N} &= \int_0^\mu \rho(E) dE = \int_0^{\mu_0} [\rho_0(E) + \rho_W(E)] dE \\ \Rightarrow \quad \int_{\mu_0}^\mu \rho(E) dE &= - \int_0^{\mu_0} \underbrace{[\rho(E) - \rho_0(E) - \rho_W(E)]}_{\rho_C(E) = \frac{d}{dE} \mathcal{N}_C(E)} dE\end{aligned}$$

Digression 3: Casimir energy in fermionic background

chem. potential $\mu = \hbar^2 k_F^2 / 2m$ or Fermi momentum k_F *natural UV-cutoff* ($\Lambda_{UV} = \mu$ or $k_{UV} = k_F$)

Casimir energy at *fixed* total number of fermions \mathcal{N} :

\Rightarrow chem. potentials μ & μ_0 at *finite* and *infinite* separation of the scatterers differ:

$$\begin{aligned}\mathcal{N} &= \int_0^\mu \rho(E) dE = \int_0^{\mu_0} [\rho_0(E) + \rho_W(E)] dE \\ \Rightarrow \quad \int_{\mu_0}^\mu \rho(E) dE &= - \int_0^{\mu_0} \underbrace{[\rho(E) - \rho_0(E) - \rho_W(E)]}_{\rho_C(E) = \frac{d}{dE} \mathcal{N}_C(E)} dE \\ \mathcal{E}_C|_{\mathcal{N}} &= \int_0^\mu E \rho(E) dE - \int_0^{\mu_0} E [\rho_0(E) + \rho_W(E)] dE\end{aligned}$$

Digression 3: Casimir energy in fermionic background

chem. potential $\mu = \hbar^2 k_F^2 / 2m$ or Fermi momentum k_F *natural UV-cutoff* ($\Lambda_{UV} = \mu$ or $k_{UV} = k_F$)

Casimir energy at *fixed* total number of fermions \mathcal{N} :

\Rightarrow chem. potentials μ & μ_0 at *finite* and *infinite* separation of the scatterers differ:

$$\begin{aligned}\mathcal{N} &= \int_0^\mu \rho(E) dE = \int_0^{\mu_0} [\rho_0(E) + \rho_W(E)] dE \\ \Rightarrow \quad \int_{\mu_0}^\mu \rho(E) dE &= - \int_0^{\mu_0} \underbrace{[\rho(E) - \rho_0(E) - \rho_W(E)]}_{\rho_C(E) = \frac{d}{dE} \mathcal{N}_C(E)} dE \\ \mathcal{E}_C|_{\mathcal{N}} &= \int_0^\mu E \rho(E) dE - \int_0^{\mu_0} E [\rho_0(E) + \rho_W(E)] dE \\ &= \int_0^{\mu_0} E \rho_C(E) dE + \mu_0 \int_{\mu_0}^\mu \rho(E) dE + \mathcal{O}(V^{-1})\end{aligned}$$

Digression 3: Casimir energy in fermionic background

chem. potential $\mu = \hbar^2 k_F^2 / 2m$ or Fermi momentum k_F *natural UV-cutoff* ($\Lambda_{UV} = \mu$ or $k_{UV} = k_F$)

Casimir energy at *fixed* total number of fermions \mathcal{N} :

\Rightarrow chem. potentials μ & μ_0 at *finite* and *infinite* separation of the scatterers differ:

$$\begin{aligned}\mathcal{N} &= \int_0^\mu \rho(E) dE = \int_0^{\mu_0} [\rho_0(E) + \rho_W(E)] dE \\ \Rightarrow \quad \int_{\mu_0}^\mu \rho(E) dE &= - \int_0^{\mu_0} \underbrace{[\rho(E) - \rho_0(E) - \rho_W(E)]}_{\rho_C(E) = \frac{d}{dE} \mathcal{N}_C(E)} dE \\ \mathcal{E}_C|_{\mathcal{N}} &= \int_0^\mu E \rho(E) dE - \int_0^{\mu_0} E [\rho_0(E) + \rho_W(E)] dE \\ &= \int_0^{\mu_0} E \rho_C(E) dE + \mu_0 \left[\int_{\mu_0}^\mu \rho(E) dE \right] + \mathcal{O}(V^{-1}) \\ &= \int_0^{\mu_0} (E - \mu_0) \rho_C(E) dE = - \int_0^{\mu_0} \mathcal{N}_C(E) dE.\end{aligned}$$

Digression 3: Casimir energy in fermionic background

chem. potential $\mu = \hbar^2 k_F^2 / 2m$ or Fermi momentum k_F natural UV-cutoff ($\Lambda_{UV} = \mu$ or $k_{UV} = k_F$)

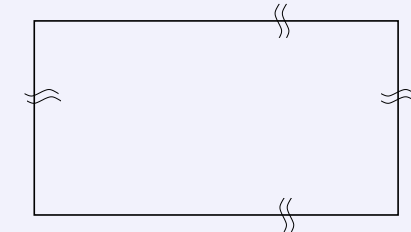
Casimir energy at *fixed* total number of fermions \mathcal{N} :

\Rightarrow chem. potentials μ & μ_0 at *finite* and *infinite* separation of the scatterers differ:

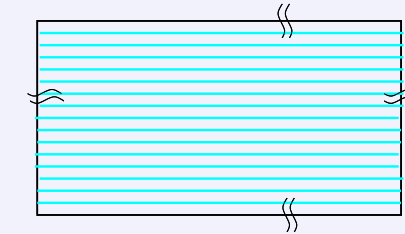
$$\begin{aligned}\mathcal{N} &= \int_0^\mu \rho(E) dE = \int_0^{\mu_0} [\rho_0(E) + \rho_W(E)] dE \\ \Rightarrow \quad \int_{\mu_0}^\mu \rho(E) dE &= - \int_0^{\mu_0} \underbrace{[\rho(E) - \rho_0(E) - \rho_W(E)]}_{\rho_C(E) = \frac{d}{dE} \mathcal{N}_C(E)} dE \\ \mathcal{E}_C|_{\mathcal{N}} &= \int_0^\mu E \rho(E) dE - \int_0^{\mu_0} E [\rho_0(E) + \rho_W(E)] dE \\ &= \int_0^{\mu_0} E \rho_C(E) dE + \mu_0 \int_{\mu_0}^\mu \rho(E) dE + \mathcal{O}(V^{-1}) \\ &= \int_0^{\mu_0} (E - \mu_0) \rho_C(E) dE = - \int_0^{\mu_0} \mathcal{N}_C(E) dE.\end{aligned}$$

Grandcanonical Casimir energy at *fixed* $\mu = \mu_0$: $\widetilde{\mathcal{E}}_C|_{\mu_0} - \mu_0 \mathcal{N}_C(\mu_0) = \mathcal{E}_C|_{\mathcal{N}} + \mathcal{O}(V^{-1})$

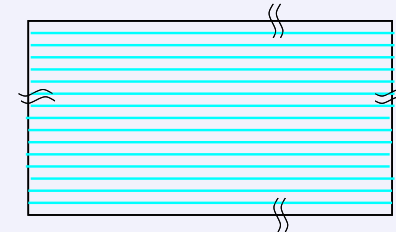
1. “infinite” container:



1. “infinite” container: $\rho(E)=\rho_0(E)$ (background field)

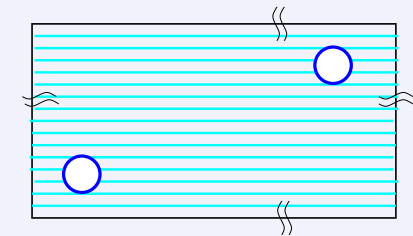


1. “*infinite*” container: $\rho(E) = \rho_0(E)$ (background field)

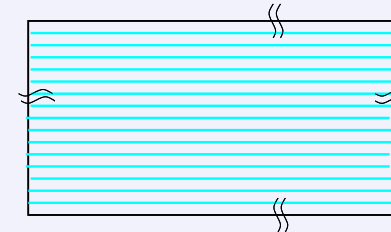


2. n bubbles (of radii a_i) “punched out” at “infinite” separation:

$$\rho(E) = \rho_0(E) + \sum_{i=1}^n \underbrace{\rho_W(E, a_i)}_{\text{Weyl-Term}} \quad (\text{note the excluded volume !})$$

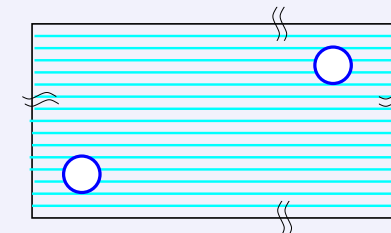


1. “*infinite*” container: $\rho(E) = \rho_0(E)$ (background field)



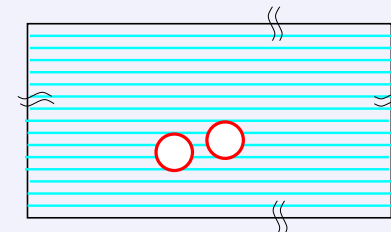
2. n bubbles (of radii a_i) “punched out” at “infinite” separation:

$$\rho(E) = \rho_0(E) + \sum_{i=1}^n \underbrace{\rho_W(E, a_i)}_{\text{Weyl-Term}} \quad (\text{note the excluded volume !})$$

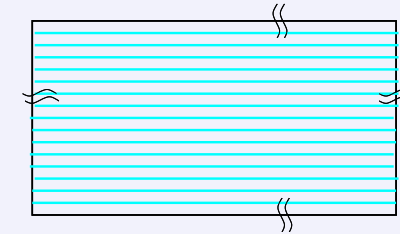


3. geometry-dependent arrangement of n bubbles:

$$\rho(E) = \rho_0(E) + \sum_{i=1}^n \rho_W(E, a_i) + \delta\rho_C(E, \{a_i\}, \{\mathbf{r}_{ij}\})$$

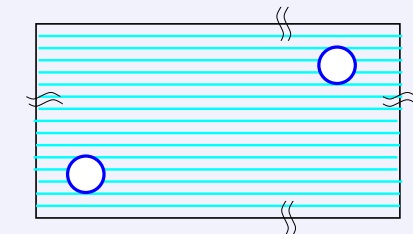


1. “*infinite*” container: $\rho(E) = \rho_0(E)$ (background field)



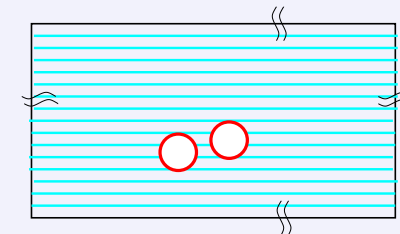
2. n bubbles (of radii a_i) “punched out” at “infinite” separation:

$$\rho(E) = \rho_0(E) + \sum_{i=1}^n \underbrace{\rho_W(E, a_i)}_{\text{Weyl-Term}} \quad (\text{note the excluded volume !})$$



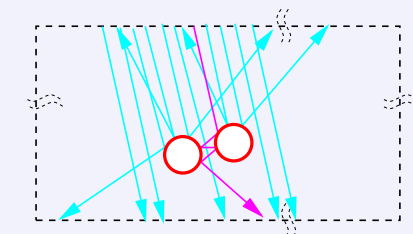
3. geometry-dependent arrangement of n bubbles:

$$\rho(E) = \rho_0(E) + \sum_{i=1}^n \rho_W(E, a_i) + \delta\rho_C(E, \{a_i\}, \{\mathbf{r}_{ij}\})$$

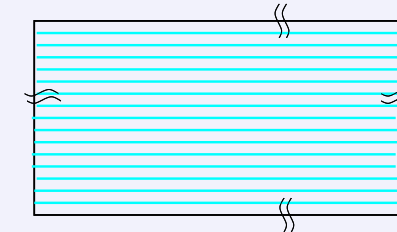


4. Krein trace formula (note the averaging):

$$\delta\rho(E) = \bar{\rho}(E) - \bar{\rho}_0(E) = \frac{1}{2\pi i} \frac{d}{dE} \overbrace{\ln \det S_n(E)}^{2i\eta_n(E)}$$

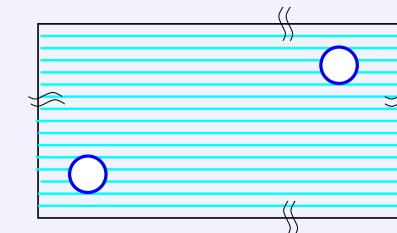


1. “*infinite*” container: $\rho(E) = \rho_0(E)$ (background field)



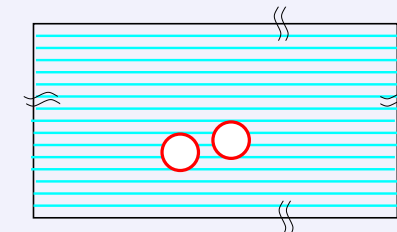
2. n bubbles (of radii a_i) “punched out” at “infinite” separation:

$$\rho(E) = \rho_0(E) + \sum_{i=1}^n \underbrace{\rho_W(E, a_i)}_{\text{Weyl-Term}} \quad (\text{note the excluded volume !})$$



3. geometry-dependent arrangement of n bubbles:

$$\rho(E) = \rho_0(E) + \sum_{i=1}^n \rho_W(E, a_i) + \delta\rho_C(E, \{a_i\}, \{\mathbf{r}_{ij}\})$$



4. Krein trace formula (note the averaging):

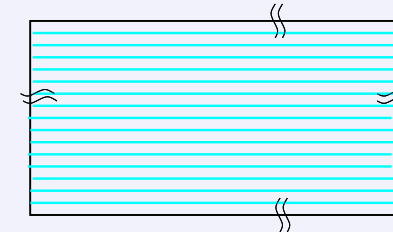
$$\delta\rho(E) = \bar{\rho}(E) - \bar{\rho}_0(E) = \frac{1}{2\pi i} \frac{d}{dE} \overbrace{\ln \det S_n(E)}^{2i\eta_n(E)}$$

5. *Multiple scattering matrix*

$$\overbrace{\det S_n(E)} = \prod_i \det S_1(E, a_i) \frac{\det \mathbf{M}^\dagger(k^*)}{\det \mathbf{M}(k)}$$

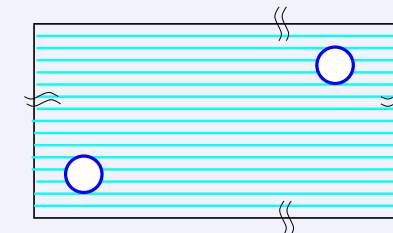
see A.W., *Phys. Rep.* **309** (1999)

1. “*infinite*” container: $\rho(E) = \rho_0(E)$ (background field)



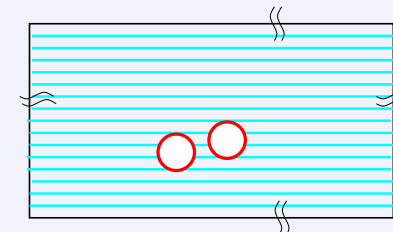
2. n bubbles (of radii a_i) “punched out” at “infinite” separation:

$$\rho(E) = \rho_0(E) + \sum_{i=1}^n \underbrace{\rho_W(E, a_i)}_{\text{Weyl-Term}} \quad (\text{note the excluded volume !})$$



3. geometry-dependent arrangement of n bubbles:

$$\rho(E) = \rho_0(E) + \sum_{i=1}^n \rho_W(E, a_i) + \delta\rho_C(E, \{a_i\}, \{\mathbf{r}_{ij}\})$$



4. Krein trace formula (note the averaging):

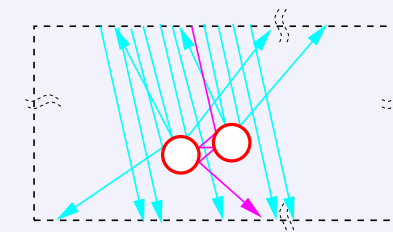
$$\delta\rho(E) = \bar{\rho}(E) - \bar{\rho}_0(E) = \frac{1}{2\pi i} \frac{d}{dE} \overbrace{\ln \det S_n(E)}^{2i\eta_n(E)}$$

5. *Multiple scattering matrix*

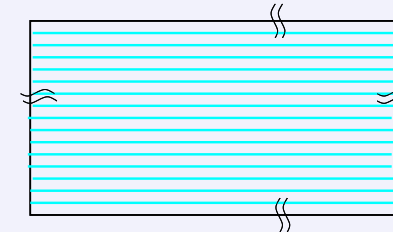
$$\rightarrow \delta\bar{\rho}_C(E, \{a_i\}, \{\mathbf{r}_{ij}\}) = -\frac{1}{\pi} \text{Im} \left(\frac{d}{dE} \ln \det \mathbf{M}(k(E)) \right)$$

$$\overbrace{\det S_n(E)}^{\text{det } S_n(E)} = \prod_i \det \mathbf{S}_1(E, a_i) \frac{\det \mathbf{M}^\dagger(k^*)}{\det \mathbf{M}(k)}$$

see A.W., *Phys. Rep.* **309** (1999)

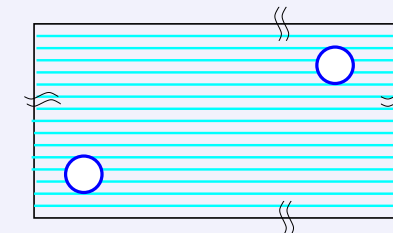


1. “*infinite*” container: $\rho(E) = \rho_0(E)$ (background field)



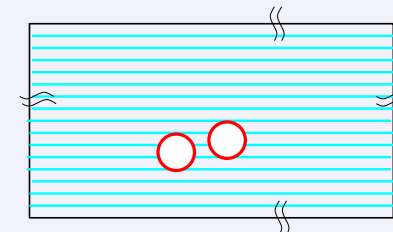
2. n bubbles (of radii a_i) “punched out” at “infinite” separation:

$$\rho(E) = \rho_0(E) + \sum_{i=1}^n \underbrace{\rho_W(E, a_i)}_{\text{Weyl-Term}} \quad (\text{note the excluded volume !})$$



3. geometry-dependent arrangement of n bubbles:

$$\rho(E) = \rho_0(E) + \sum_{i=1}^n \rho_W(E, a_i) + \delta\rho_C(E, \{a_i\}, \{\mathbf{r}_{ij}\})$$



4. Krein trace formula (note the averaging):

$$\delta\rho(E) = \bar{\rho}(E) - \bar{\rho}_0(E) = \frac{1}{2\pi i} \overbrace{\frac{d}{dE} \ln \det S_n(E)}^{2i\eta_n(E)}$$

5. *Multiple scattering matrix*

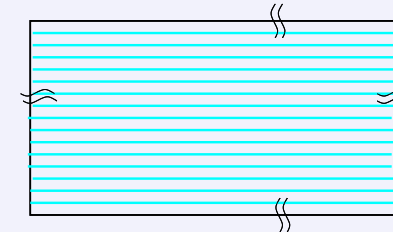
$$\rightarrow \delta\bar{\rho}_C(E, \{a_i\}, \{\mathbf{r}_{ij}\}) = -\frac{1}{\pi} \text{Im} \left(\frac{d}{dE} \ln \det \mathbf{M}(k(E)) \right)$$

$$\overbrace{\det S_n(E)}^{\text{det } S_n(E)} = \prod_i \det \mathbf{S}_1(E, a_i) \frac{\det \mathbf{M}^\dagger(k^*)}{\det \mathbf{M}(k)}$$

see A.W., *Phys. Rep.* **309** (1999)

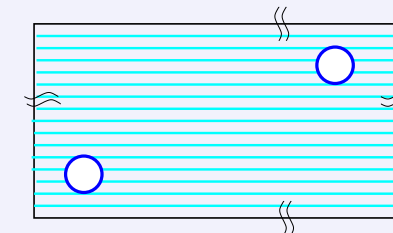
All determinants exist (although the relevant scattering matrices are infinite dimensional)
since the associated T -matrices are trace-class.

1. “*infinite*” container: $\rho(E) = \rho_0(E)$ (background field)



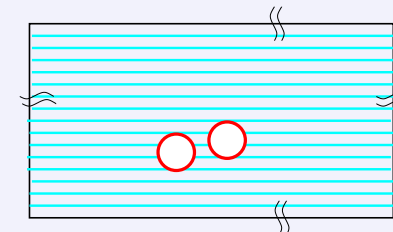
2. n bubbles (of radii a_i) “punched out” at “infinite” separation:

$$\rho(E) = \rho_0(E) + \sum_{i=1}^n \underbrace{\rho_W(E, a_i)}_{\text{Weyl-Term}} \quad (\text{note the excluded volume !})$$



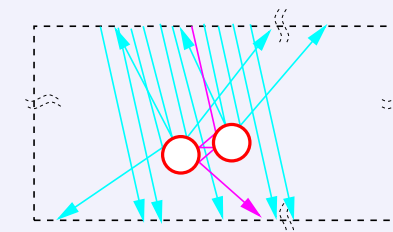
3. geometry-dependent arrangement of n bubbles:

$$\rho(E) = \rho_0(E) + \sum_{i=1}^n \rho_W(E, a_i) + \delta\rho_C(E, \{a_i\}, \{\mathbf{r}_{ij}\})$$



4. Krein trace formula (note the averaging):

$$\delta\rho(E) = \bar{\rho}(E) - \bar{\rho}_0(E) = \frac{1}{2\pi i} \frac{d}{dE} \overbrace{\ln \det S_n(E)}^{2i\eta_n(E)}$$



5. **Multiple scattering matrix**

$$\rightarrow \delta\bar{\rho}_C(E, \{a_i\}, \{\mathbf{r}_{ij}\}) = -\frac{1}{\pi} \text{Im} \left(\frac{d}{dE} \ln \det \mathbf{M}(k(E)) \right)$$

$$\overbrace{\det S_n(E)}^{\text{det } S_n(E)} = \prod_i \det S_1(E, a_i) \frac{\det \mathbf{M}^\dagger(k^*)}{\det \mathbf{M}(k)}$$

see A.W., *Phys. Rep.* **309** (1999)

6. Casimir energy:

$$\therefore \mathcal{E}_C = \int_0^\mu dE (E - \mu) \delta\bar{\rho}_C = - \int_0^\mu dE \overline{\mathcal{N}}_C$$

Multi-scattering matrix for n spheres of radii a_j and distances $r_{jj'}$ ($j, j' = 1, 2, \dots, n$)

$$\begin{aligned}
M_{lm, l'm'}^{jj'} &= \delta^{jj'} \delta_{ll'} \delta_{mm'} + (1 - \delta^{jj'}) i^{2m+l'-l} \sqrt{4\pi(2l+1)(2l'+1)} \left(\frac{a_j}{a_{j'}} \right)^2 \frac{j_l(ka_j)}{h_{l'}^{(1)}(ka_{j'})} \\
&\times \sum_{\tilde{l}=0}^{\infty} \sum_{\tilde{m}=-l'}^{l'} \sqrt{2\tilde{l}+1} i^{\tilde{l}} \begin{pmatrix} \tilde{l} & l' & l \\ 0 & 0 & 0 \end{pmatrix} \begin{pmatrix} \tilde{l} & l' & l \\ m-\tilde{m} & \tilde{m} & -m \end{pmatrix} D_{m', \tilde{m}}^{l'}(j, j') h_{\tilde{l}}^{(1)}(kr_{jj'}) Y_{\tilde{l}}^{m-\tilde{m}}(\hat{r}_{jj'}^{(j)})
\end{aligned}$$

M. Henseler, A. Wirzba & T. Guhr, *Ann. Phys.* **258** (1997) 286.

Multi-scattering matrix for n spheres of radii a_j and distances $r_{jj'}$ ($j, j' = 1, 2, \dots, n$)

$$M_{lm, l'm'}^{jj'} = \delta^{jj'} \delta_{ll'} \delta_{mm'} + (1 - \delta^{jj'}) i^{2m+l'-l} \sqrt{4\pi(2l+1)(2l'+1)} \left(\frac{a_j}{a_{j'}} \right)^2 \frac{j_l(ka_j)}{h_{l'}^{(1)}(ka_{j'})} \\ \times \sum_{\tilde{l}=0}^{\infty} \sum_{\tilde{m}=-l'}^{l'} \sqrt{2\tilde{l}+1} i^{\tilde{l}} \begin{pmatrix} \tilde{l} & l' & l \\ 0 & 0 & 0 \end{pmatrix} \begin{pmatrix} \tilde{l} & l' & l \\ m-\tilde{m} & \tilde{m} & -m \end{pmatrix} D_{m', \tilde{m}}^{l'}(j, j') h_{\tilde{l}}^{(1)}(kr_{jj'}) Y_{\tilde{l}}^{m-\tilde{m}}(\hat{r}_{jj'}^{(j)})$$

M. Henseler, A. Wirzba & T. Guhr, *Ann. Phys.* **258** (1997) 286.

In the limit of small scatterers:

$$M^{jj'}(E) \approx \delta^{jj'} - (1 - \delta^{jj'}) \underbrace{f_j(E)}_{s\text{-wave}} \frac{\exp(ikr_{jj'})}{r_{jj'}} \quad (+ p\text{-wave})$$

Two spheres of radius a at distance r

A. Bulgac & A.W., *Phys. Rev. Lett.* **87** (2001) 120404

Multi-scattering matrix for n spheres of radii a_j and distances $r_{jj'}$ ($j, j' = 1, 2, \dots, n$)

$$\begin{aligned} M_{lm, l'm'}^{jj'} &= \delta^{jj'} \delta_{ll'} \delta_{mm'} + (1 - \delta^{jj'}) i^{2m+l'-l} \sqrt{4\pi(2l+1)(2l'+1)} \left(\frac{a_j}{a_{j'}} \right)^2 \frac{j_l(ka_j)}{h_{l'}^{(1)}(ka_{j'})} \\ &\times \sum_{\tilde{l}=0}^{\infty} \sum_{\tilde{m}=-l'}^{l'} \sqrt{2\tilde{l}+1} i^{\tilde{l}} \binom{\tilde{l}}{0} \binom{l'}{0} \binom{l}{0} \binom{\tilde{l}}{m-\tilde{m}} \binom{l'}{\tilde{m}} \binom{l}{-m} D_{m', \tilde{m}}^{l'}(j, j') h_{\tilde{l}}^{(1)}(kr_{jj'}) Y_{\tilde{l}}^{m-\tilde{m}}(\hat{r}_{jj'}^{(j)}) \end{aligned}$$

M. Henseler, A. Wirzba & T. Guhr, *Ann. Phys.* **258** (1997) 286.

In the limit of small scatterers:

$$M^{jj'}(E) \approx \delta^{jj'} - (1 - \delta^{jj'}) \underbrace{f_j(E)}_{s\text{-wave}} \frac{\exp(ikr_{jj'})}{r_{jj'}} \quad (+ p\text{-wave})$$

Two spheres of radius a at distance r



A. Bulgac & A.W., *Phys. Rev. Lett.* **87** (2001) 120404

Multi-scattering matrix for n spheres of radii a_j and distances $r_{jj'}$ ($j, j' = 1, 2, \dots, n$)

$$\begin{aligned} M_{lm, l'm'}^{jj'} &= \delta^{jj'} \delta_{ll'} \delta_{mm'} + (1 - \delta^{jj'}) i^{2m+l'-l} \sqrt{4\pi(2l+1)(2l'+1)} \left(\frac{a_j}{a_{j'}} \right)^2 \frac{j_l(ka_j)}{h_{l'}^{(1)}(ka_{j'})} \\ &\times \sum_{\tilde{l}=0}^{\infty} \sum_{\tilde{m}=-l'}^{l'} \sqrt{2\tilde{l}+1} i^{\tilde{l}} \begin{pmatrix} \tilde{l} & l' & l \\ 0 & 0 & 0 \end{pmatrix} \begin{pmatrix} \tilde{l} & l' & l \\ m-\tilde{m} & \tilde{m} & -m \end{pmatrix} D_{m', \tilde{m}}^{l'}(j, j') h_{\tilde{l}}^{(1)}(kr_{jj'}) Y_{\tilde{l}}^{m-\tilde{m}}(\hat{r}_{jj'}^{(j)}) \end{aligned}$$

M. Henseler, A. Wirzba & T. Guhr, *Ann. Phys.* **258** (1997) 286.

In the limit of small scatterers:

$$M^{jj'}(E) \approx \delta^{jj'} - (1 - \delta^{jj'}) \underbrace{f_j(E)}_{s\text{-wave}} \frac{\exp(ikr_{jj'})}{r_{jj'}} \quad (+ p\text{-wave})$$

Two spheres of radius a at distance r



in the *small-scatterer* limit:

A. Bulgac & A.W., *Phys. Rev. Lett.* **87** (2001) 120404

Multi-scattering matrix for n spheres of radii a_j and distances $r_{jj'}$ ($j, j' = 1, 2, \dots, n$)

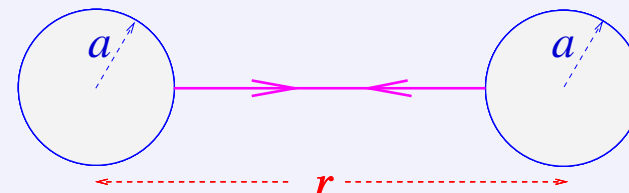
$$\begin{aligned} M_{lm, l'm'}^{jj'} &= \delta^{jj'} \delta_{ll'} \delta_{mm'} + (1 - \delta^{jj'}) i^{2m+l'-l} \sqrt{4\pi(2l+1)(2l'+1)} \left(\frac{a_j}{a_{j'}} \right)^2 \frac{j_l(ka_j)}{h_{l'}^{(1)}(ka_{j'})} \\ &\times \sum_{\tilde{l}=0}^{\infty} \sum_{\tilde{m}=-l'}^{l'} \sqrt{2\tilde{l}+1} i^{\tilde{l}} \begin{pmatrix} \tilde{l} & l' & l \\ 0 & 0 & 0 \end{pmatrix} \begin{pmatrix} \tilde{l} & l' & l \\ m-\tilde{m} & \tilde{m} & -m \end{pmatrix} D_{m', \tilde{m}}^{l'}(j, j') h_{\tilde{l}}^{(1)}(kr_{jj'}) Y_{\tilde{l}}^{m-\tilde{m}}(\hat{r}_{jj'}^{(j)}) \end{aligned}$$

M. Henseler, A. Wirzba & T. Guhr, *Ann. Phys.* **258** (1997) 286.

In the limit of small scatterers:

$$M^{jj'}(E) \approx \delta^{jj'} - (1 - \delta^{jj'}) \underbrace{f_j(E)}_{s\text{-wave}} \frac{\exp(ik\mathbf{r}_{jj'})}{r_{jj'}} \quad (+ p\text{-wave})$$

Two spheres of radius a at distance r



in the *small-scatterer* limit:

$$\mathcal{N}_C^{\text{oo}}(E) = -\frac{1}{\pi} \text{Im} \ln \det M^{\text{oo}}(E) \approx \nu_{\text{deg}} \frac{a^2}{\pi r^2} \sin[2(r-a)k] + \mathcal{O}((ka)^3),$$

A. Bulgac & A.W., *Phys. Rev. Lett.* **87** (2001) 120404

Multi-scattering matrix for n spheres of radii a_j and distances $r_{jj'}$ ($j, j' = 1, 2, \dots, n$)

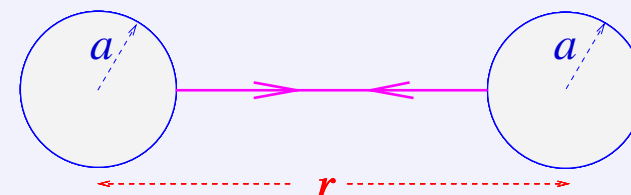
$$\begin{aligned} M_{lm, l'm'}^{jj'} &= \delta^{jj'} \delta_{ll'} \delta_{mm'} + (1 - \delta^{jj'}) i^{2m+l'-l} \sqrt{4\pi(2l+1)(2l'+1)} \left(\frac{a_j}{a_{j'}} \right)^2 \frac{j_l(ka_j)}{h_{l'}^{(1)}(ka_{j'})} \\ &\times \sum_{\tilde{l}=0}^{\infty} \sum_{\tilde{m}=-l'}^{l'} \sqrt{2\tilde{l}+1} i^{\tilde{l}} \binom{\tilde{l}}{0} \binom{l'}{0} \binom{l}{0} \binom{\tilde{l}}{m-\tilde{m}} \binom{l'}{\tilde{m}} \binom{l}{-m} D_{m', \tilde{m}}^{l'}(j, j') h_{\tilde{l}}^{(1)}(kr_{jj'}) Y_{\tilde{l}}^{m-\tilde{m}}(\hat{r}_{jj'}^{(j)}) \end{aligned}$$

M. Henseler, A. Wirzba & T. Guhr, *Ann. Phys.* **258** (1997) 286.

In the limit of small scatterers:

$$M^{jj'}(E) \approx \delta^{jj'} - (1 - \delta^{jj'}) \underbrace{f_j(E)}_{s\text{-wave}} \frac{\exp(ik\mathbf{r}_{jj'})}{r_{jj'}} \quad (+ p\text{-wave})$$

Two spheres of radius a at distance r



in the *small-scatterer* limit:

$$\mathcal{N}_C^{\text{oo}}(E) = -\frac{1}{\pi} \text{Im} \ln \det M^{\text{oo}}(E) \approx \nu_{\deg} \frac{a^2}{\pi r^2} \sin[2(r-a)k] + \mathcal{O}((ka)^3),$$

whereas the *semiclassical* result (for the single *two-bounce periodic orbit* with no repetitions) reads:

$$\mathcal{N}_{C,scl}^{\text{oo}}(E) = \nu_{\deg} \frac{a^2}{4\pi r(r-2a)} \underbrace{\sin[2(r-2a)k]}_{S_{po}(k)/\hbar} \quad (\text{Gutzwiller's trace formula})$$

A. Bulgac & A.W., *Phys. Rev. Lett.* **87** (2001) 120404

Two spheres:



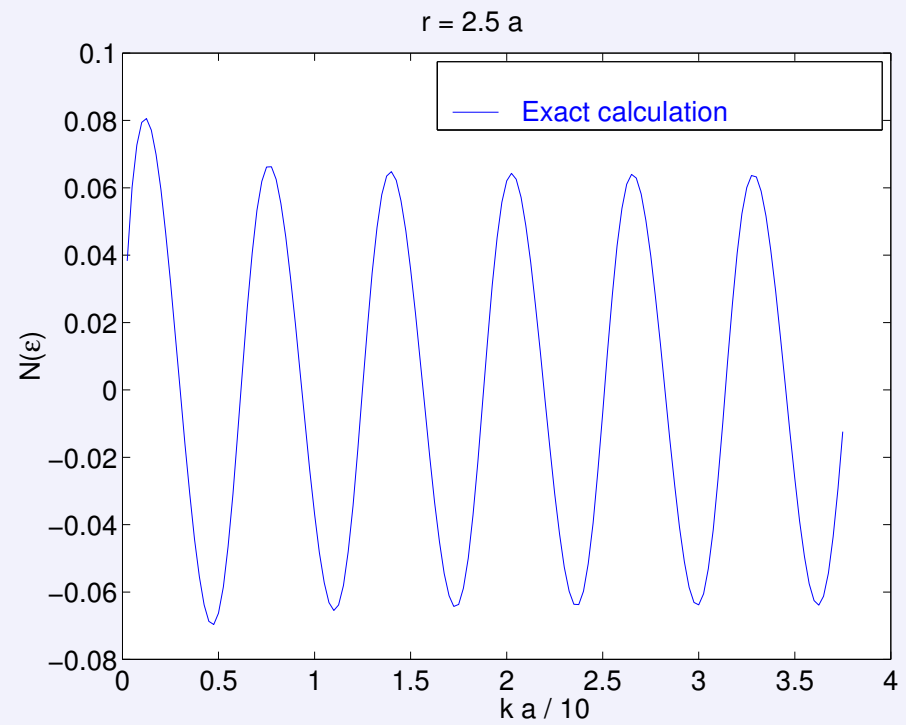
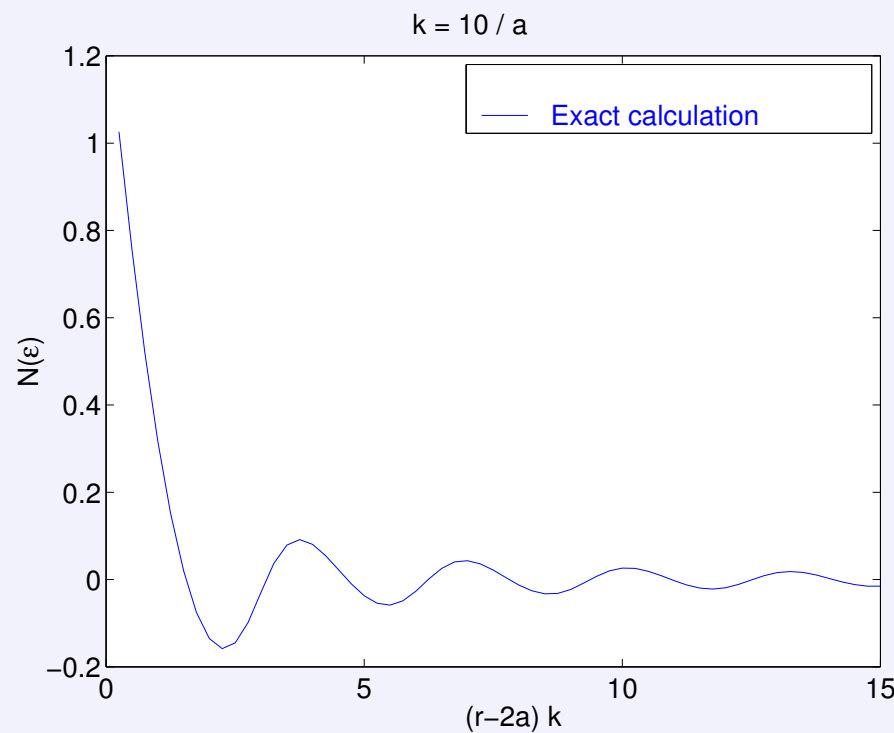
14

Two spheres:

14



$$\text{N.o.S } \mathcal{N}_C^{\text{oo}}(E) = -\frac{1}{\pi} \text{Im} \ln \det M^{\text{oo}}(E)$$

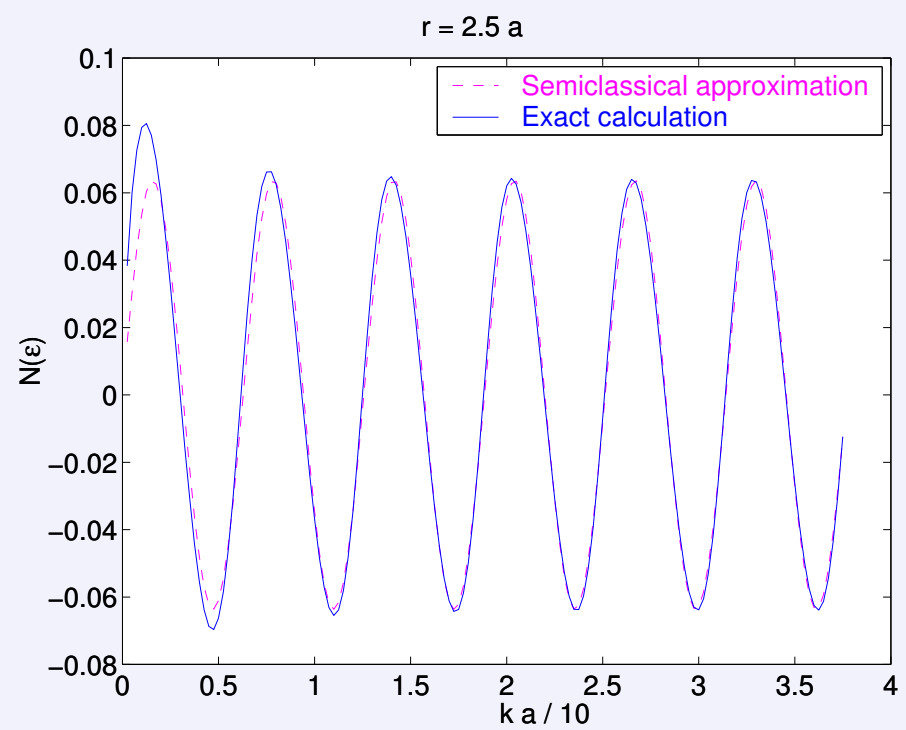
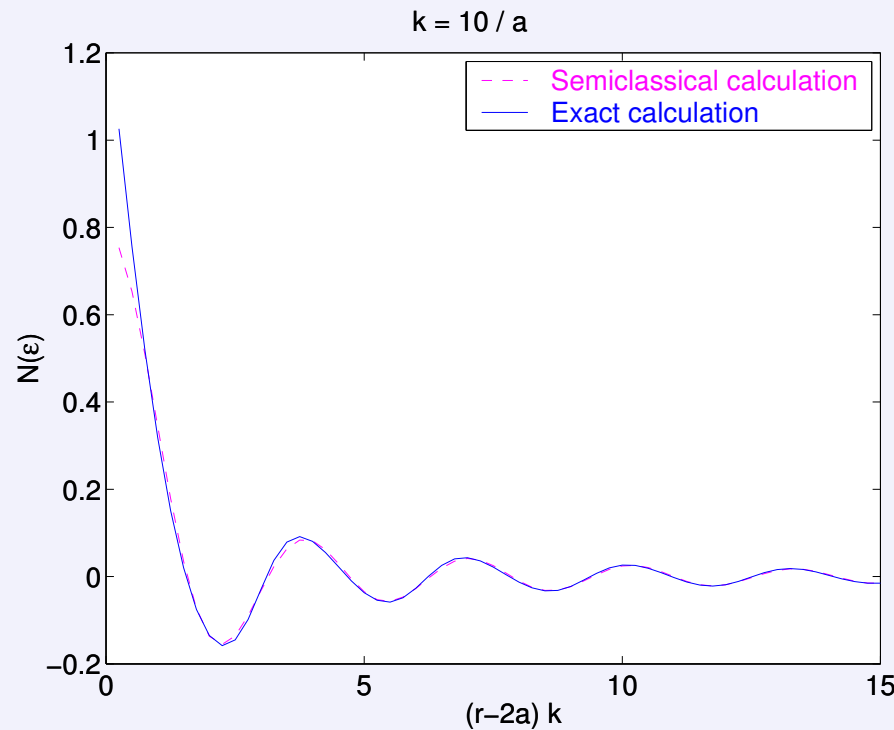


Two spheres:

14



$$\text{N.o.S } \mathcal{N}_C^{\text{oo}}(E) = -\frac{1}{\pi} \text{Im} \ln \det M^{\text{oo}}(E) \approx \frac{a^2}{4\pi r(r-2a)} \sin[2(r-2a)k]$$

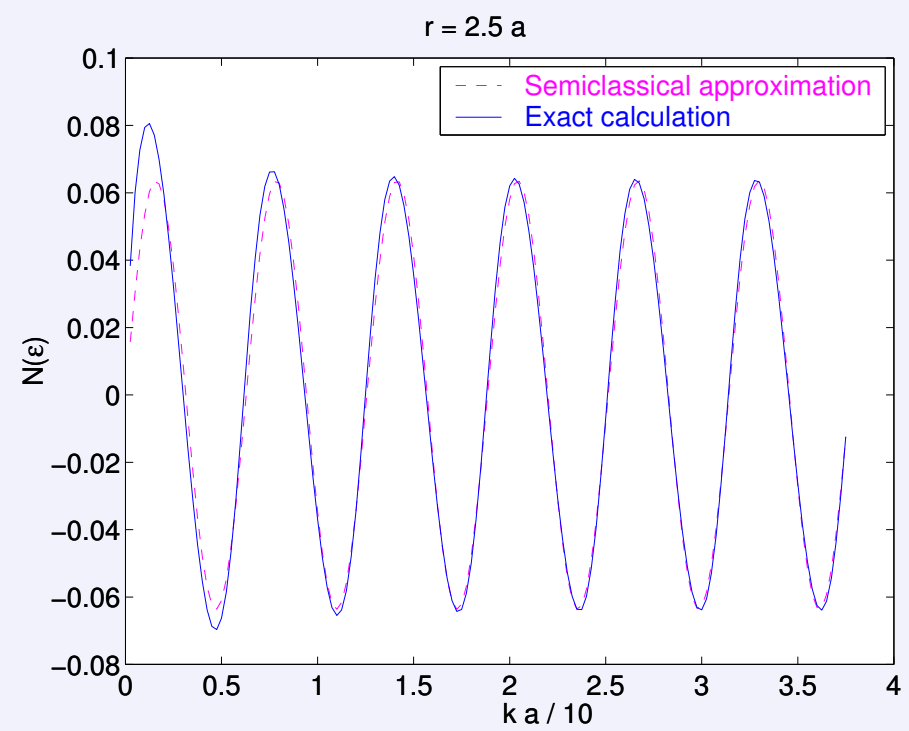
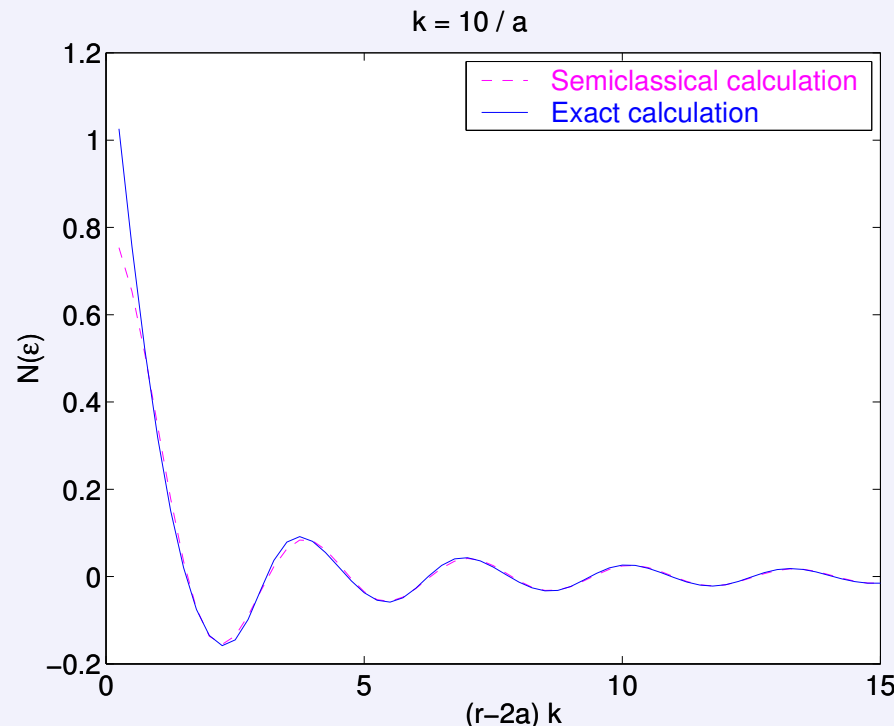


Two spheres:

14



$$\text{N.o.S } \mathcal{N}_C^{oo}(E) = -\frac{1}{\pi} \text{Im} \ln \det M^{oo}(E) \approx \frac{a^2}{4\pi r(r-2a)} \sin[2(r-2a)k]$$



$$\mathcal{E}_C^{oo} = - \int_0^{\mu(k_F)} dE \mathcal{N}_C^{oo}(E) \approx -\mu \frac{a^2}{2\pi r(r-2a)} j_1[2(r-2a)k_F] \sim \frac{a^2}{L^3}$$

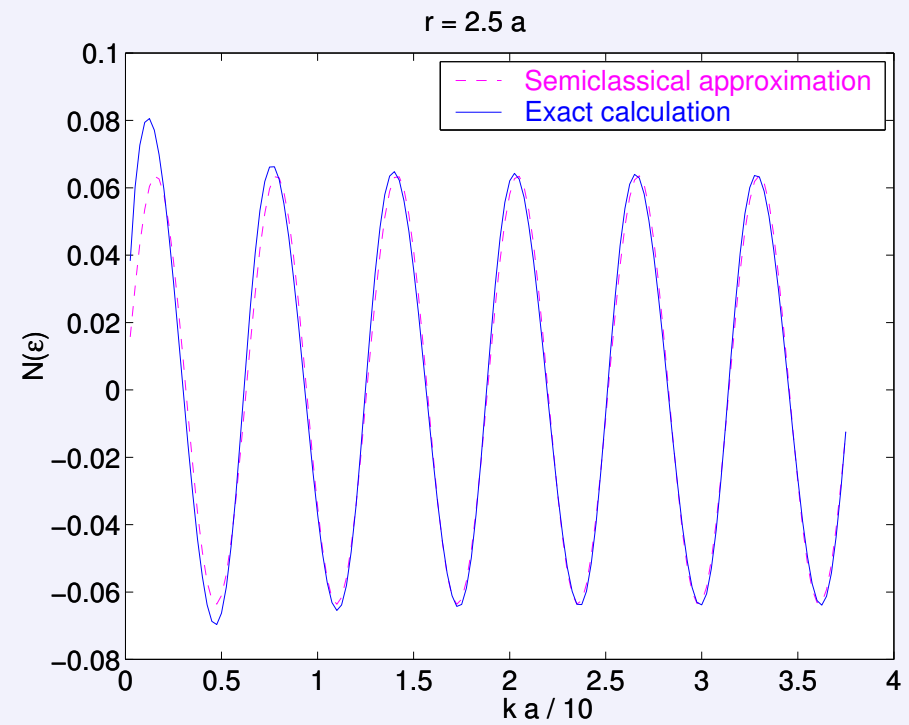
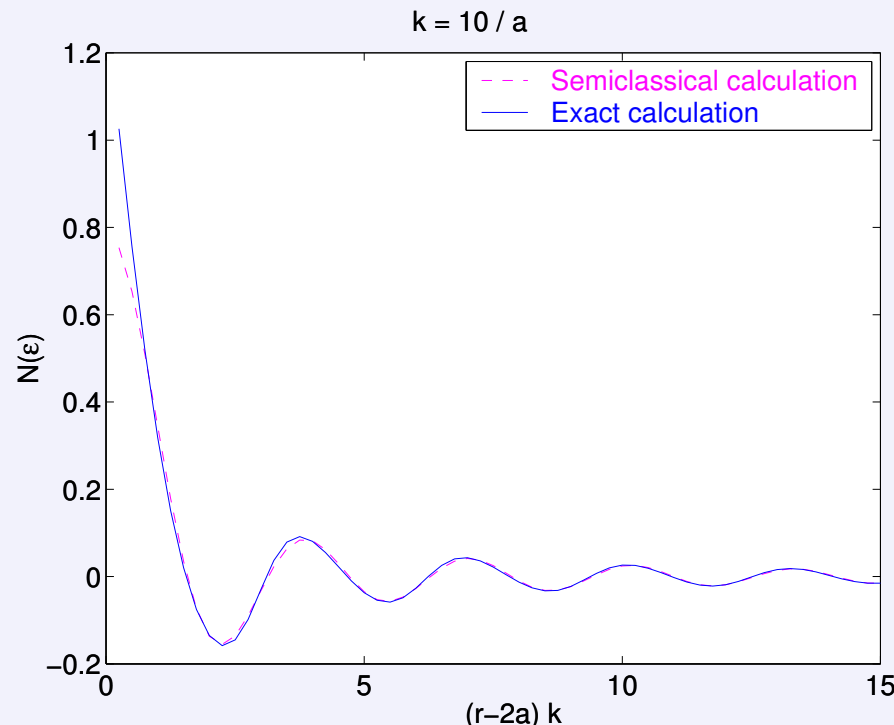
(oscillating and of longer range than molecular van der Waals forces !)

Two spheres:

14



$$\text{N.o.S } \mathcal{N}_C^{oo}(E) = -\frac{1}{\pi} \text{Im} \ln \det M^{oo}(E) \approx \frac{a^2}{4\pi r(r-2a)} \sin[2(r-2a)k]$$



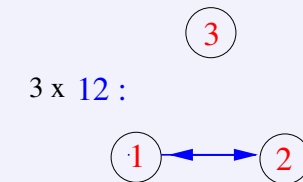
$$\mathcal{E}_C^{oo} = - \int_0^{\mu(k_F)} dE \mathcal{N}_C^{oo}(E) \approx -\mu \frac{a^2}{2\pi r(r-2a)} j_1[2(r-2a)k_F] \sim \frac{a^2}{L^3}$$

(oscillating and of longer range than molecular van der Waals forces !)

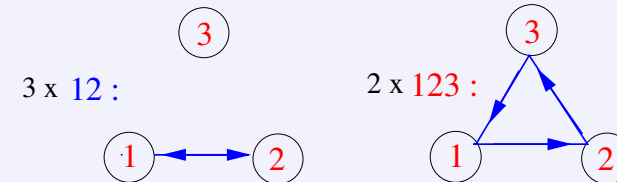
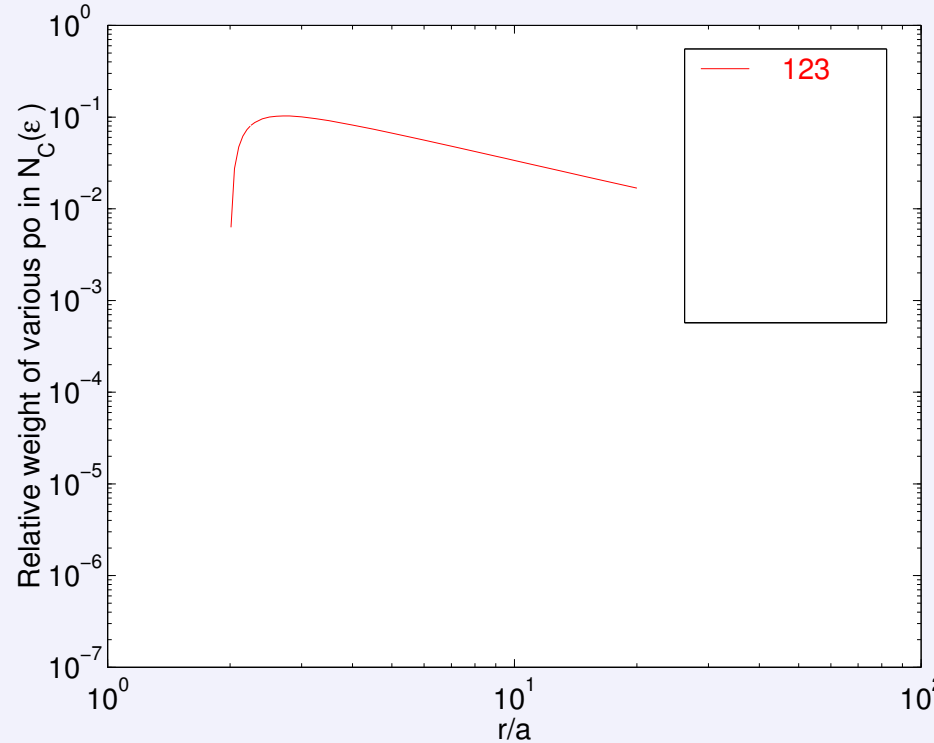
Sphere-plate geometry: $\mathcal{E}_C^{o|} \approx -\mu \frac{a}{\pi(r-a)} j_1[2(r-a)k_F] \sim \frac{a}{L^2}$

- *periodic orbit summation*: \exists of genuine *three and more-body* interactions

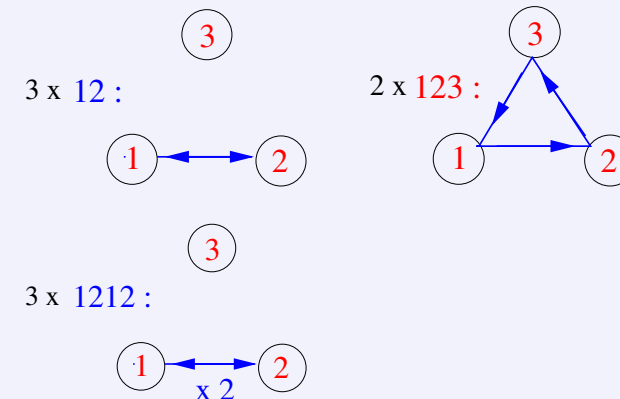
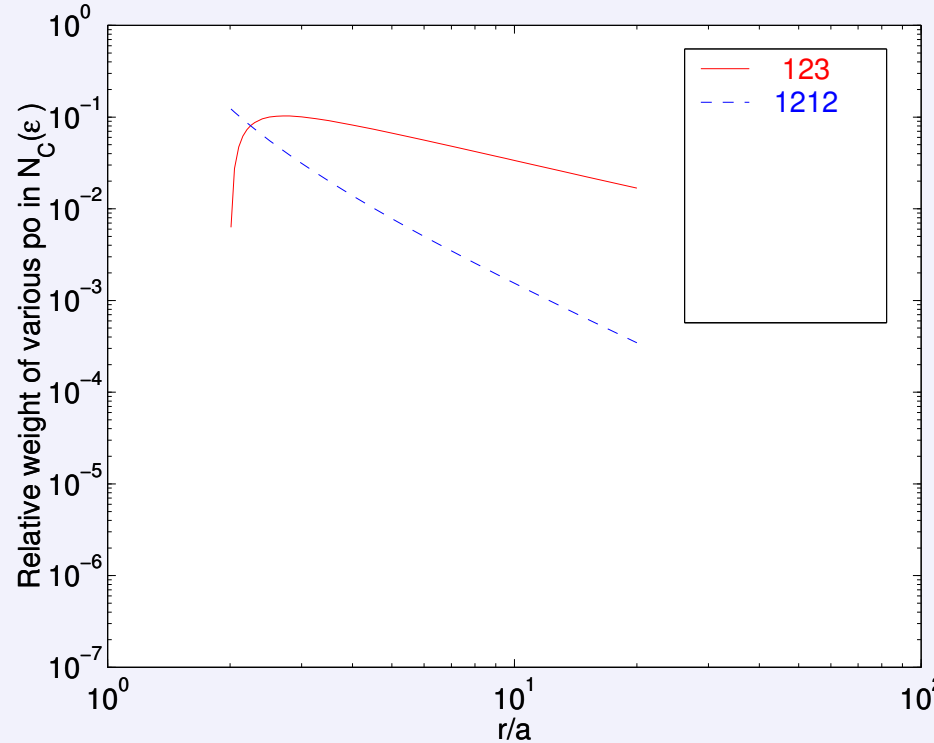
- *periodic orbit summation*: \exists of genuine *three and more-body* interactions
- However, **2-bounce orbit dominates** in equilateral three- and four sphere systems



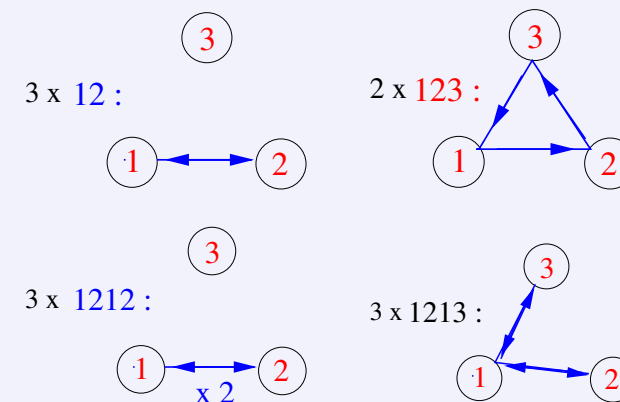
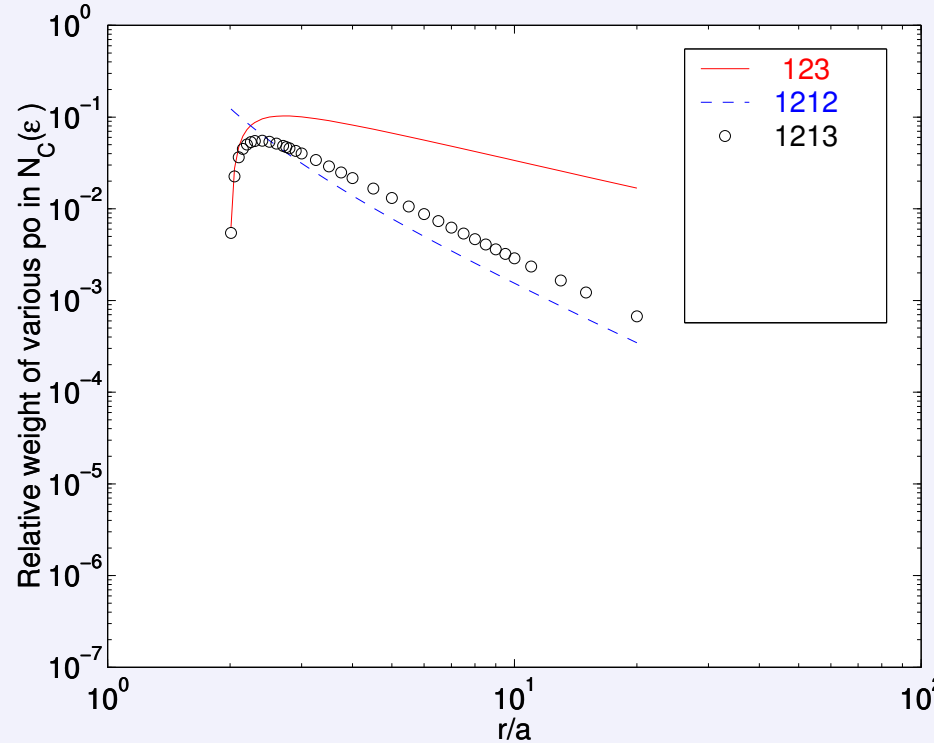
- *periodic orbit summation*: \exists of genuine *three and more-body* interactions
- However, **2-bounce orbit dominates** in equilateral three- and four sphere systems
(max. correction due to 3-bounce orbit is $\sim 10\%$ at $r \approx 2.5a$)



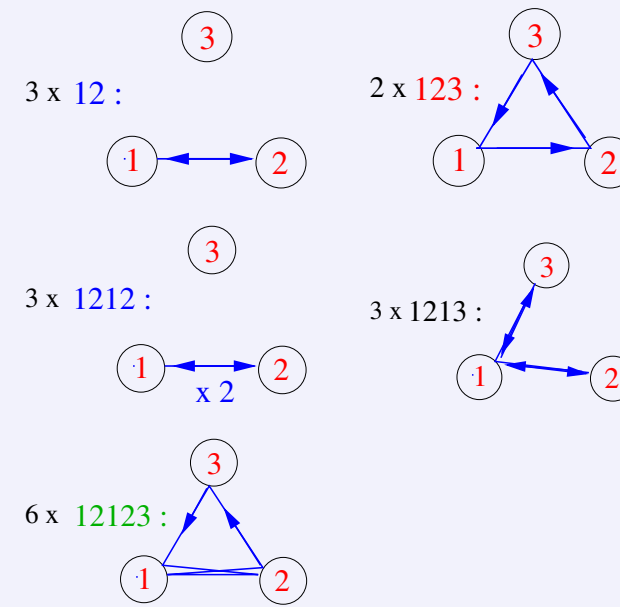
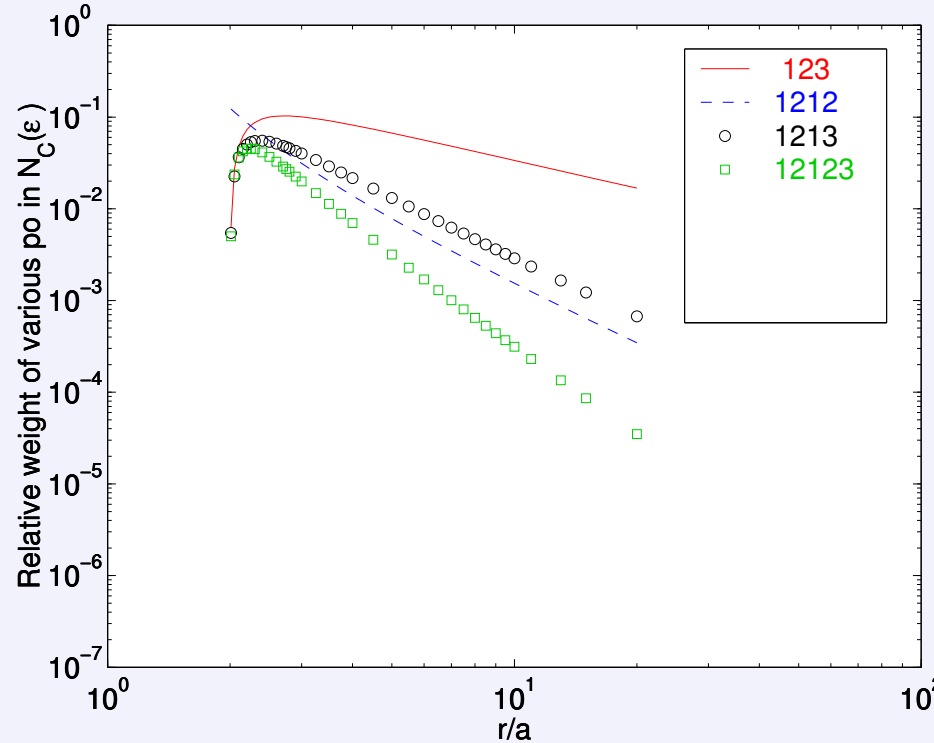
- *periodic orbit summation*: \exists of genuine *three and more-body* interactions
- However, **2-bounce orbit dominates** in equilateral three- and four sphere systems
(max. correction due to 3-bounce orbit is $\sim 10\%$ at $r \approx 2.5a$)



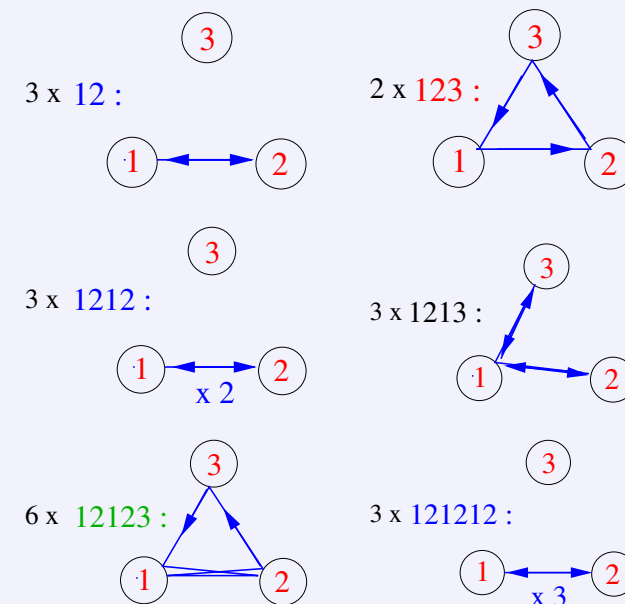
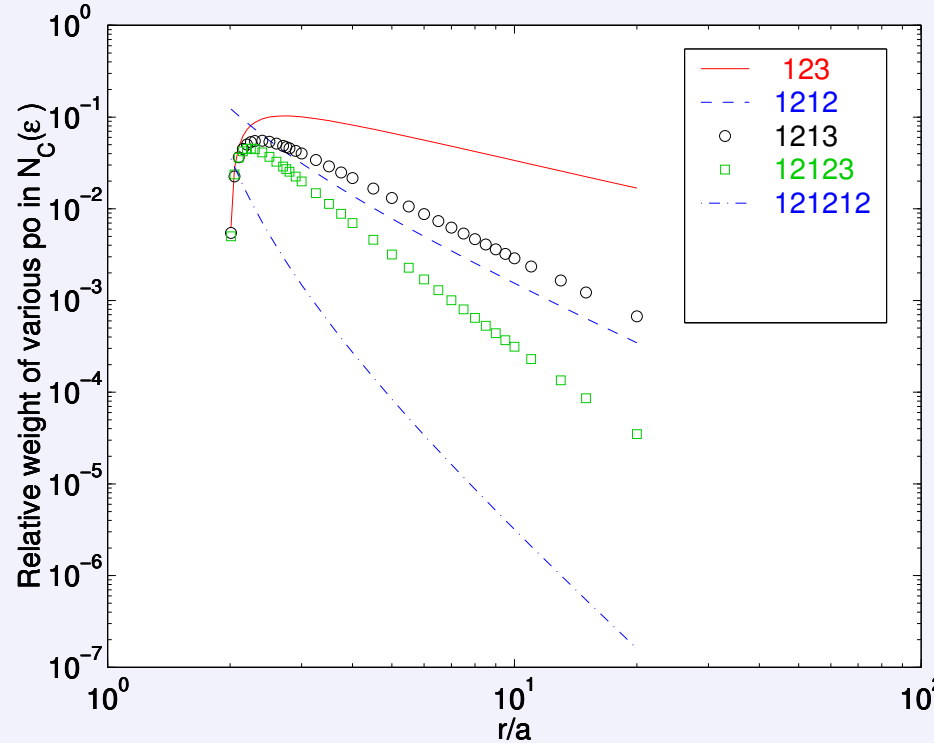
- *periodic orbit summation*: \exists of genuine *three and more-body* interactions
- However, **2-bounce orbit dominates** in equilateral three- and four sphere systems
(max. correction due to 3-bounce orbit is $\sim 10\%$ at $r \approx 2.5a$)



- *periodic orbit summation*: \exists of genuine *three and more-body* interactions
- However, **2-bounce orbit dominates** in equilateral three- and four sphere systems
(max. correction due to 3-bounce orbit is $\sim 10\%$ at $r \approx 2.5a$)



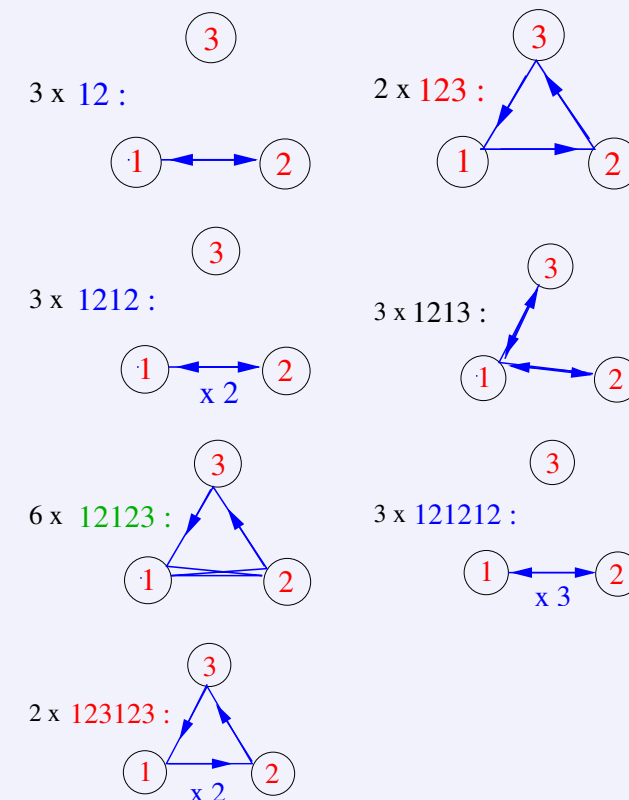
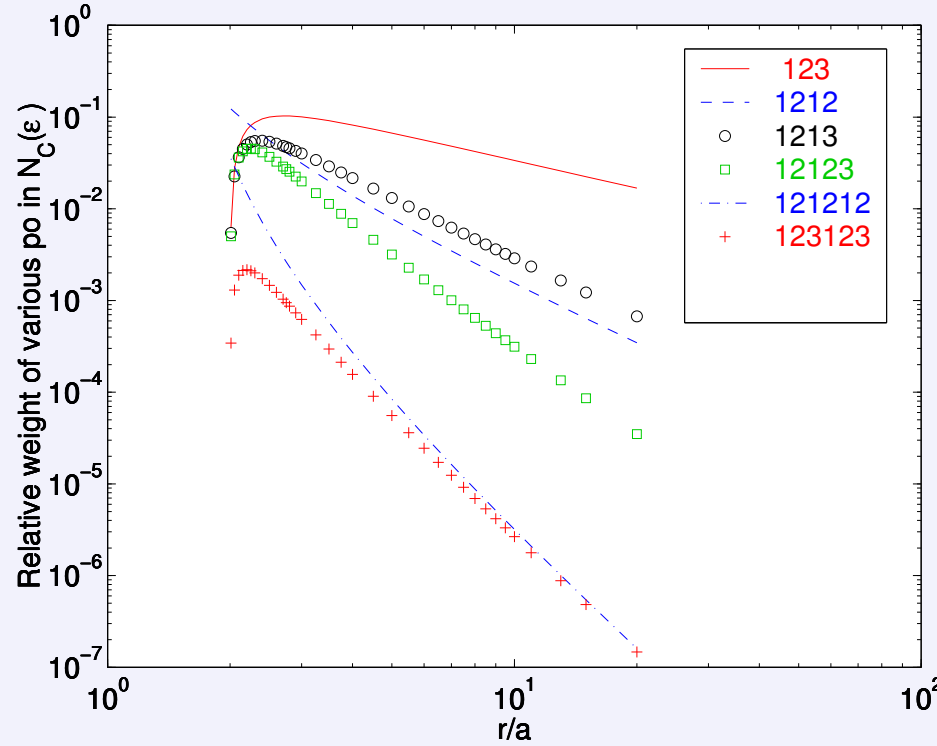
- *periodic orbit summation*: \exists of genuine *three and more-body* interactions
- However, **2-bounce orbit dominates** in equilateral three- and four sphere systems
(max. correction due to 3-bounce orbit is $\sim 10\%$ at $r \approx 2.5a$)



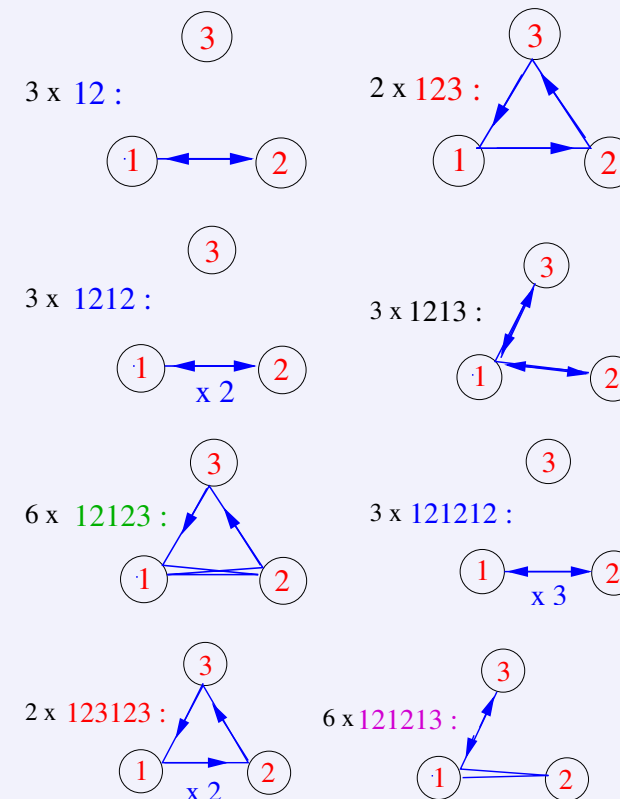
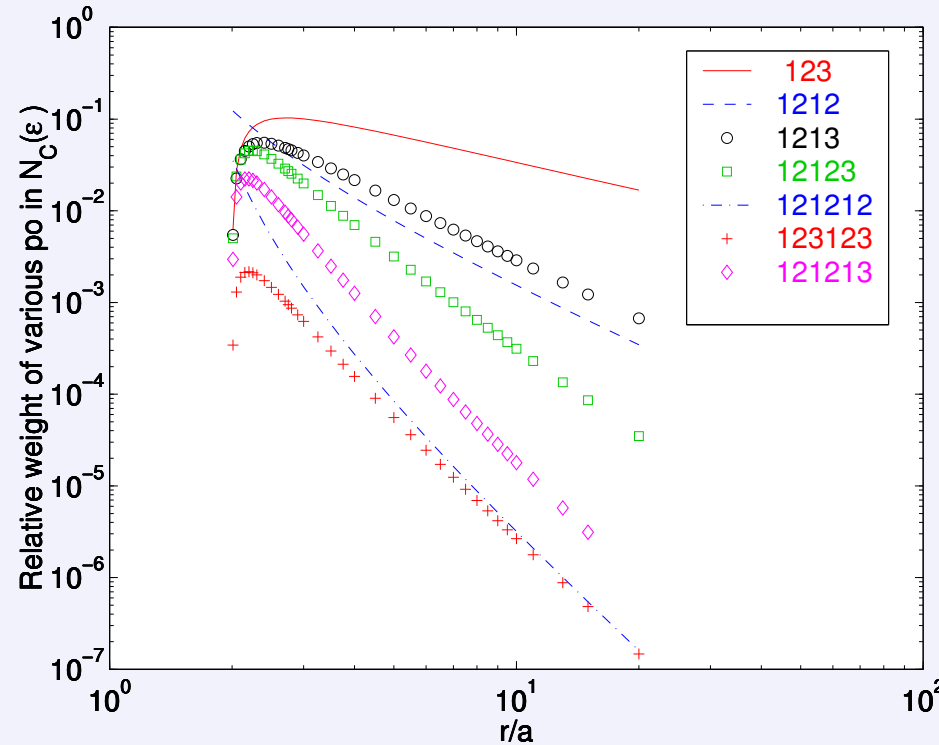
Three and four spheres:

A.Bulgac & A.W., PRL 87 (2001) 120404.

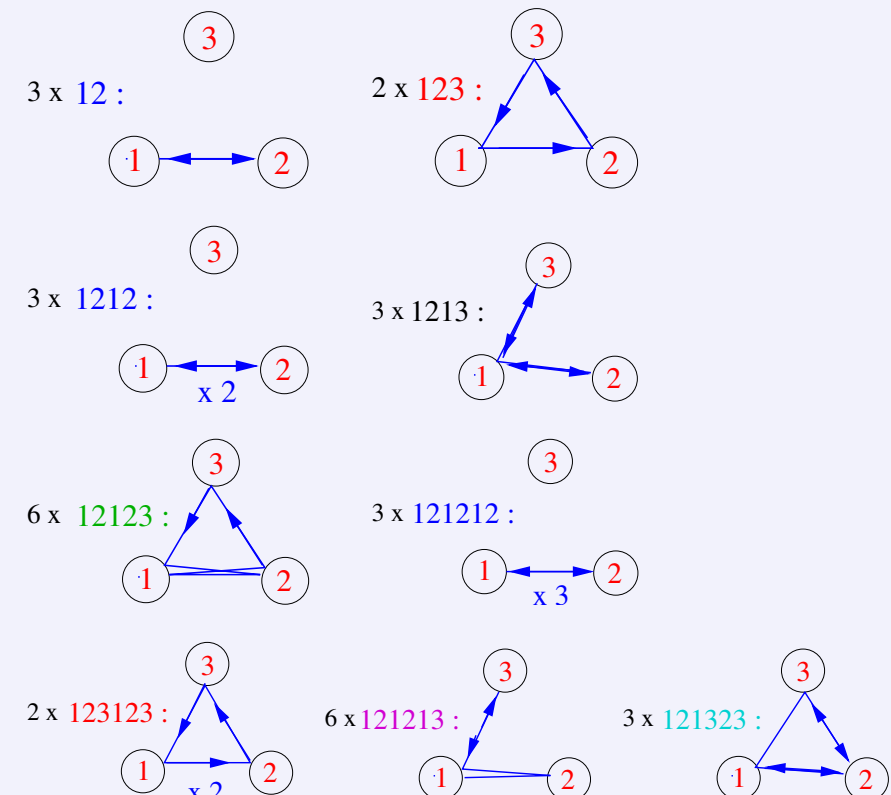
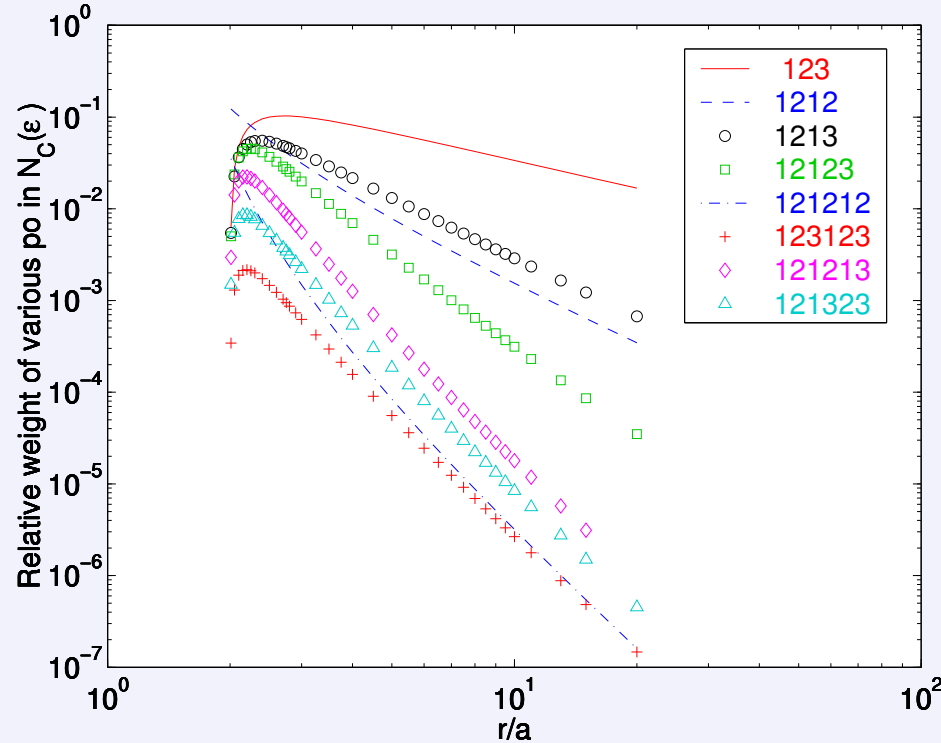
- *periodic orbit summation*: \exists of genuine *three and more-body* interactions
- However, **2-bounce orbit dominates** in equilateral three- and four sphere systems
(max. correction due to 3-bounce orbit is $\sim 10\%$ at $r \approx 2.5a$)



- *periodic orbit summation*: \exists of genuine *three and more-body* interactions
- However, **2-bounce orbit dominates** in equilateral three- and four sphere systems
(max. correction due to 3-bounce orbit is $\sim 10\%$ at $r \approx 2.5a$)



- *periodic orbit summation*: \exists of genuine *three and more-body* interactions
- However, **2-bounce orbit dominates** in equilateral three- and four sphere systems
(max. correction due to 3-bounce orbit is $\sim 10\%$ at $r \approx 2.5a$)



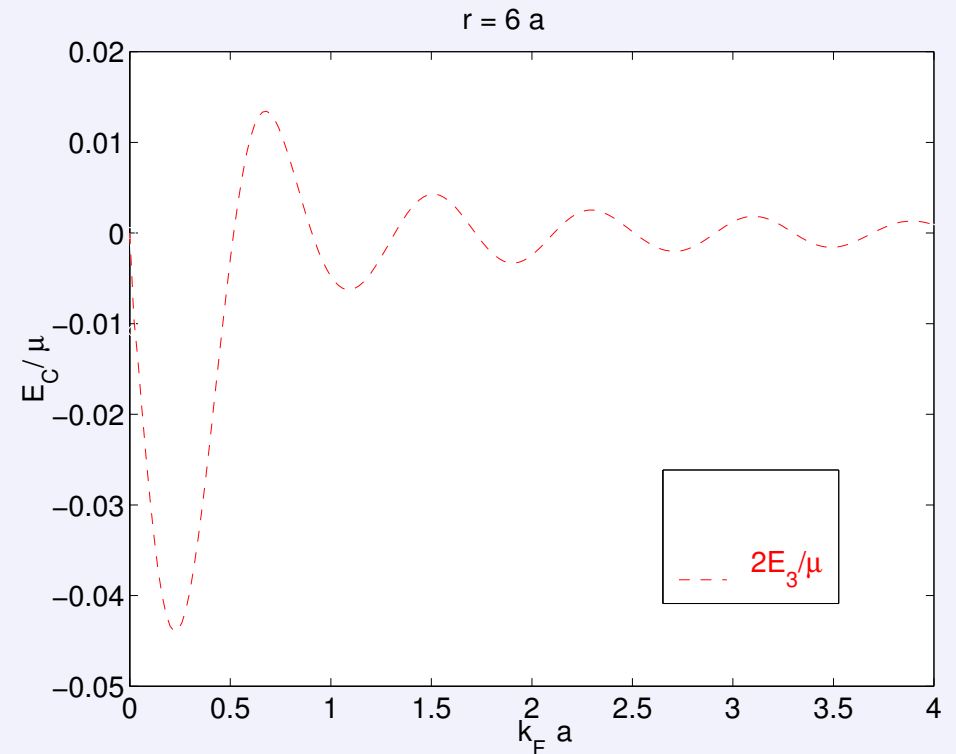
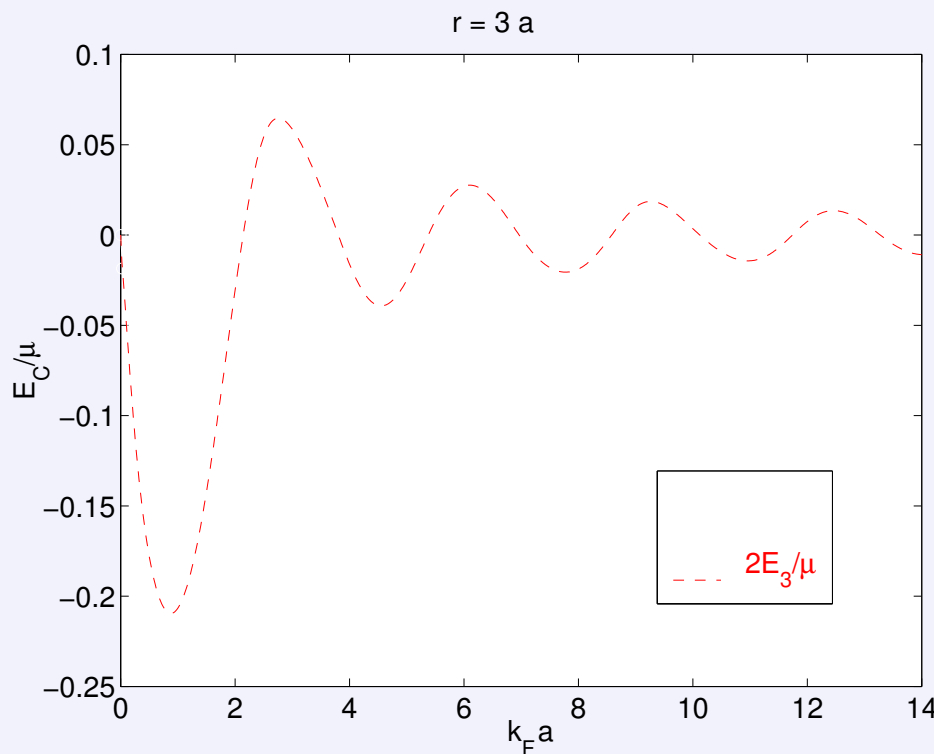
- *Billiard analogy*: difficult to make **long** shots, especially with **many bounces**
– the slightest error ruins the shot.

- *period orbits* summations \Rightarrow genuine *three- and more-body* interactions,
- However, **2-bounce orbit dominantes** as shortest and simplest (billiard analog!)

- *period orbits* summations \Rightarrow genuine *three- and more-body* interactions,
- However, **2-bounce orbit dominantes** as shortest and simplest (billiard analog!)

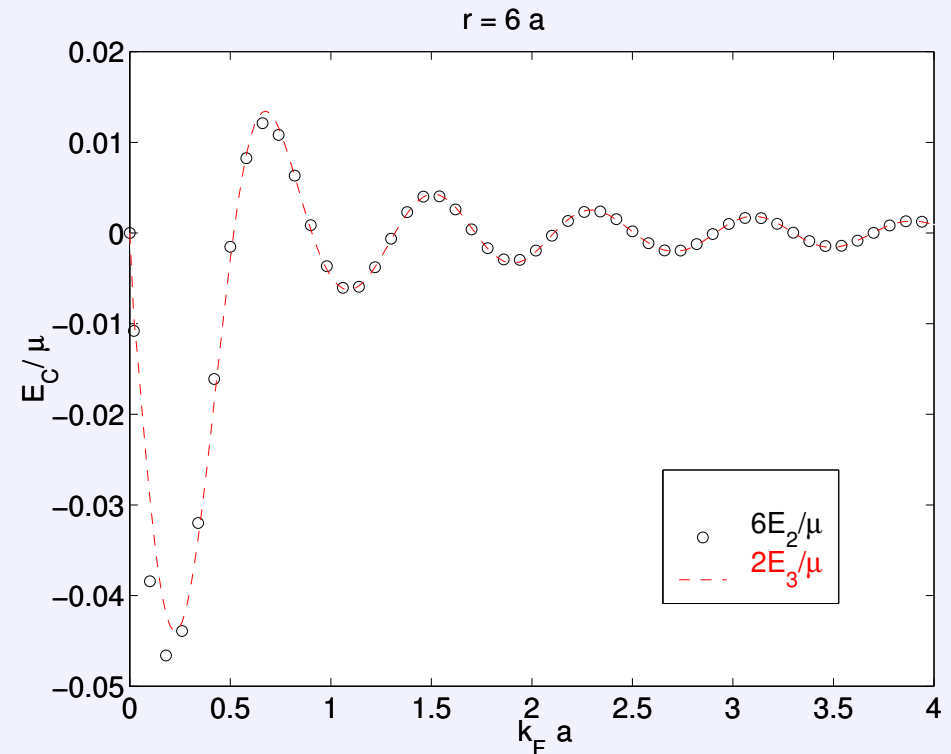
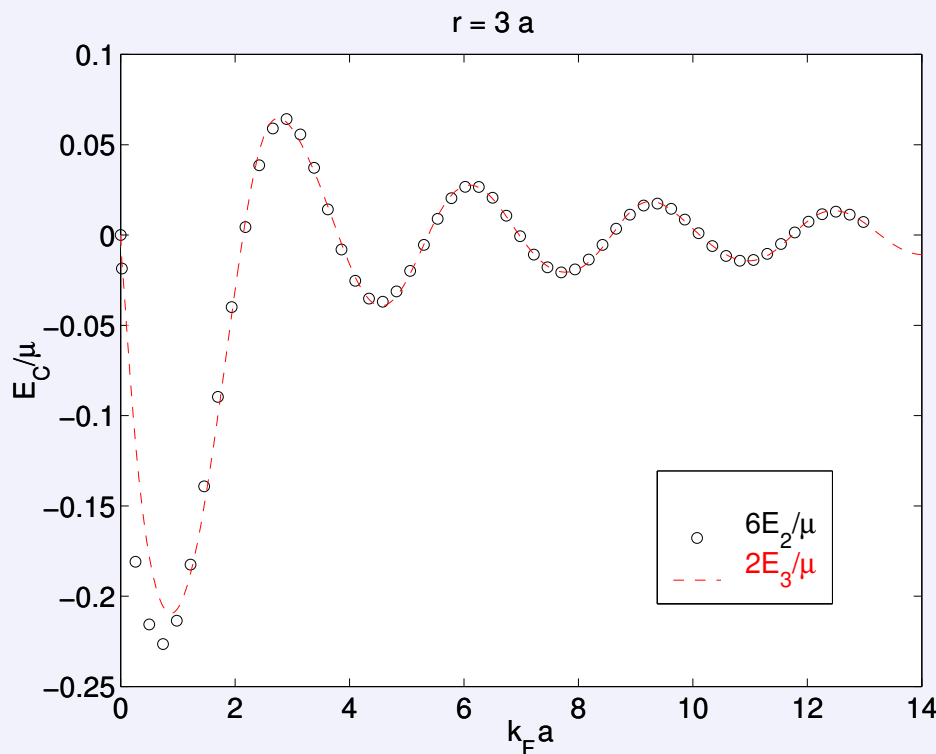
the Casimir energy

for **3 ident. spheres (*equilateral triangle*)**



- *period orbits* summations \Rightarrow genuine *three- and more-body* interactions,
- However, **2-bounce orbit dominantes** as shortest and simplest (billiard analog!)

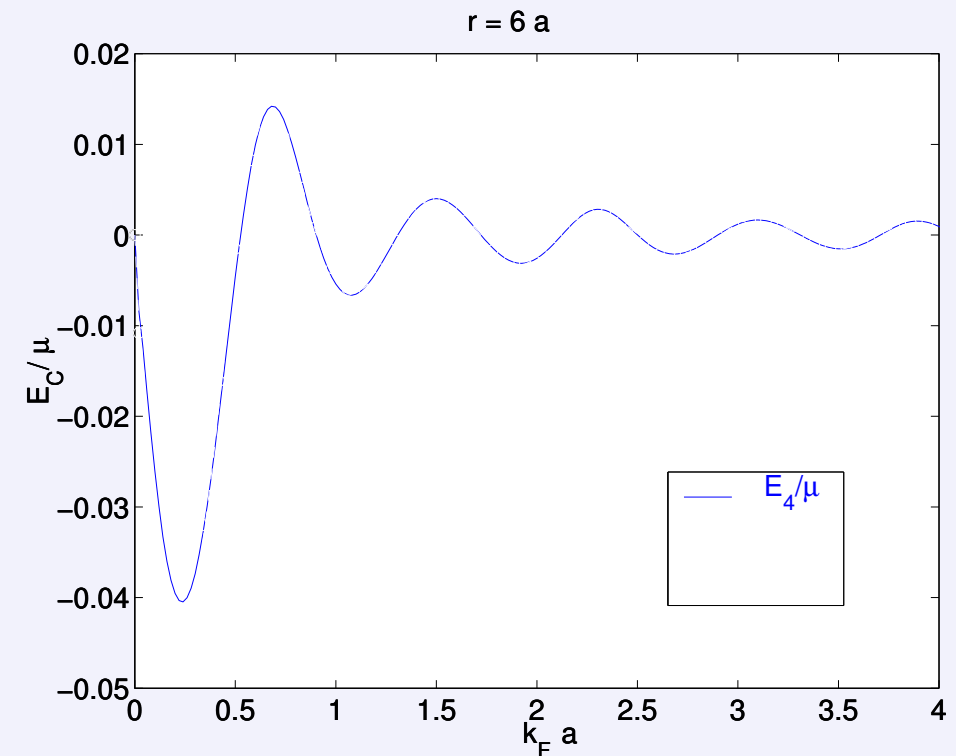
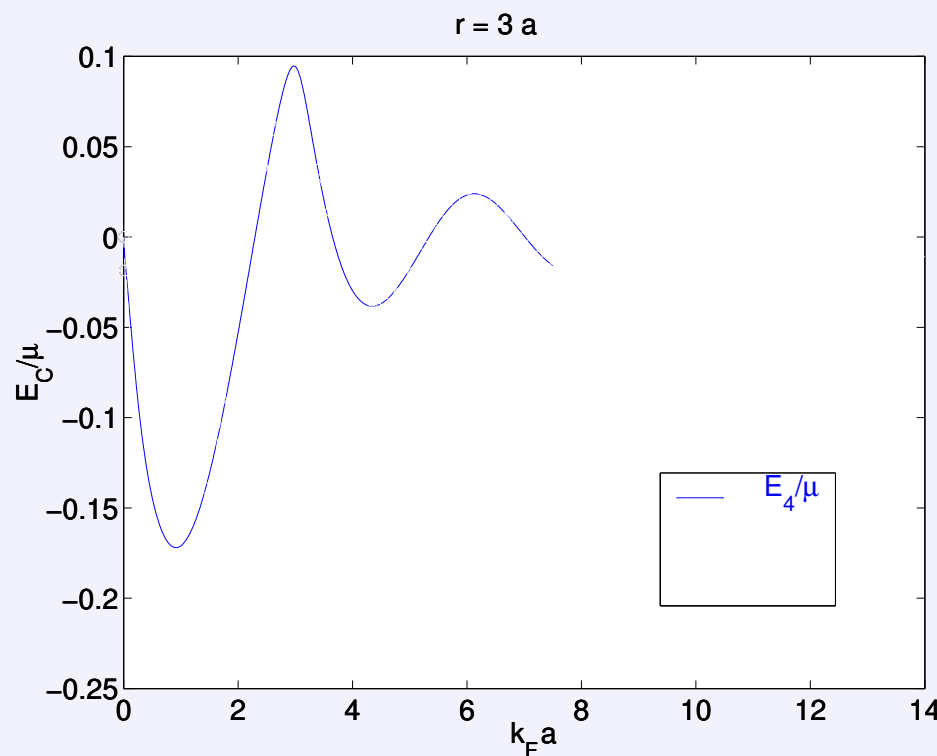
the Casimir energy satisfies the rule $E_3 \approx 3E_2$ for **3 ident. spheres (*equilateral triangle*)**



- *period orbits* summations \Rightarrow genuine *three- and more-body* interactions,
- However, **2-bounce orbit dominantes** as shortest and simplest (billiard analog!)

the Casimir energy

for 4 identical spheres (*symmetric tetrahedron*),

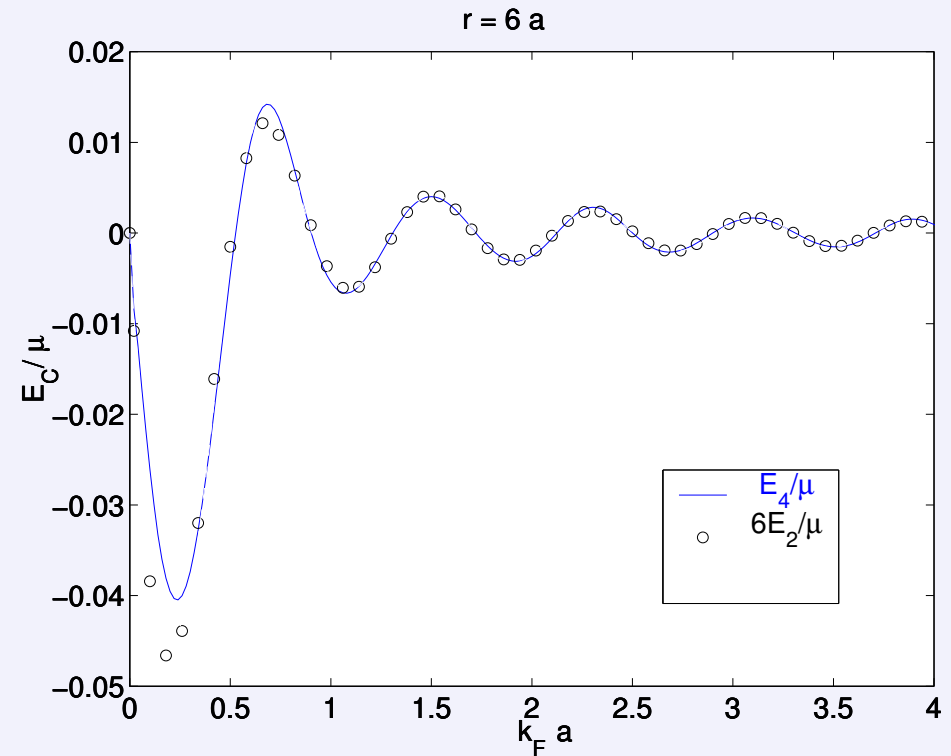
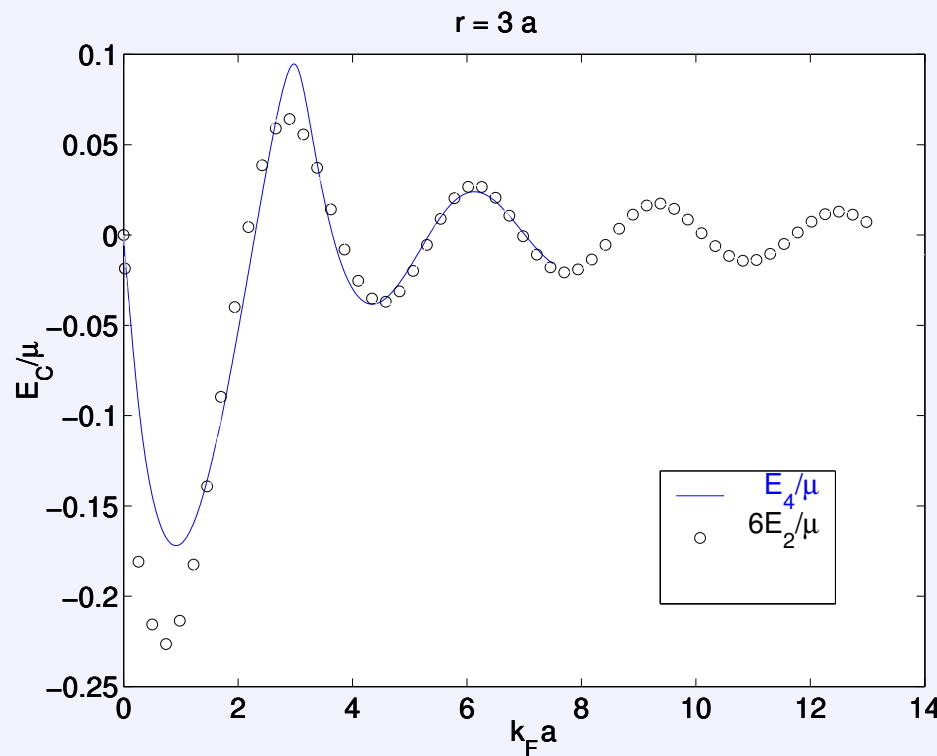


- *period orbits* summations \Rightarrow genuine *three- and more-body* interactions,
- However, **2-bounce orbit dominantes** as shortest and simplest (billiard analog!)

the Casimir energy satisfies the rule

$$E_4 \approx 6E_2$$

for 4 identical spheres (*symmetric tetrahedron*),

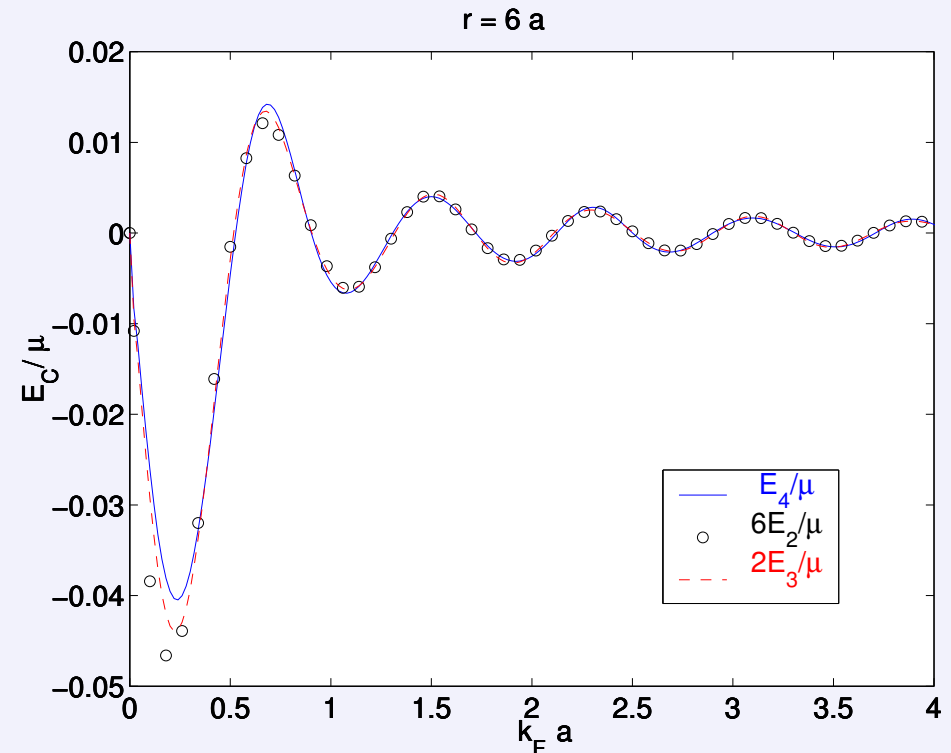
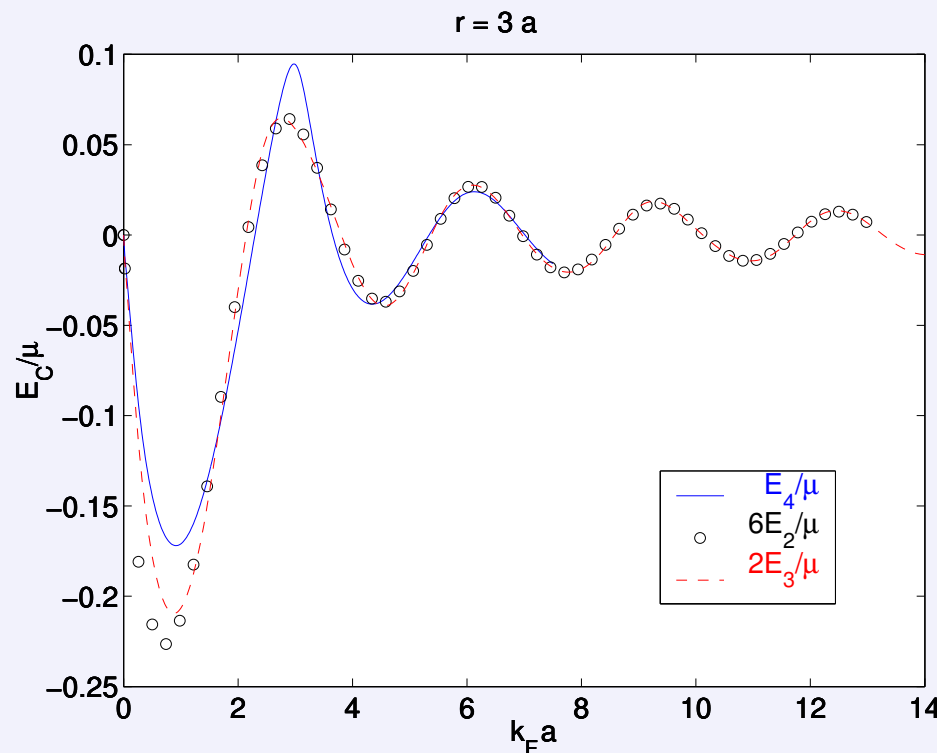


- *period orbits* summations \Rightarrow genuine *three- and more-body* interactions,
- However, **2-bounce orbit dominantes** as shortest and simplest (billiard analog!)

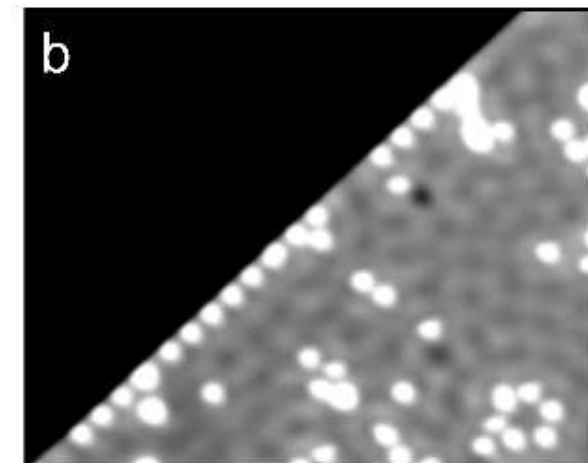
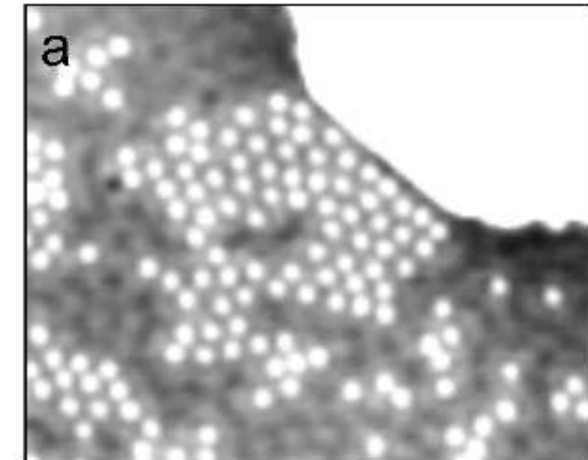
the Casimir energy satisfies the rule $E_3 \approx 3E_2$ for **3 ident. spheres (*equilateral triangle*)**

and $E_4 \approx 6E_2 \approx 2E_3$ for **4 identical spheres (*symmetric tetrahedron*)**, if $k_F a \gg 1$.

$(k_F a \leq 1$: corrections up to **10 %** and **25 %** for **3 & 4** spheres)

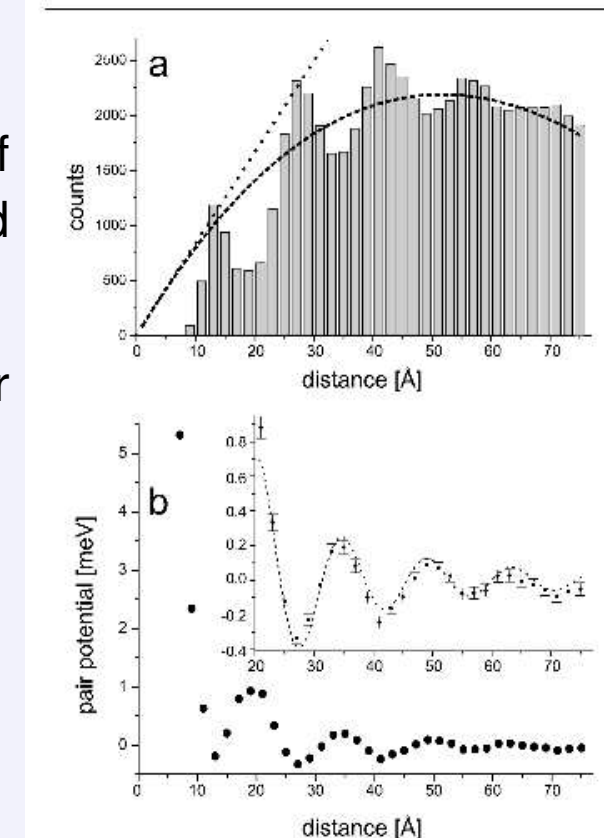


J. Repp et al., PRL 85 (2000) 2981



STM snap-shots ($200 \text{ \AA} \times 250 \text{ \AA}$) of Cu-adatoms on a closed packed Cu(111)-surface (at 9 K)

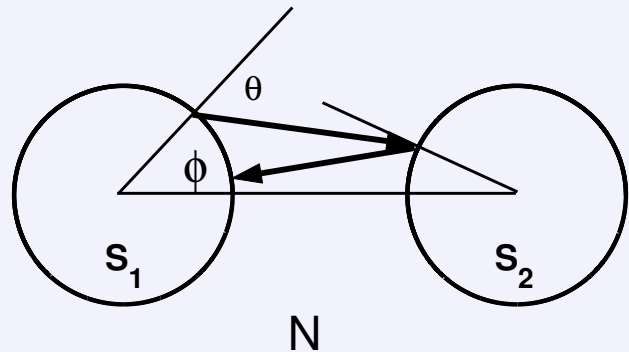
- islands with local hexagonal order
- average adatom-distance 12.5 \AA
- $E(R) \simeq -A \frac{4E_F \sin^2(\delta)}{\pi^2} \frac{\sin(2k_F R + 2\delta)}{(k_F R)^2}$
 $E_F = 0.3 \text{ eV}$, $k_F = 0.22/\text{\AA}$, $A = 0.08$,
 $\delta = 0.3\pi$.
- minima of pot.: 12.9 \AA , 26.7 \AA ,
maximum of potential: 20.7 \AA



P. Hyldgaard & M. Persson, J.Phys.:Cond.Mat. **12** (2000) L13
K.H. Lau & W. Kohn, Surf. Sci. **75** (1978) 69.

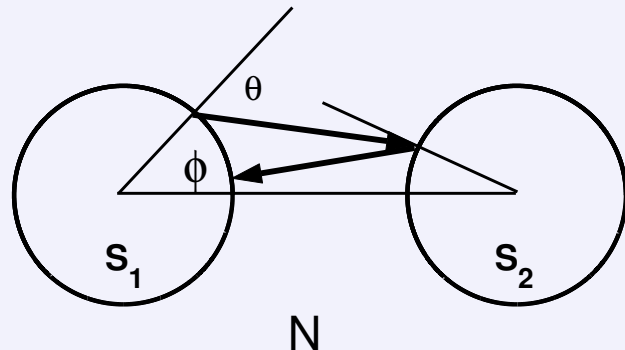
Fermionic Casimir Effect of two superfluid grains in a normal Fermi gas

Fermionic Casimir Effect of two superfluid grains in a normal Fermi gas



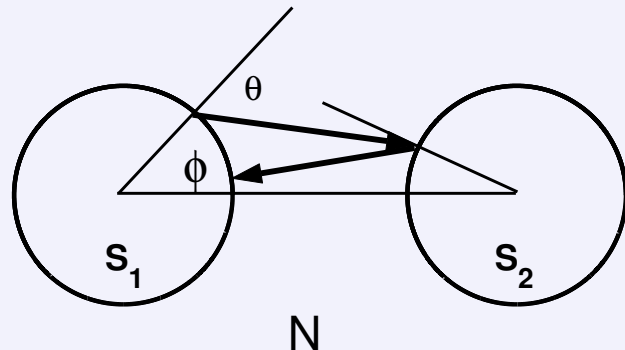
Specular reflection replaced by *Andreev reflection*

Fermionic Casimir Effect of two superfluid grains in a normal Fermi gas



Specular reflection replaced by *Andreev reflection*
 \Rightarrow particle retro-reflected as a hole.

Fermionic Casimir Effect of two superfluid grains in a normal Fermi gas

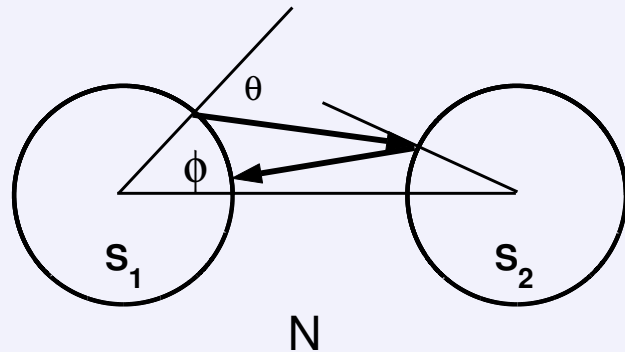


Specular reflection replaced by *Andreev reflection*
 \Rightarrow particle retro-reflected as a hole.

$$k_p^2/2 + k_h^2/2 = k_F^2 \text{ (particle/hole states symmetric).}$$

$$k_p \sin \theta_p = k_h \sin \theta_h \text{ (modified Snell's law)}$$

Fermionic Casimir Effect of two superfluid grains in a normal Fermi gas



Specular reflection replaced by *Andreev reflection*

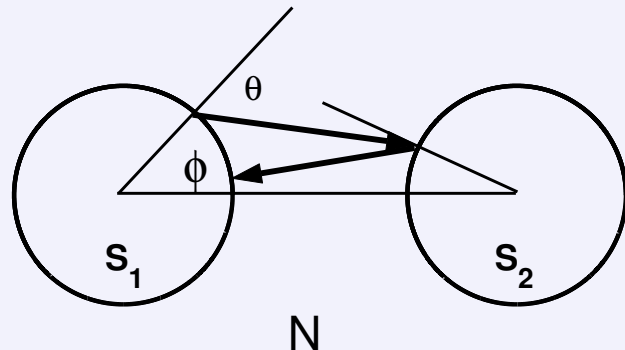
⇒ particle retro-reflected as a hole.

$$k_p^2/2 + k_h^2/2 = k_F^2 \text{ (particle/hole states symmetric).}$$

$$k_p \sin \theta_p = k_h \sin \theta_h \text{ (modified Snell's law),}$$

⇒ disks/spheres have **focusing effect**.

Fermionic Casimir Effect of two superfluid grains in a normal Fermi gas



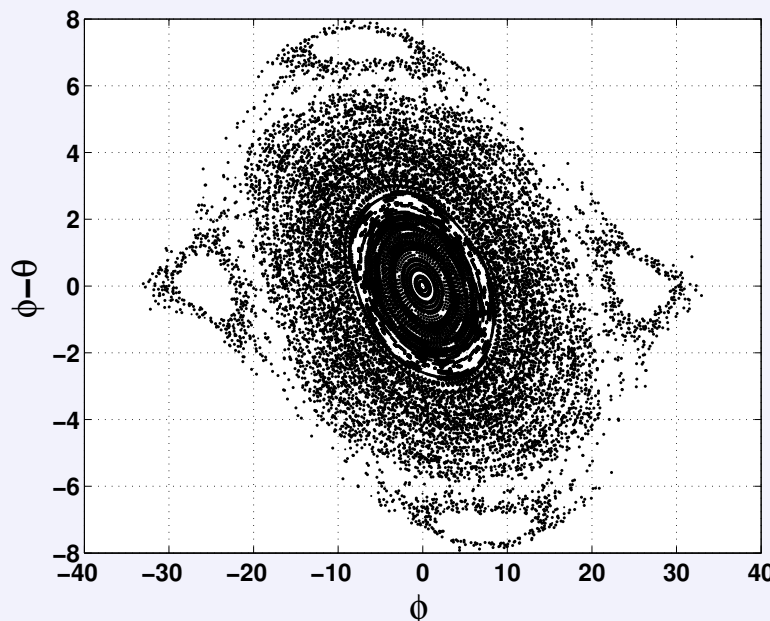
Specular reflection replaced by *Andreev reflection*

⇒ particle retro-reflected as a hole.

$$k_p^2/2 + k_h^2/2 = k_F^2 \text{ (particle/hole states symmetric).}$$

$$k_p \sin \theta_p = k_h \sin \theta_h \text{ (modified Snell's law),}$$

⇒ disks/spheres have **focusing effect**.



Stable orbits if $\frac{R}{2a} \leq \frac{k_p}{k_p - k_h}$ satisfied.

(here $R = 6a$ and $k_p/k_h = 1.5$)

A. Bulgac, P. Magierski & A.W., *Europhys. Lett.* **72** (2005) 327

1) Apply Bogoliubov-de Gennes equations in the p-h-space for quasi-particle energy $E = \pm \frac{k^2_{p/h}}{2m} \mp \mu$

$$\begin{pmatrix} H_0 - \mu & \Delta(\vec{r}) \\ \Delta(\vec{r}) & -(H_0 - \mu) \end{pmatrix} \begin{pmatrix} u(\vec{r}) \\ v(\vec{r}) \end{pmatrix} = E \begin{pmatrix} u(\vec{r}) \\ v(\vec{r}) \end{pmatrix} \text{ with } \text{pair field } \Delta(\vec{r}) = \begin{cases} \Delta e^{+i\phi_\Delta/2} & \text{for } r \in \text{grain 1,} \\ \Delta e^{-i\phi_\Delta/2} & \text{for } r \in \text{grain 2,} \\ 0 & \text{otherwise.} \end{cases}$$

1) Apply Bogoliubov-de Gennes equations in the p-h-space for quasi-particle energy $E = \pm \frac{k^2_{p/h}}{2m} \mp \mu$

$$\begin{pmatrix} H_0 - \mu & \Delta(\vec{r}) \\ \Delta(\vec{r}) & -(H_0 - \mu) \end{pmatrix} \begin{pmatrix} u(\vec{r}) \\ v(\vec{r}) \end{pmatrix} = E \begin{pmatrix} u(\vec{r}) \\ v(\vec{r}) \end{pmatrix} \text{ with pair field } \Delta(\vec{r}) = \begin{cases} \Delta e^{+i\phi_\Delta/2} & \text{for } r \in \text{grain 1,} \\ \Delta e^{-i\phi_\Delta/2} & \text{for } r \in \text{grain 2,} \\ 0 & \text{otherwise.} \end{cases}$$

2) Modify Krein formula $\delta N(E) = -\frac{1}{\pi} \text{Im} \ln \det M(E)$ for the p-h space.

1) Apply Bogoliubov-de Gennes equations in the p-h-space for quasi-particle energy $E = \pm \frac{k^2_{p/h}}{2m} \mp \mu$

$$\begin{pmatrix} H_0 - \mu & \Delta(\vec{r}) \\ \Delta(\vec{r}) & -(H_0 - \mu) \end{pmatrix} \begin{pmatrix} u(\vec{r}) \\ v(\vec{r}) \end{pmatrix} = E \begin{pmatrix} u(\vec{r}) \\ v(\vec{r}) \end{pmatrix} \text{ with pair field } \Delta(\vec{r}) = \begin{cases} \Delta e^{+i\phi_\Delta/2} & \text{for } r \in \text{grain 1,} \\ \Delta e^{-i\phi_\Delta/2} & \text{for } r \in \text{grain 2,} \\ 0 & \text{otherwise.} \end{cases}$$

2) Modify Krein formula $\delta N(E) = -\frac{1}{\pi} \text{Im} \ln \det M(E)$ for the p-h space.

$$\text{For } R \gg a: \quad \delta N(E) \approx \frac{4|T_{ph}(a, \mu, \Delta)| \cos \phi_\Delta}{\pi^2 \sqrt{k_h k_p} R} \sin[(k_p - k_h)R + \phi_{ph}] \\ - \frac{2|T_{pp}(a, \mu, \Delta)|}{\pi^2 k_p R} \cos(2k_p R + \phi_{pp}) + \frac{2|T_{hh}(a, \mu, \Delta)|}{\pi^2 k_h R} \cos(2k_h R - \phi_{hh})$$

1) Apply Bogoliubov-de Gennes equations in the p-h-space for quasi-particle energy $E = \pm \frac{k^2_{p/h}}{2m} \mp \mu$

$$\begin{pmatrix} H_0 - \mu & \Delta(\vec{r}) \\ \Delta(\vec{r}) & -(H_0 - \mu) \end{pmatrix} \begin{pmatrix} u(\vec{r}) \\ v(\vec{r}) \end{pmatrix} = E \begin{pmatrix} u(\vec{r}) \\ v(\vec{r}) \end{pmatrix} \text{ with pair field } \Delta(\vec{r}) = \begin{cases} \Delta e^{+i\phi_\Delta/2} & \text{for } r \in \text{grain 1,} \\ \Delta e^{-i\phi_\Delta/2} & \text{for } r \in \text{grain 2,} \\ 0 & \text{otherwise.} \end{cases}$$

2) Modify Krein formula $\delta N(E) = -\frac{1}{\pi} \text{Im} \ln \det M(E)$ for the p-h space.

$$\text{For } R \gg a: \quad \delta N(E) \approx \frac{4|T_{ph}(a, \mu, \Delta)| \cos \phi_\Delta}{\pi^2 \sqrt{k_h k_p} R} \sin[(k_p - k_h)R + \phi_{ph}] \\ - \frac{2|T_{pp}(a, \mu, \Delta)|}{\pi^2 k_p R} \cos(2k_p R + \phi_{pp}) + \frac{2|T_{hh}(a, \mu, \Delta)|}{\pi^2 k_h R} \cos(2k_h R - \phi_{hh})$$

$T_{ph} = (\sum_m t_{ph}^m / 2)^2$, $T_{pp} = (\sum_m (-1)^m t_{pp}^m / 2)^2$ etc. structure functions (only dep. on single scatterer)

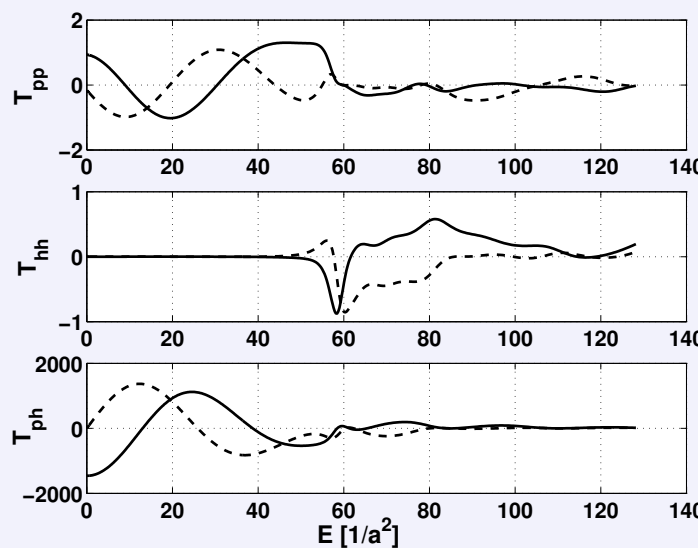
1) Apply Bogoliubov-de Gennes equations in the p-h-space for quasi-particle energy $E = \pm \frac{k^2_{p/h}}{2m} \mp \mu$

$$\begin{pmatrix} H_0 - \mu & \Delta(\vec{r}) \\ \Delta(\vec{r}) & -(H_0 - \mu) \end{pmatrix} \begin{pmatrix} u(\vec{r}) \\ v(\vec{r}) \end{pmatrix} = E \begin{pmatrix} u(\vec{r}) \\ v(\vec{r}) \end{pmatrix} \text{ with pair field } \Delta(\vec{r}) = \begin{cases} \Delta e^{+i\phi_\Delta/2} & \text{for } r \in \text{grain 1}, \\ \Delta e^{-i\phi_\Delta/2} & \text{for } r \in \text{grain 2}, \\ 0 & \text{otherwise.} \end{cases}$$

2) Modify Krein formula $\delta N(E) = -\frac{1}{\pi} \text{Im} \ln \det M(E)$ for the p-h space.

$$\text{For } R \gg a: \delta N(E) \approx \frac{4|T_{ph}(a, \mu, \Delta)| \cos \phi_\Delta}{\pi^2 \sqrt{k_h k_p} R} \sin[(k_p - k_h)R + \phi_{ph}] - \frac{2|T_{pp}(a, \mu, \Delta)|}{\pi^2 k_p R} \cos(2k_p R + \phi_{pp}) + \frac{2|T_{hh}(a, \mu, \Delta)|}{\pi^2 k_h R} \cos(2k_h R - \phi_{hh})$$

$T_{ph} = (\sum_m t_{ph}^m / 2)^2$, $T_{pp} = (\sum_m (-1)^m t_{pp}^m / 2)^2$ etc. structure functions (only dep. on single scatterer)



$\mu = 200/a^2$, gap $\Delta = 50/a^2$,
rel. gap-phase $\phi_\Delta = 0$,

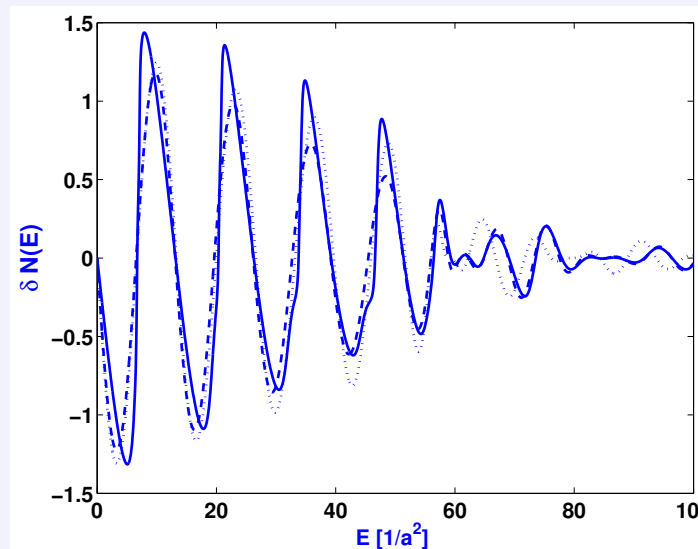
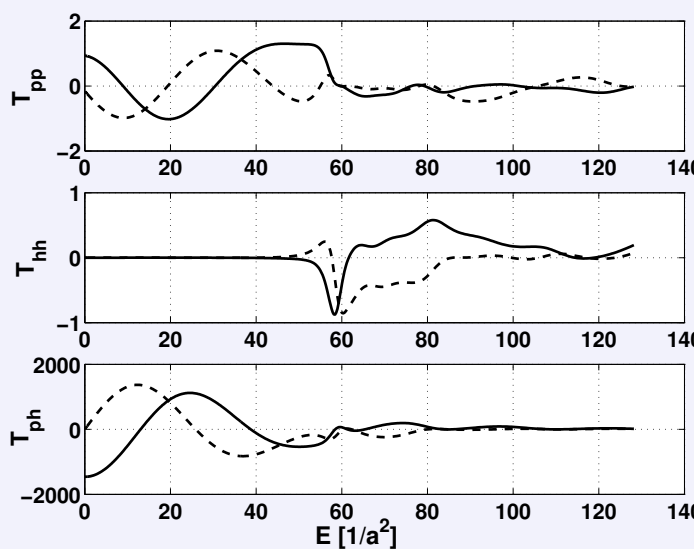
1) Apply Bogoliubov-de Gennes equations in the p-h-space for quasi-particle energy $E = \pm \frac{k^2_{p/h}}{2m} \mp \mu$

$$\begin{pmatrix} H_0 - \mu & \Delta(\vec{r}) \\ \Delta(\vec{r}) & -(H_0 - \mu) \end{pmatrix} \begin{pmatrix} u(\vec{r}) \\ v(\vec{r}) \end{pmatrix} = E \begin{pmatrix} u(\vec{r}) \\ v(\vec{r}) \end{pmatrix} \text{ with pair field } \Delta(\vec{r}) = \begin{cases} \Delta e^{+i\phi_\Delta/2} & \text{for } r \in \text{grain 1}, \\ \Delta e^{-i\phi_\Delta/2} & \text{for } r \in \text{grain 2}, \\ 0 & \text{otherwise.} \end{cases}$$

2) Modify Krein formula $\delta N(E) = -\frac{1}{\pi} \text{Im} \ln \det M(E)$ for the p-h space.

$$\text{For } R \gg a: \delta N(E) \approx \frac{4|T_{ph}(a, \mu, \Delta)| \cos \phi_\Delta}{\pi^2 \sqrt{k_h k_p} R} \sin[(k_p - k_h)R + \phi_{ph}] - \frac{2|T_{pp}(a, \mu, \Delta)|}{\pi^2 k_p R} \cos(2k_p R + \phi_{pp}) + \frac{2|T_{hh}(a, \mu, \Delta)|}{\pi^2 k_h R} \cos(2k_h R - \phi_{hh})$$

$T_{ph} = (\sum_m t_{ph}^m / 2)^2$, $T_{pp} = (\sum_m (-1)^m t_{pp}^m / 2)^2$ etc. structure functions (only dep. on single scatterer)



$\mu = 200/a^2$, gap $\Delta = 50/a^2$,
rel. gap-phase $\phi_\Delta = 0$, $R = 6a$,

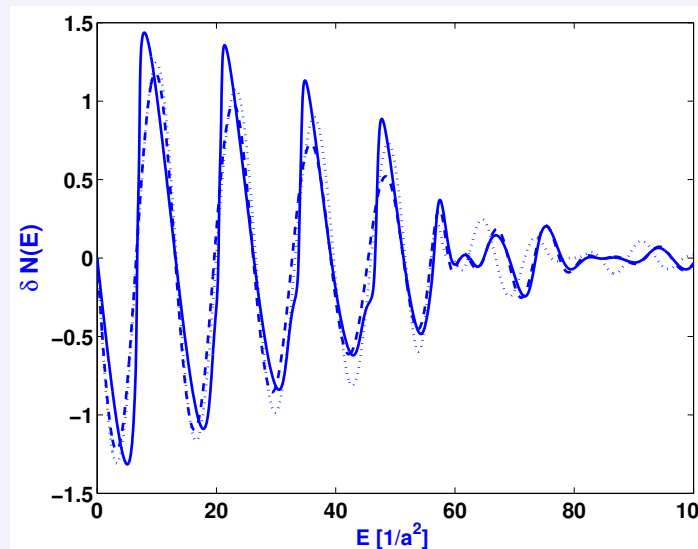
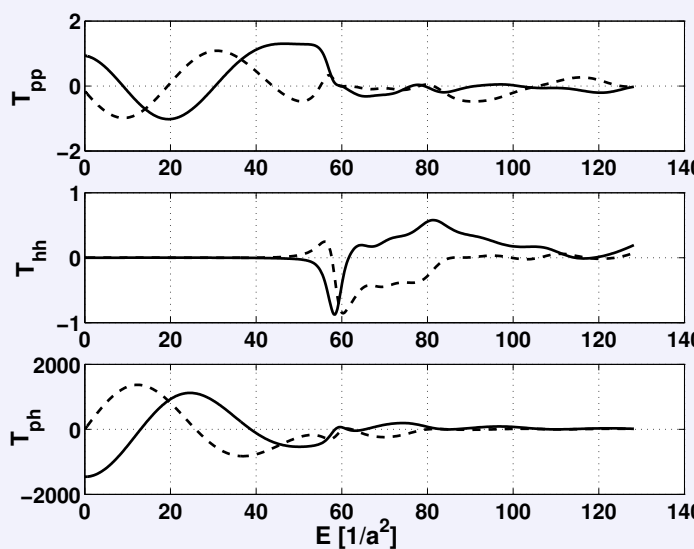
1) Apply Bogoliubov-de Gennes equations in the p-h-space for quasi-particle energy $E = \pm \frac{k^2_{p/h}}{2m} \mp \mu$

$$\begin{pmatrix} H_0 - \mu & \Delta(\vec{r}) \\ \Delta(\vec{r}) & -(H_0 - \mu) \end{pmatrix} \begin{pmatrix} u(\vec{r}) \\ v(\vec{r}) \end{pmatrix} = E \begin{pmatrix} u(\vec{r}) \\ v(\vec{r}) \end{pmatrix} \text{ with pair field } \Delta(\vec{r}) = \begin{cases} \Delta e^{+i\phi_\Delta/2} & \text{for } r \in \text{grain 1}, \\ \Delta e^{-i\phi_\Delta/2} & \text{for } r \in \text{grain 2}, \\ 0 & \text{otherwise.} \end{cases}$$

2) Modify Krein formula $\delta N(E) = -\frac{1}{\pi} \text{Im} \ln \det M(E)$ for the p-h space.

$$\text{For } R \gg a: \delta N(E) \approx \frac{4|T_{ph}(a, \mu, \Delta)| \cos \phi_\Delta}{\pi^2 \sqrt{k_h k_p} R} \sin[(k_p - k_h)R + \phi_{ph}] - \frac{2|T_{pp}(a, \mu, \Delta)|}{\pi^2 k_p R} \cos(2k_p R + \phi_{pp}) + \frac{2|T_{hh}(a, \mu, \Delta)|}{\pi^2 k_h R} \cos(2k_h R - \phi_{hh})$$

$T_{ph} = (\sum_m t_{ph}^m / 2)^2$, $T_{pp} = (\sum_m (-1)^m t_{pp}^m / 2)^2$ etc. structure functions (only dep. on single scatterer)



$\mu = 200/a^2$, gap $\Delta = 50/a^2$,
rel. gap-phase $\phi_\Delta = 0$, $R = 6a$,
 $E \leq \Delta$ behavior **dominant**,

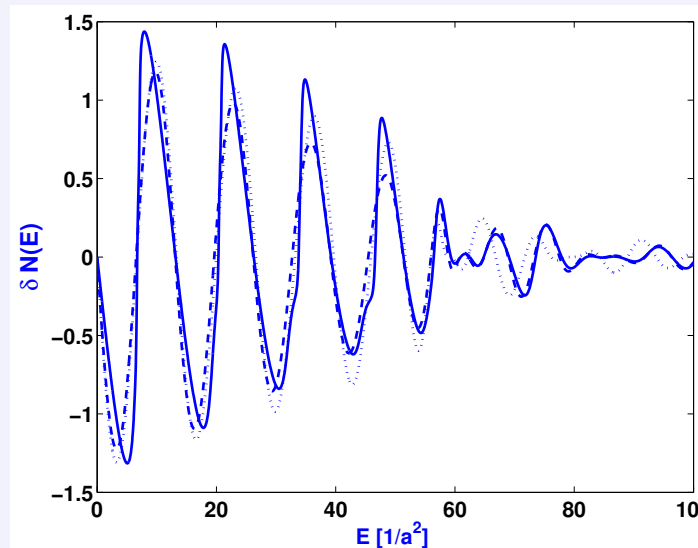
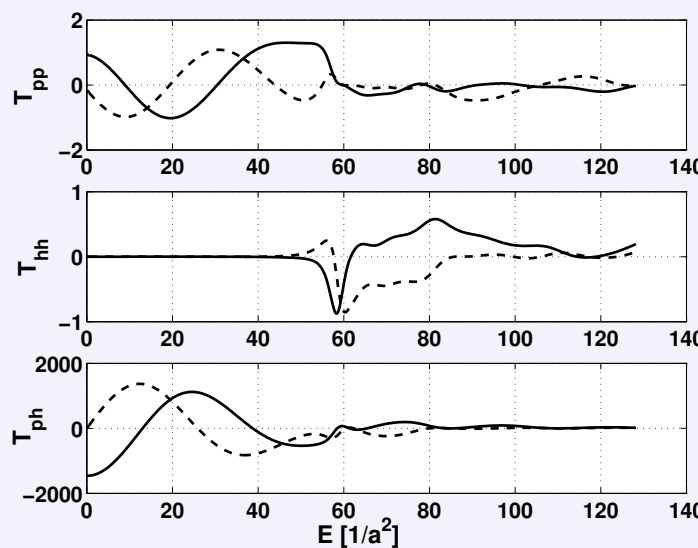
1) Apply Bogoliubov-de Gennes equations in the p-h-space for quasi-particle energy $E = \pm \frac{k^2_{p/h}}{2m} \mp \mu$

$$\begin{pmatrix} H_0 - \mu & \Delta(\vec{r}) \\ \Delta(\vec{r}) & -(H_0 - \mu) \end{pmatrix} \begin{pmatrix} u(\vec{r}) \\ v(\vec{r}) \end{pmatrix} = E \begin{pmatrix} u(\vec{r}) \\ v(\vec{r}) \end{pmatrix} \text{ with pair field } \Delta(\vec{r}) = \begin{cases} \Delta e^{+i\phi_\Delta/2} & \text{for } r \in \text{grain 1}, \\ \Delta e^{-i\phi_\Delta/2} & \text{for } r \in \text{grain 2}, \\ 0 & \text{otherwise.} \end{cases}$$

2) Modify Krein formula $\delta N(E) = -\frac{1}{\pi} \text{Im} \ln \det M(E)$ for the p-h space.

$$\text{For } R \gg a: \delta N(E) \approx \frac{4|T_{ph}(a, \mu, \Delta)| \cos \phi_\Delta}{\pi^2 \sqrt{k_h k_p} R} \sin[(k_p - k_h)R + \phi_{ph}] - \frac{2|T_{pp}(a, \mu, \Delta)|}{\pi^2 k_p R} \cos(2k_p R + \phi_{pp}) + \frac{2|T_{hh}(a, \mu, \Delta)|}{\pi^2 k_h R} \cos(2k_h R - \phi_{hh})$$

$T_{ph} = (\sum_m t_{ph}^m / 2)^2$, $T_{pp} = (\sum_m (-1)^m t_{pp}^m / 2)^2$ etc. structure functions (only dep. on single scatterer)



$\mu = 200/a^2$, gap $\Delta = 50/a^2$,
rel. gap-phase $\phi_\Delta = 0$, $R = 6a$,

$E \leq \Delta$ behavior **dominant**,
Quantization condition of
shortest periodic orbit:

$$(k_p - k_h)(R - 2a) - 2 \arccos(E/\Delta) = 2\pi n, \quad n = 0, 1, 2, \dots$$

For $E \ll |\Delta|$:

$$\delta N(E) = -\text{Im} \underbrace{\left[\int_{-a \min(k_p, k_h)}^{a \min(k_p, k_h)} d\nu \exp\left(\frac{i(k_p - k_h)\nu^2}{2k_p k_h a}\right) \right]^2}_{\rightarrow (2k_F a)^2 \text{ if } E=0} \frac{e^{i(k_p - k_h)(R-2a)}}{\pi^2 R \sqrt{k_p k_h}} \cos(\phi_\Delta).$$

- **Exponent:** classical action of shortest periodic orbit (hole momentum negative!); quantization condition: $(k_p - k_h)(R - 2a) - 2 \arccos(E/\Delta) = 2\pi n$, $n = 0, 1, 2, \dots$.
- **Weight:** quadratic number of partial waves under Andreev reflection i.e. the quadratic range of impact-parameters $4m_{max}^2 = (2k_F a)^2$.

For $E \ll |\Delta|$:

$$\delta N(E) = -\text{Im} \underbrace{\left[\int_{-a \min(k_p, k_h)}^{a \min(k_p, k_h)} d\nu \exp\left(\frac{i(k_p - k_h)\nu^2}{2k_p k_h a}\right) \right]^2}_{\rightarrow (2k_F a)^2 \text{ if } E=0} \frac{e^{i(k_p - k_h)(R-2a)}}{\pi^2 R \sqrt{k_p k_h}} \cos(\phi_\Delta).$$

- **Exponent:** classical action of shortest periodic orbit (hole momentum negative!); quantization condition: $(k_p - k_h)(R - 2a) - 2 \arccos(E/\Delta) = 2\pi n$, $n = 0, 1, 2, \dots$.
- **Weight:** quadratic number of partial waves under Andreev reflection i.e. the quadratic range of impact-parameters $4m_{max}^2 = (2k_F a)^2$.
- Casimir energy of superfluid grains in the Fermi sea:

$$\mathcal{E}_{SC}(R) = \nu_{\text{deg}} \int_0^\infty dE E \frac{d\delta N(E)}{dE} = -\nu_{\text{deg}} \int_0^\infty dE \delta N(E).$$

For $E \ll |\Delta|$:

$$\delta N(E) = -\text{Im} \underbrace{\left[\int_{-a \min(k_p, k_h)}^{a \min(k_p, k_h)} d\nu \exp\left(\frac{i(k_p - k_h)\nu^2}{2k_p k_h a}\right) \right]^2}_{\rightarrow (2k_F a)^2 \text{ if } E=0} \frac{e^{i(k_p - k_h)(R-2a)}}{\pi^2 R \sqrt{k_p k_h}} \cos(\phi_\Delta).$$

- **Exponent**: classical action of shortest periodic orbit (hole momentum negative!); quantization condition: $(k_p - k_h)(R - 2a) - 2 \arccos(E/\Delta) = 2\pi n$, $n = 0, 1, 2, \dots$.
- **Weight**: quadratic number of partial waves under Andreev reflection i.e. the quadratic range of impact-parameters $4m_{max}^2 = (2k_F a)^2$.
- Casimir energy of superfluid grains in the Fermi sea:

$$\mathcal{E}_{SC}(R) = \nu_{\deg} \int_0^\infty dE E \frac{d\delta N(E)}{dE} = -\nu_{\deg} \int_0^\infty dE \delta N(E).$$

Numerical result for two spherical three-dimensional grains at separation R :

$$\mathcal{E}_{SC}(R) \approx \nu_{\deg} \frac{\hbar^2 k_F^2}{2m} \frac{k_F a^4}{2\pi R^2 (R - 2a)} X \gg \left| -\nu_{\deg} \frac{\hbar^2 k_F^2}{2m} \frac{a^2}{2\pi R (R - 2a)} j_1(2k_F(R - 2a)) \right|$$

with $X = \mathcal{O}(1)$, positive (i.e. repulsive!) and weakly dependent on R, k_F, Δ .

A. Bulgac, P. Magierski & A.W., *Europhys. Lett.* **72** (2005) 327

Conclusions:

21

Conclusions:

- \exists effective interaction between voids inside a non-interacting fermion background.

Conclusions:

- \exists effective interaction between voids inside a non-interacting fermion background.
New form of Casimir energy neither attractive nor repulsive, but *changes sign* according to relative arrangement of scatterers.

Conclusions:

- \exists effective interaction between voids inside a non-interacting fermion background.
New form of Casimir energy neither attractive nor repulsive, but *changes sign* according to relative arrangement of scatterers.
- Casimir contributions well approximated semiclassically.

Conclusions:

- \exists effective interaction between voids inside a non-interacting fermion background.
New form of Casimir energy neither attractive nor repulsive, but *changes sign* according to relative arrangement of scatterers.
- Casimir contributions well approximated semiclassically.
- \exists many-body Casimir contributions in n-sphere systems

Conclusions:

- \exists effective interaction between voids inside a non-interacting fermion background.
New form of Casimir energy neither attractive nor repulsive, but *changes sign* according to relative arrangement of scatterers.
- Casimir contributions well approximated semiclassically.
- \exists many-body Casimir contributions in n-sphere systems:
 - However short-ranged and dominated by long-ranged two-body interactions.

Conclusions:

- \exists effective interaction between voids inside a non-interacting fermion background.
New form of Casimir energy neither attractive nor repulsive, but *changes sign* according to relative arrangement of scatterers.
- Casimir contributions well approximated semiclassically.
- \exists many-body Casimir contributions in n-sphere systems:
– However short-ranged and dominated by long-ranged two-body interactions.
- Presented results only for symmetric arrangements of spheres.

Conclusions:

- \exists effective interaction between voids inside a non-interacting fermion background.
New form of Casimir energy neither attractive nor repulsive, but *changes sign* according to relative arrangement of scatterers.
- Casimir contributions well approximated semiclassically.
- \exists many-body Casimir contributions in n-sphere systems:
– However short-ranged and dominated by long-ranged two-body interactions.
- Presented results only for symmetric arrangements of spheres.
However, tests of various asymmetrical configurations of three and four spheres show the same general pattern: d.o.s. \approx sum of corresponding pairwise contributions.

Conclusions:

- \exists effective interaction between voids inside a non-interacting fermion background.
New form of Casimir energy neither attractive nor repulsive, but *changes sign* according to relative arrangement of scatterers.
- Casimir contributions well approximated semiclassically.
- \exists many-body Casimir contributions in n-sphere systems:
– However short-ranged and dominated by long-ranged two-body interactions.
- Presented results only for symmetric arrangements of spheres.
However, tests of various asymmetrical configurations of three and four spheres show the same general pattern: d.o.s. \approx sum of corresponding pairwise contributions.
- The spheres can be replaced with other objects, if curvature radii larger than the Fermi wave length.

Conclusions:

- \exists effective interaction between voids inside a non-interacting fermion background.
New form of Casimir energy neither attractive nor repulsive, but *changes sign* according to relative arrangement of scatterers.
- Casimir contributions well approximated semiclassically.
- \exists many-body Casimir contributions in n-sphere systems:
– However short-ranged and dominated by long-ranged two-body interactions.
- Presented results only for symmetric arrangements of spheres.
However, tests of various asymmetrical configurations of three and four spheres show the same general pattern: d.o.s. \approx sum of corresponding pairwise contributions.
- The spheres can be replaced with other objects, if curvature radii larger than the Fermi wave length. Effects of finite surface thickness can be booked as Weyl-term contributions if the objects do not overlap.

Conclusions:

- \exists effective interaction between voids inside a non-interacting fermion background.
New form of Casimir energy neither attractive nor repulsive, but *changes sign* according to relative arrangement of scatterers.
- Casimir contributions well approximated semiclassically.
- \exists many-body Casimir contributions in n-sphere systems:
– However short-ranged and dominated by long-ranged two-body interactions.
- Presented results only for symmetric arrangements of spheres.
However, tests of various asymmetrical configurations of three and four spheres show the same general pattern: d.o.s. \approx sum of corresponding pairwise contributions.
- The spheres can be replaced with other objects, if curvature radii larger than the Fermi wave length. Effects of finite surface thickness can be booked as Weyl-term contributions if the objects do not overlap.
- Possible lab case: Buckyball-lattices in liquid mercury or liquid ^3He .

Conclusions:

- \exists effective interaction between voids inside a non-interacting fermion background.
New form of Casimir energy neither attractive nor repulsive, but *changes sign* according to relative arrangement of scatterers.
- Casimir contributions well approximated semiclassically.
- \exists many-body Casimir contributions in n-sphere systems:
– However short-ranged and dominated by long-ranged two-body interactions.
- Presented results only for symmetric arrangements of spheres.
However, tests of various asymmetrical configurations of three and four spheres show the same general pattern: d.o.s. \approx sum of corresponding pairwise contributions.
- The spheres can be replaced with other objects, if curvature radii larger than the Fermi wave length. Effects of finite surface thickness can be booked as Weyl-term contributions if the objects do not overlap.
- Possible lab case: Buckyball-lattices in liquid mercury or liquid ^3He .
- Nuclei immersed in neutron gas in a neutron star crust: Casimir interactions of same order ($\sim \text{keV/fm}^3$) as energy differences between various liquid drop phases.

Conclusions:

- \exists effective interaction between voids inside a non-interacting fermion background.
New form of Casimir energy neither attractive nor repulsive, but *changes sign* according to relative arrangement of scatterers.
- Casimir contributions well approximated semiclassically.
- \exists many-body Casimir contributions in n-sphere systems:
– However short-ranged and dominated by long-ranged two-body interactions.
- Presented results only for symmetric arrangements of spheres.
However, tests of various asymmetrical configurations of three and four spheres show the same general pattern: d.o.s. \approx sum of corresponding pairwise contributions.
- The spheres can be replaced with other objects, if curvature radii larger than the Fermi wave length. Effects of finite surface thickness can be booked as Weyl-term contributions if the objects do not overlap.
- Possible lab case: Buckyball-lattices in liquid mercury or liquid ^3He .
- Nuclei immersed in neutron gas in a neutron star crust: Casimir interactions of same order ($\sim \text{keV/fm}^3$) as energy differences between various liquid drop phases. Long-range and oscillating: → disordered lattices expected.

Conclusions:

- \exists effective interaction between voids inside a non-interacting fermion background.
New form of Casimir energy neither attractive nor repulsive, but *changes sign* according to relative arrangement of scatterers.
- Casimir contributions well approximated semiclassically.
- \exists many-body Casimir contributions in n-sphere systems:
– However short-ranged and dominated by long-ranged two-body interactions.
- Presented results only for symmetric arrangements of spheres.
However, tests of various asymmetrical configurations of three and four spheres show the same general pattern: d.o.s. \approx sum of corresponding pairwise contributions.
- The spheres can be replaced with other objects, if curvature radii larger than the Fermi wave length. Effects of finite surface thickness can be booked as Weyl-term contributions if the objects do not overlap.
- Possible lab case: Buckyball-lattices in liquid mercury or liquid ^3He .
- Nuclei immersed in neutron gas in a neutron star crust: Casimir interactions of same order ($\sim \text{keV}/\text{fm}^3$) as energy differences between various liquid drop phases. Long-range and oscillating: → disordered lattices expected.
- Pairing interaction: enhancement of Casimir contributions.

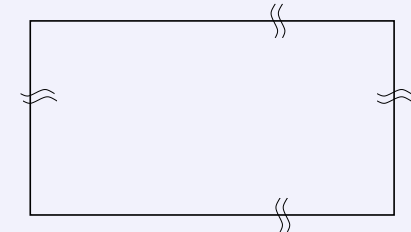
Conclusions:

- \exists effective interaction between voids inside a non-interacting fermion background.
New form of Casimir energy neither attractive nor repulsive, but *changes sign* according to relative arrangement of scatterers.
- Casimir contributions well approximated semiclassically.
- \exists many-body Casimir contributions in n-sphere systems:
– However short-ranged and dominated by long-ranged two-body interactions.
- Presented results only for symmetric arrangements of spheres.
However, tests of various asymmetrical configurations of three and four spheres show the same general pattern: d.o.s. \approx sum of corresponding pairwise contributions.
- The spheres can be replaced with other objects, if curvature radii larger than the Fermi wave length. Effects of finite surface thickness can be booked as Weyl-term contributions if the objects do not overlap.
- Possible lab case: Buckyball-lattices in liquid mercury or liquid ^3He .
- Nuclei immersed in neutron gas in a neutron star crust: Casimir interactions of same order ($\sim \text{keV}/\text{fm}^3$) as energy differences between various liquid drop phases. Long-range and oscillating: \rightarrow disordered lattices expected.
- Pairing interaction: enhancement of Casimir contributions.
Andreev reflection: focusing (and defocusing) scattering; p-h dominant; repulsive.

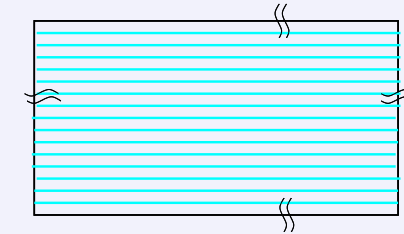
Conclusions:

- \exists effective interaction between voids inside a non-interacting fermion background.
New form of Casimir energy neither attractive nor repulsive, but *changes sign* according to relative arrangement of scatterers.
- Casimir contributions well approximated semiclassically.
- \exists many-body Casimir contributions in n-sphere systems:
– However short-ranged and dominated by long-ranged two-body interactions.
- Presented results only for symmetric arrangements of spheres.
However, tests of various asymmetrical configurations of three and four spheres show the same general pattern: d.o.s. \approx sum of corresponding pairwise contributions.
- The spheres can be replaced with other objects, if curvature radii larger than the Fermi wave length. Effects of finite surface thickness can be booked as Weyl-term contributions if the objects do not overlap.
- Possible lab case: Buckyball-lattices in liquid mercury or liquid ^3He .
- Nuclei immersed in neutron gas in a neutron star crust: Casimir interactions of same order ($\sim \text{keV/fm}^3$) as energy differences between various liquid drop phases. Long-range and oscillating: \rightarrow disordered lattices expected.
- Pairing interaction: enhancement of Casimir contributions.
Andreev reflection: focusing (and defocusing) scattering; p-h dominant; repulsive.
- Map-method onto scattering systems also applicable to traditional Casimir problems:

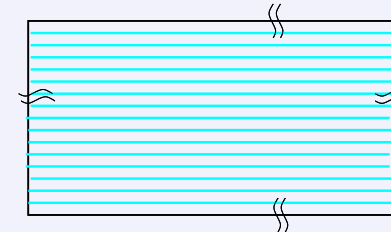
1. “infinite” container:



1. “infinite” container: $\rho(E)=\rho_0(E)$ (background field)

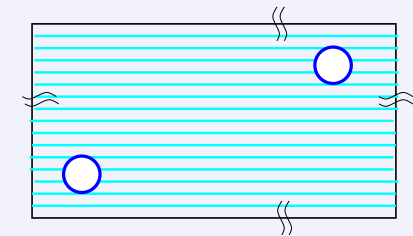


1. “*infinite*” container: $\rho(E) = \rho_0(E)$ (background field)

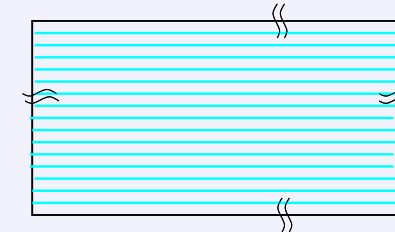


2. n bubbles (of radii a_i) “punched out” at “infinite” separation:

$$\rho(E) = \rho_0(E) + \sum_{i=1}^n \underbrace{\rho_W(E, a_i)}_{\text{Weyl-Term}} \quad (\text{note the excluded volume !})$$

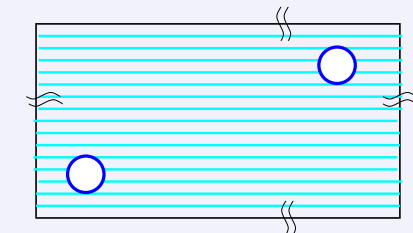


1. “*infinite*” container: $\rho(E) = \rho_0(E)$ (background field)



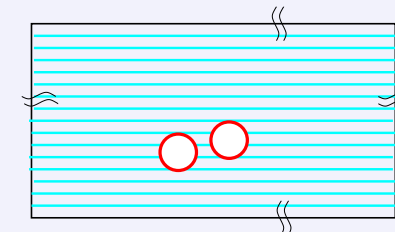
2. n bubbles (of radii a_i) “punched out” at “infinite” separation:

$$\rho(E) = \rho_0(E) + \sum_{i=1}^n \underbrace{\rho_W(E, a_i)}_{\text{Weyl-Term}} \quad (\text{note the excluded volume !})$$

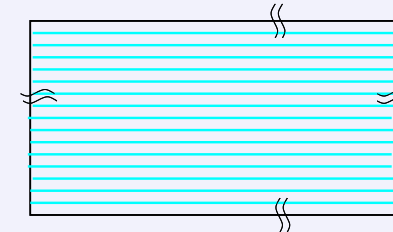


3. geometry-dependent arrangement of n bubbles:

$$\rho(E) = \rho_0(E) + \sum_{i=1}^n \rho_W(E, a_i) + \delta\rho_C(E, \{a_i\}, \{\mathbf{r}_{ij}\})$$

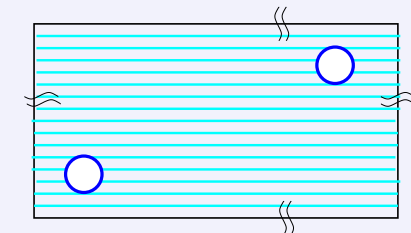


1. “*infinite*” container: $\rho(E) = \rho_0(E)$ (background field)



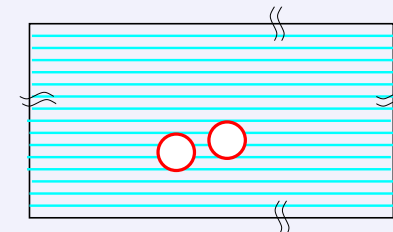
2. n bubbles (of radii a_i) “punched out” at “infinite” separation:

$$\rho(E) = \rho_0(E) + \sum_{i=1}^n \underbrace{\rho_W(E, a_i)}_{\text{Weyl-Term}} \quad (\text{note the excluded volume !})$$



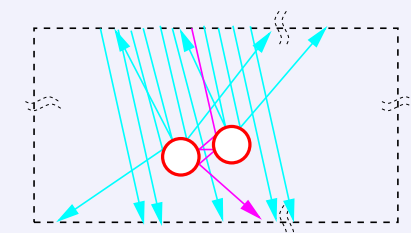
3. geometry-dependent arrangement of n bubbles:

$$\rho(E) = \rho_0(E) + \sum_{i=1}^n \rho_W(E, a_i) + \delta\rho_C(E, \{a_i\}, \{\mathbf{r}_{ij}\})$$

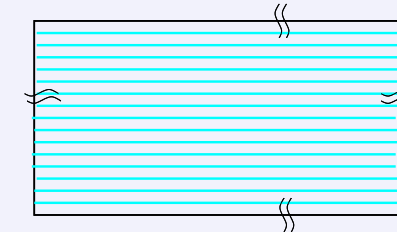


4. Krein trace formula (note the averaging):

$$\delta\rho(E) = \bar{\rho}(E) - \bar{\rho}_0(E) = \frac{1}{2\pi i} \frac{d}{dE} \overbrace{\ln \det S_n(E)}^{2i\eta_n(E)}$$

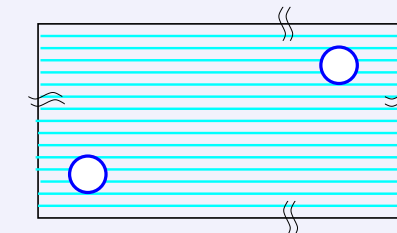


1. “*infinite*” container: $\rho(E) = \rho_0(E)$ (background field)



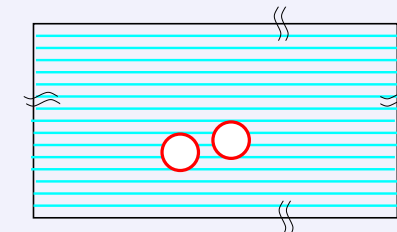
2. n bubbles (of radii a_i) “punched out” at “*infinite*” separation:

$$\rho(E) = \rho_0(E) + \sum_{i=1}^n \underbrace{\rho_W(E, a_i)}_{\text{Weyl-Term}} \quad (\text{note the excluded volume !})$$



3. geometry-dependent arrangement of n bubbles:

$$\rho(E) = \rho_0(E) + \sum_{i=1}^n \rho_W(E, a_i) + \delta\rho_C(E, \{a_i\}, \{\mathbf{r}_{ij}\})$$



4. Krein trace formula (note the averaging):

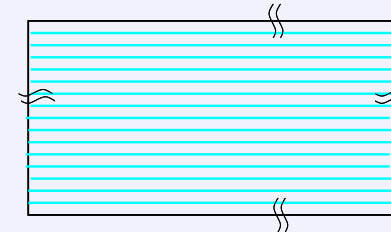
$$\delta\rho(E) = \bar{\rho}(E) - \bar{\rho}_0(E) = \frac{1}{2\pi i} \frac{d}{dE} \overbrace{\ln \det S_n(E)}^{2i\eta_n(E)}$$

5. *Multiple scattering matrix*

$$\overbrace{\det S_n(E)} = \prod_i \det S_1(E, a_i) \frac{\det \mathbf{M}^\dagger(k^*)}{\det \mathbf{M}(k)}$$

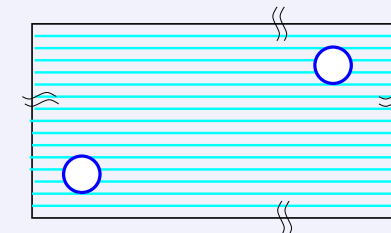
see A.W., *Phys. Rep.* **309** (1999)

1. “*infinite*” container: $\rho(E) = \rho_0(E)$ (background field)



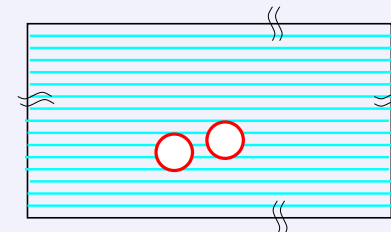
2. n bubbles (of radii a_i) “punched out” at “infinite” separation:

$$\rho(E) = \rho_0(E) + \sum_{i=1}^n \underbrace{\rho_W(E, a_i)}_{\text{Weyl-Term}} \quad (\text{note the excluded volume !})$$



3. geometry-dependent arrangement of n bubbles:

$$\rho(E) = \rho_0(E) + \sum_{i=1}^n \rho_W(E, a_i) + \delta\rho_C(E, \{a_i\}, \{\mathbf{r}_{ij}\})$$



4. Krein trace formula (note the averaging):

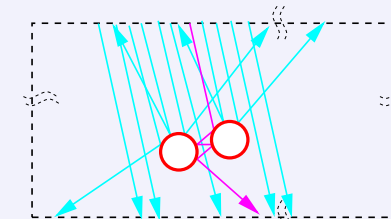
$$\delta\rho(E) = \bar{\rho}(E) - \bar{\rho}_0(E) = \frac{1}{2\pi i} \frac{d}{dE} \overbrace{\ln \det S_n(E)}^{2i\eta_n(E)}$$

5. *Multiple scattering matrix*

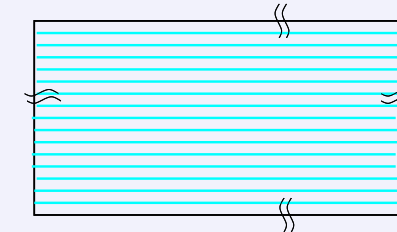
$$\rightarrow \delta\bar{\rho}_C(E, \{a_i\}, \{\mathbf{r}_{ij}\}) = -\frac{1}{\pi} \text{Im} \left(\frac{d}{dE} \ln \det \mathbf{M}(k(E)) \right)$$

$$\overbrace{\det S_n(E)}^{\text{det } S_n(E)} = \prod_i \det \mathbf{S}_1(E, a_i) \frac{\det \mathbf{M}^\dagger(k^*)}{\det \mathbf{M}(k)}$$

see A.W., *Phys. Rep.* **309** (1999)

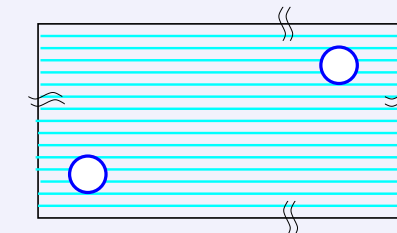


1. “*infinite*” container: $\rho(E) = \rho_0(E)$ (background field)



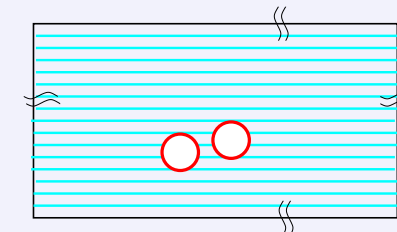
2. n bubbles (of radii a_i) “punched out” at “infinite” separation:

$$\rho(E) = \rho_0(E) + \sum_{i=1}^n \underbrace{\rho_W(E, a_i)}_{\text{Weyl-Term}} \quad (\text{note the excluded volume !})$$



3. geometry-dependent arrangement of n bubbles:

$$\rho(E) = \rho_0(E) + \sum_{i=1}^n \rho_W(E, a_i) + \delta\rho_C(E, \{a_i\}, \{\mathbf{r}_{ij}\})$$



4. Krein trace formula (note the averaging):

$$\delta\rho(E) = \bar{\rho}(E) - \bar{\rho}_0(E) = \frac{1}{2\pi i} \overbrace{\frac{d}{dE} \ln \det S_n(E)}^{2i\eta_n(E)}$$

5. *Multiple scattering matrix*

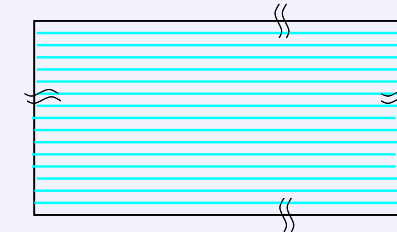
$$\rightarrow \delta\bar{\rho}_C(E, \{a_i\}, \{\mathbf{r}_{ij}\}) = -\frac{1}{\pi} \text{Im} \left(\frac{d}{dE} \ln \det \mathbf{M}(k(E)) \right)$$

$$\overbrace{\det S_n(E)}^{\text{det } S_n(E)} = \prod_i \det \mathbf{S}_1(E, a_i) \frac{\det \mathbf{M}^\dagger(k^*)}{\det \mathbf{M}(k)}$$

see A.W., *Phys. Rep.* **309** (1999)

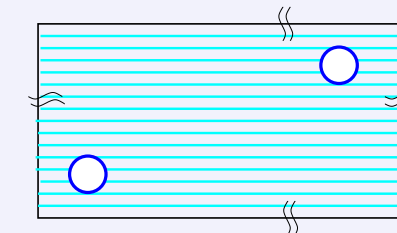
All determinants exist (although the relevant scattering matrices are infinite dimensional)
since the associated T -matrices are trace-class.

1. “*infinite*” container: $\rho(E) = \rho_0(E)$ (background field)



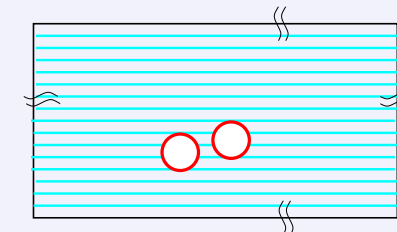
2. n bubbles (of radii a_i) “punched out” at “infinite” separation:

$$\rho(E) = \rho_0(E) + \sum_{i=1}^n \underbrace{\rho_W(E, a_i)}_{\text{Weyl-Term}} \quad (\text{note the excluded volume !})$$



3. geometry-dependent arrangement of n bubbles:

$$\rho(E) = \rho_0(E) + \sum_{i=1}^n \rho_W(E, a_i) + \delta\rho_C(E, \{a_i\}, \{\mathbf{r}_{ij}\})$$



4. Krein trace formula (note the averaging):

$$\delta\rho(E) = \bar{\rho}(E) - \bar{\rho}_0(E) = \frac{1}{2\pi i} \overbrace{\frac{d}{dE} \ln \det S_n(E)}^{2i\eta_n(E)}$$

5. *Multiple scattering matrix*

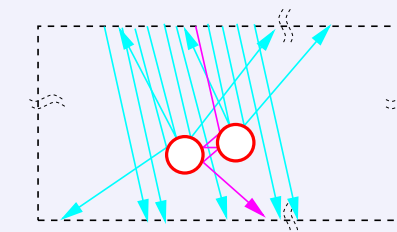
$$\rightarrow \delta\bar{\rho}_C(E, \{a_i\}, \{\mathbf{r}_{ij}\}) = -\frac{1}{\pi} \text{Im} \left(\frac{d}{dE} \ln \det \mathbf{M}(k(E)) \right)$$

$$\overbrace{\det S_n(E)}^{\text{det } S_n(E)} = \prod_i \det \mathbf{S}_1(E, a_i) \frac{\det \mathbf{M}^\dagger(k^*)}{\det \mathbf{M}(k)}$$

see A.W., *Phys. Rep.* **309** (1999)

6. Casimir energy:

$$\therefore \mathcal{E}_C = \int_0^\infty dE \frac{1}{2} E \delta\bar{\rho}_C = -\frac{1}{2} \int_0^\infty dE \overline{\mathcal{N}}_C = \frac{1}{2\pi} \int_0^\infty dE \text{Im} \ln \det \mathbf{M}(k(E))$$



$$\begin{aligned}
\mathcal{E}_{\textcolor{red}{C}} &= \int_0^\infty dE \frac{1}{2} \hbar c k \delta \bar{\rho}_{\textcolor{red}{C}}(k(E)) = -\frac{\hbar c}{2} \int_0^\infty dk \overline{\mathcal{N}}_{\textcolor{red}{C}}(k) = \frac{\hbar c}{2\pi} \int_0^\infty dk \operatorname{Im} \ln \det \textcolor{red}{M}(k) \\
&= \frac{\hbar c}{4\pi i} \left[\int_0^{\infty(1+i0_+)} dk \ln \det \textcolor{red}{M}(k) - \int_0^{\infty(1-i0_+)} dk \ln \det \textcolor{red}{M}(k)^\dagger \right] \\
&= \frac{\hbar c}{2\pi} \int_0^\infty dk_4 \ln \det \textcolor{red}{M}(ik_4) \quad \text{for relativistic disp. } E = \hbar c k \text{ and after Wick-rotation}
\end{aligned}$$

$$\begin{aligned}
\mathcal{E}_{\textcolor{red}{C}} &= \int_0^\infty dE \frac{1}{2} \hbar c k \delta \bar{\rho}_{\textcolor{red}{C}}(k(E)) = -\frac{\hbar c}{2} \int_0^\infty dk \overline{\mathcal{N}}_{\textcolor{red}{C}}(k) = \frac{\hbar c}{2\pi} \int_0^\infty dk \operatorname{Im} \ln \det \textcolor{red}{M}(k) \\
&= \frac{\hbar c}{4\pi i} \left[\int_0^{\infty(1+i0_+)} dk \ln \det \textcolor{red}{M}(k) - \int_0^{\infty(1-i0_+)} dk \ln \det \textcolor{red}{M}(k)^\dagger \right] \\
&= \frac{\hbar c}{2\pi} \int_0^\infty dk_4 \ln \det \textcolor{red}{M}(ik_4) \quad \text{for relativistic disp. } E = \hbar c k \text{ and after Wick-rotation}
\end{aligned}$$

Note that $\det M(ik_4)^\dagger = \det M(ik_4)$ since $\det M(k) = \det M((-k^*))^\dagger$;

$$\begin{aligned}
\mathcal{E}_C &= \int_0^\infty dE \frac{1}{2} \hbar c k \delta \bar{\rho}_C(k(E)) = -\frac{\hbar c}{2} \int_0^\infty dk \overline{\mathcal{N}}_C(k) = \frac{\hbar c}{2\pi} \int_0^\infty dk \operatorname{Im} \ln \det \textcolor{red}{M}(k) \\
&= \frac{\hbar c}{4\pi i} \left[\int_0^{\infty(1+i0_+)} dk \ln \det \textcolor{red}{M}(k) - \int_0^{\infty(1-i0_+)} dk \ln \det \textcolor{red}{M}(k)^\dagger \right] \\
&= \frac{\hbar c}{2\pi} \int_0^\infty dk_4 \ln \det \textcolor{red}{M}(ik_4) \quad \text{for relativistic disp. } E = \hbar c k \text{ and after Wick-rotation}
\end{aligned}$$

Note that $\det M(ik_4)^\dagger = \det M(ik_4)$ since $\det M(k) = \det M((-k^*))^\dagger$; therefore corollary:

$$\frac{\hbar c}{2\pi} \int_0^\infty dk k^{2n+1} \operatorname{Im} \ln \det M(k) = i(-1)^n \frac{\hbar c}{4\pi} \int_0^\infty dk_4 k_4^{2n+1} [\ln \det M(ik_4) - \ln \det M(ik_4)^\dagger] = 0$$

e.g. Casimir energy over modes with non-relativistic dispersion $E = \hbar^2 k^2 / 2m$ integrates to zero, unless there is a *finite upper cutoff*, as e.g. the *Fermi momentum k_F* in the case of the so-called *fermionic Casimir effect*

– see A. Bulgac & AW., Phys. Rev. Lett. 87 (2001).

Scalar Casimir effect of Dirichlet-spheres and -plates – or *How good is the PFA?*

24

Scalar Casimir effect of Dirichlet-spheres and -plates – or *How good is the PFA?*

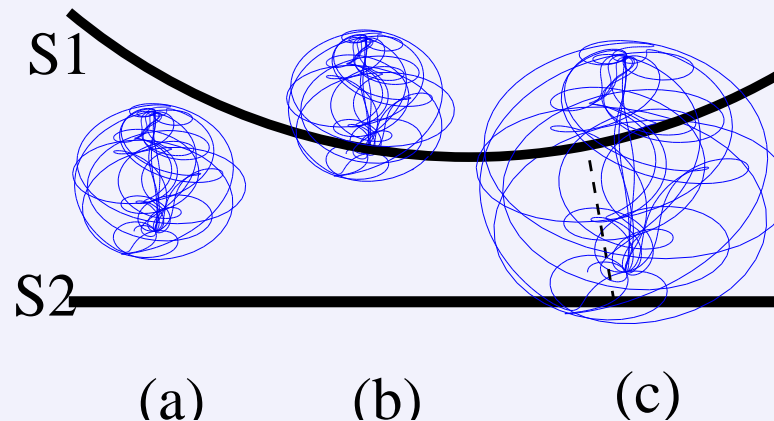
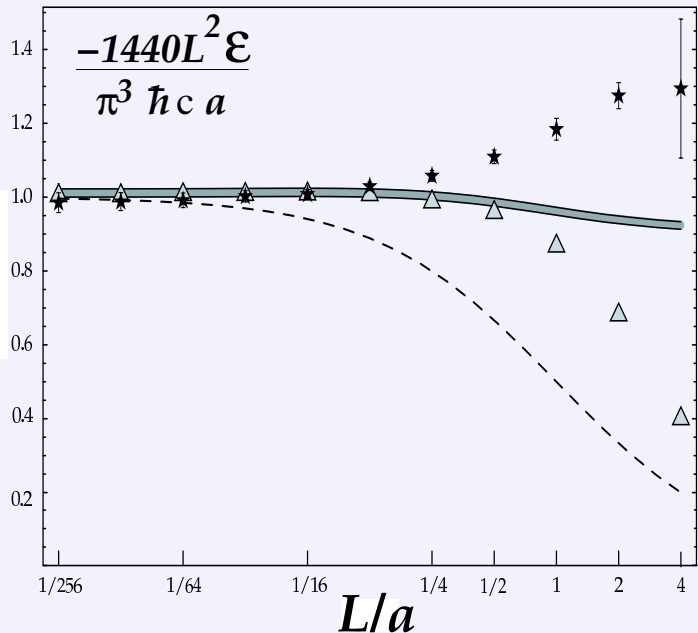
24

M. Schaden, L. Spruch, PRA **58** (1998): *short-distance PFA confirmed by semiclassics (periodic orbits)*

Scalar Casimir effect of Dirichlet-spheres and -plates – or *How good is the PFA?*

24

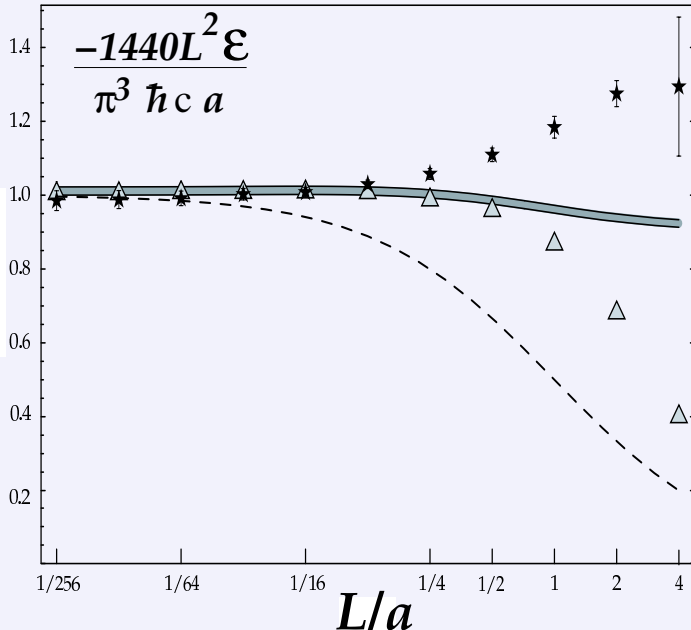
H. Gies, K. Langfeld, L. Moyaerts, JHEP **0306** (2003): *world-line approach (Feynman integral in x-space)*
A. Scardicchio, R.L. Jaffe, NPB **704** (2005): *optical ansatz (summation over closed orbits)*



Scalar Casimir effect of Dirichlet-spheres and -plates – or *How good is the PFA?*

H. Gies, K. Langfeld, L. Moyaerts, JHEP **0306** (2003): *world-line approach (Feynman integral in x-space)*

A. Scardicchio, R.L. Jaffe, NPB **704** (2005): *optical ansatz (summation over closed orbits)*



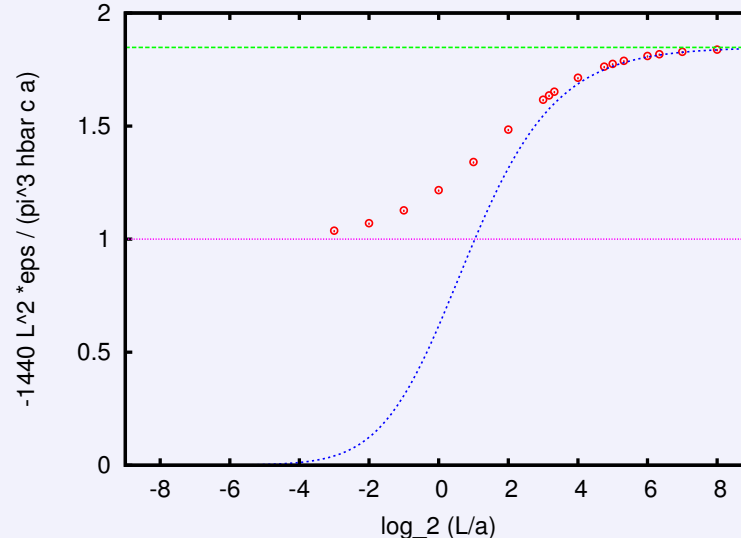
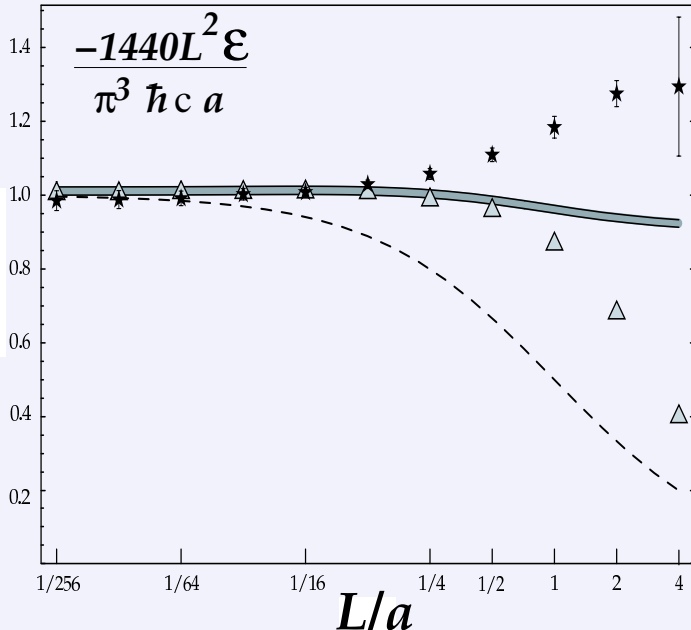
Note: asymptotically ($L/a \gg 1$) s-wave scattering dominates:

$$\mathcal{E}(L) \sim -\frac{\pi^3 \hbar c a}{1440 L^2} \frac{90}{\pi^4} \frac{2}{(1 + a/L)(1 + a/2L)} \rightarrow -\frac{\pi^3 \hbar c a}{1440 L^2} \frac{90}{\pi^4} \times 2 = -\frac{\pi^3 \hbar c a}{1440 L^2} \times 1.847 \dots$$

Scalar Casimir effect of Dirichlet-spheres and -plates – or *How good is the PFA?*

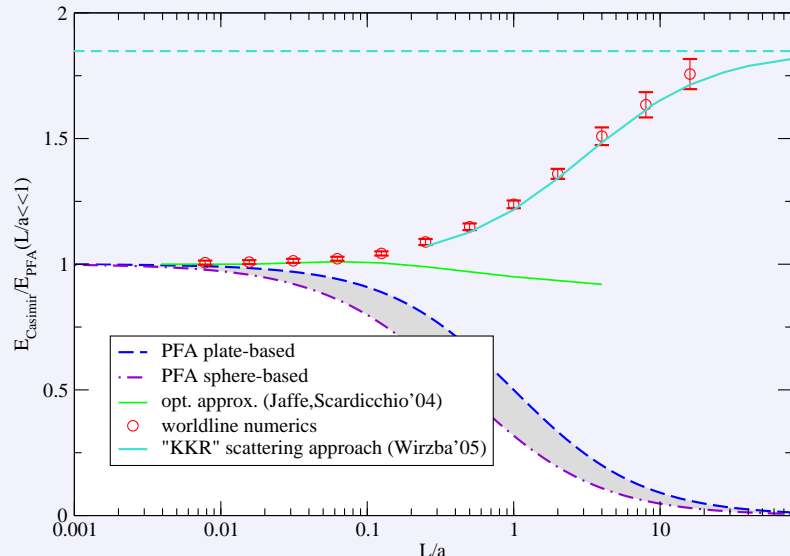
H. Gies, K. Langfeld, L. Moyaerts, JHEP **0306** (2003): *world-line approach (Feynman integral in x-space)*

A. Scardicchio, R.L. Jaffe, NPB **704** (2005): *optical ansatz (summation over closed orbits)*

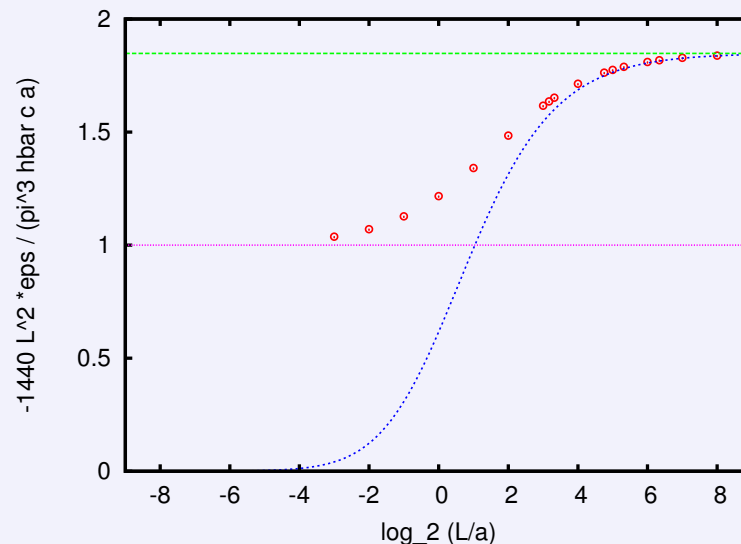


Note: asymptotically ($L/a \gg 1$) s-wave scattering dominates:

$$\mathcal{E}(L) \sim -\frac{\pi^3 \hbar c a}{1440 L^2} \frac{90}{\pi^4} \frac{2}{(1 + a/L)(1 + a/2L)} \rightarrow -\frac{\pi^3 \hbar c a}{1440 L^2} \frac{90}{\pi^4} \times 2 = -\frac{\pi^3 \hbar c a}{1440 L^2} \times 1.847 \dots$$



H. Gies & K. Klingmüller, 2006



Note: asymptotically ($L/a \gg 1$) s-wave scattering dominates:

$$\mathcal{E}(L) \sim -\frac{\pi^3 \hbar c a}{1440 L^2} \frac{90}{\pi^4} \frac{2}{(1+a/L)(1+a/2L)} \rightarrow -\frac{\pi^3 \hbar c a}{1440 L^2} \frac{90}{\pi^4} \times 2 = -\frac{\pi^3 \hbar c a}{1440 L^2} \times 1.847 \dots$$

while

$$\mathcal{E}_{\text{p-wave}}(L) \sim -\frac{5\pi^3 \hbar c a^3}{1440 L^4} \frac{90}{\pi^4}$$

(i.e. no Casimir-Polder behavior in the scalar case)
A. Bulgac, P. Magierski & A.W., *Phys. Rev. D* **73** (2006) 025007

Additional Conclusions:

- Casimir energy re-defined as vacuum energy of the geometry-dependent part of the level density (connected to the multi-scattering phase shift by a modified Krein trace formula).
- The non-overlapping (i.g. non-separable) N-sphere, sphere-plate, N-disk (and N-cylinder) Casimir problems can be solved exactly in the scalar (and also in the fermionic) case.
- Calculation not plagued by subtraction of single-sphere contributions or by the removal of diverging ultraviolet contributions; all involved determinants exist and are finite since the pertinent T -matrices are trace-class.
- Large-distance behavior dominated by s -wave scattering in the case of the scalar Casimir effect and by p -wave scattering for the EM Casimir effect.
- The presented method can easily be applied to any number of spheres or cylinders with or without planes (in 2D disks with or without lines).
- Moreover, the Dirichlet boundary conditions can be replaced by Neumann or mixed boundary conditons.
- The Casimir energy is dominated by momenta $k \sim 1/L$ where L is the separation scale. For the scalar sphere-plate case the integration can be truncated at $k_{\max} \sim 10/L$ corresponding to a truncation in the angular momentum $l_{\max} \geq (e/2)k_{\max}a \approx 14a/L$.

Publications:

Aurel Bulgac & A.W., *Phys. Rev. Lett.* **87** (2001) 120404

Physics News Update, No. 556, #1, Sep. 13, 2001.

Aurel Bulgac, Piotr Magierski & A.W., *Europhys. Lett.* **72** (2005) 372.

Aurel Bulgac, Piotr Magierski & A.W., *Phys. Rev. D* **73** (2006) 025007.

A.W., Aurel Bulgac & Piotr Magierski, *J. Phys. A: Math. Gen.* **39** (2006) 6815.

A.W., *J. Phys. A: Math. Theor.* **41** (2008) 164003.